OPTICAL ASSEMBLY OF FAR-FIELD SUPER-RESOLUTION IMAGING VIA OPTICAL GAIN

By

Joshua.S. Deaver

A Thesis
Submitted to the
Faculty of the Graduate School
of
Western Carolina University
in Partial Fulfillment of
the Requirements for the Degree
of
Master of Science in Technology

Committee:

_____ Director

_____

_____

_____ Dean of the Graduate School

Date: _____

Spring 2011
Western Carolina University
Cullowhee, North Carolina

OPTICAL ASSEMBLY OF FAR-FIELD SUPER-RESOLUTION
IMAGING VIA OPTICAL GAIN

A thesis presented to the faculty of the Graduate School of
Western Carolina University in partial fulfillment of the
requirements for the degree of Master of Science in Technology.

By

Joshua.S. Deaver

Director: Dr. Yang
Assistant Professor
Department of Engineering Technology Western Carolina University

Committee Members: Dr. Michael Fiddy, Physics, ECE UNC Charlotte
Dr. Mesfin Woldeyohannes, Physics Western Carolina University
Dr. James Zhang, Engineering and Technology Western Carolina
University

March 2011

This thesis is dedicated to my fiance, and to my family. To my fiance, without your continued support and love I would not possess the ability to function, let alone finish such a demanding project. To my family, the sacrifices you made have given me opportunities which to you I will always be indebted. Many thanks to all others who have helped me along the way, God bless you all.

TABLE OF CONTENTS

LIST OF TABLES

LIST OF FIGURES

ABSTRACT

OPTICAL ASSEMBLY OF FAR-FIELD SUPER-RESOLUTION IMAGING VIA
OPTICAL GAIN

Joshua.S. Deaver, M.S.T.

Western Carolina University (March 2011)

Director: Dr. Yang

The performance of an optical imaging system is fundamentally limited by the wave nature of light. More specifically the lateral resolution of an image has traditionally been dictated by Abbe's limit, to be approximately one-half of the wavelength. The pursuit of exceeding this limit is a growing interest in several research areas. The goal of these pursuits is to achieve super-resolution imaging, as in breaking what have long been thought of as insurmountable restrictions. There have been several methods proposed and demonstrated to overcome Abbe's limits. Some of the aforementioned methods include the perfect lens made from negative refractive index materials and Structured Illumination Microscopy (SIM). This paper highlights a novel approach to achieving super-resolution imaging. In this case the means to obtaining super-resolution imaging will be through optical gain by using an active objective lens. This gain will allow for the retention of spatial frequencies beyond Abbes limit, by the conversion of evanescent waves into sustainable propagating waves. An optical assembly was constructed to verify the theory of optical gain assisted evanescent wave conversion. The experimental results show that for two specific situa-

tions, where one (Pump angle A) provides the possibility of optical gain assisted evanescent wave conversion and one (Pump angle C) does not, Pump angle A position allows for the detection of higher spatial frequency information than Pump angle C position in the far-field pattern. This confirms the hypothesis and the theory of evanescent wave conversion via optical gain, providing the potential for far-field super-resolution.

CHAPTER 1: INTRODUCTION

For many years a major tool of scientists has been the optical lens. Optical lenses' operation is understood on the basis of classical optics: curved surfaces bend light due to the refractive index contrast. The optical lenses' limitation is that no lens can focus light onto an area smaller than a square wavelength. Accordingly the resolution of the far-field optical microscopy is limited to approximately one-half of the wavelength as dictated by Abbe's limit. [1] For visible light, the best performing optical microscope can only distinguish particles that are more than 200 nano-meters apart. [2] The limit of the resolving power of a lens was long thought to be an immutable law of nature. As any follower of the sciences knows, any limit or "immutable law of nature" stands to be put through the most rigorous scrutiny. This scrutiny gave birth to the research into super-resolution imaging, or imaging systems that surpass this imaging limit. Any method which surpasses Abbe's limit can be a very significant scientific breakthrough, having broad and fundamental impact on almost every scientific research field from fundamental physics to biology.

There are current theories and practices that propose and demonstrate super-resolution imaging, and in particular, there are many articles published and studies being conducted in the field of super-lenses. These super-lenses derive their foundation from Pendry's seminal work [3] which proposes that a slab of negative refractive index material of n = -1 has the power to focus all spatial frequency components of a point source, including those carried by evanescent waves. However, the applications of these existing methods for far-field super-resolution imaging are limited. The deficiencies of the super-lens methods

along with other methods which are capable of far-field super-resolution imaging will be discussed in further detail in the literature review section.

We propose to accomplish breaking the Abbe limit by optical gain assisted evanescent wave conversion. The goal of this thesis study is to build an active objective lens set-up that performs proof-of-concept experiments, and compare the experimental results to the theory in order to identify any experimental evidence of the optical gain assisted evanescent wave conversion. The theory of optical gain assisted evanescent wave conversion and the design of experimentation will be explained in further detail in the remaining sections.

CHAPTER 2: BACKGROUND/LITERATURE SURVEY

This chapter outlines the methods currently being used in far-field super-resolution imaging and describes our proposed theory and its anticipated outcome. It explains the proposed evanescent wave conversion via optical gain, and the design of an optical experimental set-up incorporating an active objective lens.

2.1   Background

As stated previously Abbe's limit restricts every optical imaging system. This limit is represented as:

$$Abbe'sLimit :\Rightarrow d = \frac{\lambda}{2nsin\theta}$$

where d is the lateral resolution, λ is the wavelength, and n is the refractive index. To understand how to improve upon Abbe's limit one must first understand evanescent waves that carry the high spatial frequency component of a sub-wavelength object.

As illustrated in Figure (2.1) the purple circle represents $k_{||} = k_0$ where $k_0 = \frac{\omega^2}{c^2}$, where ω is the frequency of light and c is the speed of light in a vacuum. $k_{||} = \sqrt{k_x^2 + k_y^2}$, denotes the magnitude of the spatial frequency. Without losing generality, we can assume $k_y = 0$. Accordingly, $k_z = \sqrt{k_0^2 - k_{||}^2}$ is the propagation vector in the direction of wave propagation. When $k_{||} < k_0$, k_z is a real number and the plane waves are propagating.
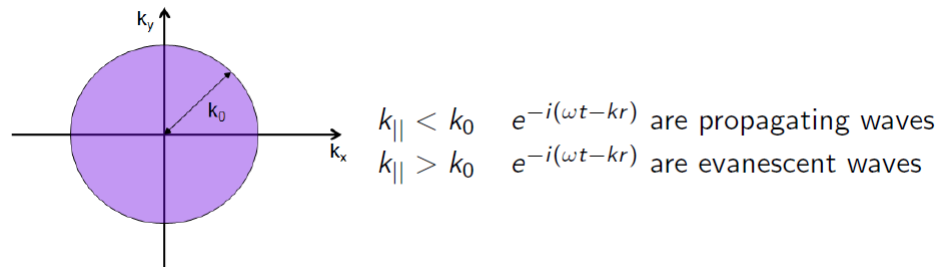
Figure 2.1: Propagating v. Evanescent Waves

Sub-wavelength objects generate higher spatial frequency components where $k_{||} > k_0$. For such cases, k_z is an imaginary number and the plane waves are decaying exponentially in the direction of wave propagation. These fast decaying plane waves are referred to as evanescent waves. Evanescent waves carry high spatial frequency information that is responsible for small feature sizes below the Abbe limit. To break the diffraction limit and achieve super-resolution the high spatial frequency component carried by these evanescent waves must be sustained and transported to the image plane.

Evanescent waves can also be formed at the boundary between two media with different wave motion properties. More specifically evanescent waves are formed when waves travelling in a medium are subject to total internal reflection at its boundary. The waves undergo total internal reflection because they strike the interface at an angle greater than the "critical angle". Evanescent waves exist because the electric and magnetic fields cannot be discontinuous at a boundary (interface between two media), as they would be if there were no evanescent wave field. For our experimentation the evanescent waves which we hope to image are generated on scattering from sub-wavelength scale structures.

2.2   Established Far-field Super-resolution Imaging Methods

The research field of super-resolution imaging is an exciting and rapidly growing area of study. Already in existence are several techniques that are able to improve spatial resolution of optical imaging systems beyond the Abbe diffraction limit. These techniques do so by retaining the spatial information contained in evanescent waves. Several such techniques are highlighted in [4]. One set of approaches utilizes non-linear optics (e.g. coherent anti-Stokes scattering or saturable fluorescence transitions). Coherent anti-Stokes Raman scattering (CARS) is a multi-photon microscopy that was put forward as an alternative way of providing vibrational contrast. [5] In CARS spectroscopy a pump laser and a Stokes laser beam, with center frequencies of V_p and V_s are spatially overlapped. High peak powers are necessary for the efficient generation of a CARS signal. This is also similar in other non-linear optical processes. [5] The widespread availability of these methods are limited due to the complexity and expensive nature of non-linear optics. The deficiencies of CARS and other non-linear optical processes may be overcome by the emergence of meta-materials-based devices. [4]

Another established method that breaks Abbe's limit is Structured Illumination Microscopy (SIM). The resolution of optical microscopes is limited by the diffraction nature of light and equates to approximately 200nm for point objects imaged with green light and high numerical aperture objectives. [6] One method that breaks the resolution limit of microscopes is called harmonic excitation light microscopy. 2D structured illumination produced by four interfering laser beams increases the resolution by a factor of 2 to reach 100nm. [6] Structure illumination enhances the resolution since spatial frequencies beyond the cut-off frequency are brought into the passband of the optical microscope, by using frequency mixing. [6] This clearly suggests that present methods of SIM only provide a linear improvement factor of approximately 2.

During the previous two decades fluorescence microscopy has become an experimental tool in modern biology. The fluorescence microscope operates through the use of multiple fluorescence labelling. Although the detection of fluorescing molecules below the diffraction limit has been achieved, the fluorescence microscope cannot provide spatial resolution below the diffraction limit of specific features.

Meta-materials, that is materials that derive their properties from structure more than their composition often possess special properties that are not easily available with naturally occurring materials. One special type of meta-materials is negative refractive index materials (NIM). These meta-materials are often referred to as left-handed media, that is media with simultaneously negative dielectric permittivity and magnetic permeability. The main potential application of the left-handed media(LHM) is found in super-resolution research. While in the near field, left hand media may show super-resolution capabilities, but due to losses, the super-lens cannot sustain sub-wavelength resolution at a focal distance which is large when compared to wavelength [7]. Previous experiments involving meta-materials indicate exponential sensitivity to losses. Podolskiy and Narimanov pointed out that the implementation of a super-lens made from LHM could lead to an advance in imaging, sensing, fabrication, communications, and related areas, while the underlying physics has initiated a lot of controversy [7]. The theory on which these devices operate hinges on the recovering of the evanescent waves and the concomitant information about the object's fine structure. Pendry maintains that a slab of negative index material (NIM) with n = -1 can amplify all evanescent waves, and therefore, is capable of perfect imaging [3]. However, there is a self-inconsistency in Pendry's theory of the perfect lens and the subsequent experimental verification of Pendry's theory is based on a different mechanism of evanescent wave transport, namely surface plasmon resonant coupling which does not result in evanescent wave amplification [8]. Regardless of this

controversy our theory of super-resolution imaging based on optical gain assisted evanescent wave conversion was inspired by Pendry's work.

All of the mentioned "super-resolution" methods leave something to be desired. The established methods can be difficult to implement, and the underlying physics of some methods have initiated a lot of controversy. These methods also only allow for a limited linear amount of improvement. Thus, a new method to achieve super-resolution is extremely desirable in optics.

2.3   Principles of Proposed Research

The principles of our proposed research begin by showing that, when the imaginary parts of a medium's permittivity $\varepsilon = \varepsilon' + j\varepsilon''$ and permeability $\mu = \mu' + j\mu''$ are not zero (correlating to a gain or loss), all evanescent waves will be converted into non-uniform plane waves in the medium at an interface between air and the medium. For a lossy medium, all evanescent waves in air will become decaying non-uniform propagating waves in the medium. In gain media, however, the non-uniform propagating waves will grow due to the optical gain. To fully understand the theory one needs to investigate the difference between uniform and non-uniform propagating plane waves. The equal amplitude and phase planes of a uniform propagating plane wave are parallel to one another. This means that the energy and direction of the wave propagation are both heading in the same direction, allowing the wave to propagate. In an evanescent wave the equal phase planes and equal amplitude planes are perpendicular to one another. The evanescent wave still contains energy, but this energy is not in its direction of travel and therefore will not propagate. A non-uniform propagating wave is somewhere between a uniform propagating plane wave and an evanescent wave. For non-uniform propagating plane waves, the equal phase and equal amplitude planes will differ by some degree between $0°$ and $90°$, illustrated in Figure

(2.2).
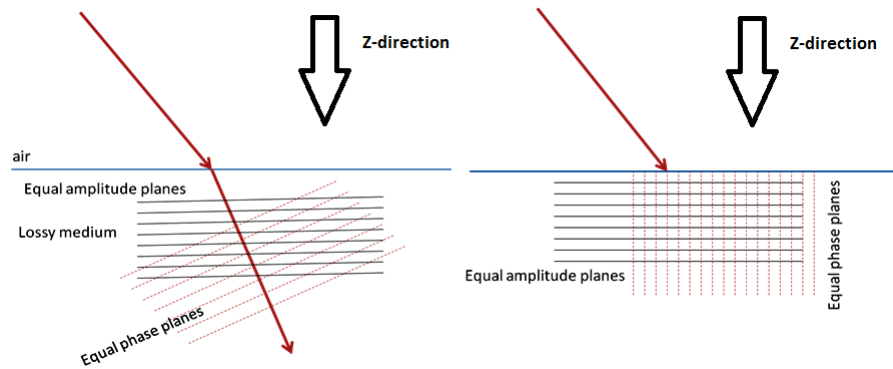
Figure 2.2: Non-uniform Plane Waves

In Figure (2.2) the non-uniform plane propagating plane wave is shown on the left. As you can see, the equal phase and equal amplitude planes differ by some degree between $0°$ and $90°$, after the interface between air and the lossy medium. This will be similar in a gain medium. The difference will be that in a lossy medium the non-uniform propagating plane waves will be decaying and in a gain medium the non-uniform propagating plane waves will be growing. The evanescent wave is shown in the right picture in Figure (2.2). This picture helps to illustrate why the evanescent wave cannot propagate without conversion. The equal amplitude and equal phase planes are perpendicular to one another. The technique by which evanescent waves are converted into non-uniform propagating waves is explained mathematically below.

From the Wave Equation:

$$\bigtriangledown^2 E + \omega^2 \mu \varepsilon E = 0 \tag{2.1}$$

where

$$E = e^{-jk\hat{r}}(PlaneWave) \tag{2.2}$$

and

$$k'^2 = \omega^2 \mu_2 \varepsilon_2 \mu_0 \varepsilon_0 \tag{2.3}$$

as well as

$$k'^2 = k_x'^2 + k_y'^2 + k_z'^2 \tag{2.4}$$

Without losing generality, assume

$$k_y = k_y' = 0 \tag{2.5}$$

one has

$$k_z'^2 + k_x'^2 = \omega^2 \mu_2 \varepsilon_2 \mu_0 \varepsilon_0 \tag{2.6}$$

where $'$ indicates these are directional components inside the medium

Since

$$\mu \varepsilon = \mu_2 \mu_0 \varepsilon_2 \varepsilon_0 \tag{2.7}$$

therefore,

$$k_z'^2 + k_x'^2 = \omega^2 \mu_2 \mu_0 \varepsilon_2 \varepsilon_0 \tag{2.8}$$

where

$$\mu_2 \varepsilon_2 = (\varepsilon' + j\varepsilon'')(\mu' + j\mu'') \tag{2.9}$$

(in equation (2.9) the ' and '' refer to the real and imaginary parts of μ and ε), and

$$\omega^2 \mu_0 \varepsilon_0 = \frac{\omega^2}{c^2} = k_0^2 \tag{2.10}$$

$$k_x = k_x' \tag{2.11}$$

which can be recognized as snell's refraction law.

This produces

$$k_z'^2 = (\mu' + j\mu'')(\varepsilon' + j\varepsilon'')k_0^2 - k_x^2 \tag{2.12}$$

So taking the real and imaginary parts of equation (2.12) you get

$$\mathscr{R}\left\{k_z'^2\right\} = (\mu'\varepsilon' - \mu''\varepsilon'')k_0^2 - k_x^2 \tag{2.13}$$

and

$$\mathscr{I}\left\{k_z'^2\right\} = (\mu'\varepsilon'' + \varepsilon'\mu'')k_0^2 \tag{2.14}$$

$$k_z' = \mathscr{R}\left\{k_z'\right\} + j\mathscr{I}\left\{k_z'\right\} \tag{2.15}$$

Going back to equation (2.15) and squaring it gives:

$$k_z'^2 = \mathscr{R}\left\{k_z'\right\}^2 + j2\mathscr{R}\left\{k_z'\right\}\mathscr{I}\left\{k_z'\right\} - \mathscr{I}\left\{k_z'\right\}^2 \tag{2.16}$$

Therefore the real part of equation (2.16) is:

$$\mathscr{R}\left\{k_z'\right\}^2 - \mathscr{I}\left\{k_z'\right\}^2 = (\mu'\varepsilon' - \mu''\varepsilon'')k_0^2 - k_x^2 \tag{2.17}$$

and the imaginary part is:

$$2\mathscr{R}\left\{k_z'\right\}\mathscr{I}\left\{k_z'\right\} = (\mu'\varepsilon'' + \varepsilon'\mu'')k_0^2 \tag{2.18}$$

Solving for the real part of k_z' gives:

$$\mathscr{R}\left\{k_z'\right\} = [\frac{1}{2}(b + \sqrt{b^2 + a^2})]^{\frac{1}{2}} \tag{2.19}$$

the imaginary part of k_z' is now given by:

$$\mathscr{I}\left\{k_z'\right\} = \frac{a}{[2(b + \sqrt{b^2 + a^2})]^{\frac{1}{2}}} \tag{2.20}$$

where

$$a = (\mu'\varepsilon'' + \varepsilon'\mu'')k_0^2 \tag{2.21}$$

and

$$b = (\mu'\varepsilon'' + \varepsilon'\mu'')k_0^2 - k_x^2 \tag{2.22}$$

An illustration is shown in Figure (2.3) which shows how the propagating waves react at an interface between air and a gain medium. From this visualization one needs to know the transmission coefficient and θ inside the gain medium.
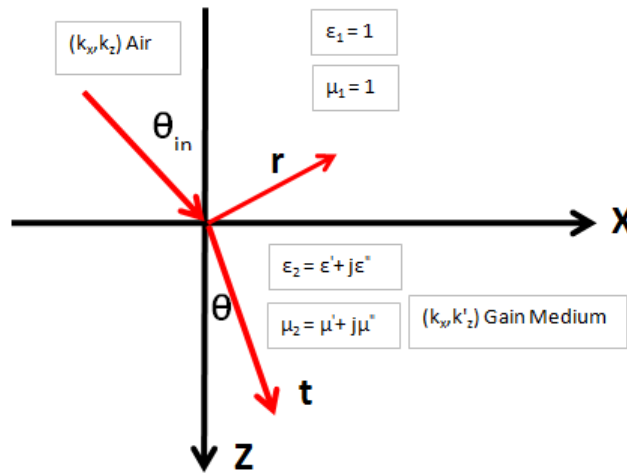
Figure 2.3: Transmitted and Reflected

In Figure (2.3) you can see that the permittivity and permeability of air are equal to 1. Inside the gain medium the permittivity and permeability are equal to $\varepsilon_2 = \varepsilon' + j\varepsilon''$ and $\mu_2 = \mu' + j\mu''$. This allows us to solve for the transmission and the refracted angle θ.

The transmission coefficient is given by: [3]

$$t' = \frac{2k_z'}{\mu k_z + k_z'} \tag{2.23}$$

and the angle θ by:

$$tan(\theta) = \frac{k_x}{\mathscr{R}\{k_z'\}} \tag{2.24}$$

The transmission coefficient t, and the angle θ are vital in characterizing the spatial performance of an optical system. These variables are used together in a spatial frequency domain transfer function. This function is discussed further in the following chapter. For $\varepsilon'' \neq 0$ or $\mu'' \neq 0$, one has $\mathscr{R}\left\{k_z'\right\} \mathscr{I}\left\{k_z'\right\} \neq 0$. Thus equation (2.18) implies that in general neither the real nor the imaginary part of k_z' is zero after refraction at the interface. Due to the resulting non-zero real and imaginary parts of k_z', all evanescent waves will now be transformed into non-uniform propagating waves inside the medium. For the majority of normal dielectrics at optical frequencies i.e, $\varepsilon' > 1, \mu' = 1, \mu'' = 0$, and (2.18) simplifies to, $2\mathscr{R}\left\{k_z'\right\} \mathscr{I}\left\{k_z'\right\} = \varepsilon'' \frac{\omega^2}{c^2}$ For passive dielectrics, $\varepsilon'' < 0$ and $\mathscr{I}(k_z') < 0$, and the non-uniform propagating waves are decaying waves. On the other hand, in a gain medium, $\varepsilon'' > 0$ and $\mathscr{I}(k_z') > 0$, and the non-uniform propagating waves grow in the z direction. The remaining sustainable propagating waves, which are converted from evanescent waves, can keep the high spatial frequency information about an object into the far field, providing the opportunity for far-field sub-diffraction-limited imaging and more specifically, sub-wavelength imaging. In principle, due to the fact that all evanescent waves excited by an object can be converted into the sustainable propagating waves with the assistance of optical gain, then perfect imaging in the far field is also possible.

2.3.1 Spatial Frequency Domain Transfer Function

Abbe's limit arises from the fact that propagating waves able to reach the far-field plane have a limited range of spatial frequencies. This is described by a Spatial Frequency Domain Function (SFTF). For spatial frequencies where $k_{||} < k_0$, the plane waves represented by (k_x, k_y) are propagating waves and for spatial frequencies where $k_{||} > k_0$, the plane waves represented by (k_x, k_y) are evanescent waves as k_z will be imaginary and the

waves can never reach the far field. In the case of the interface of a gain medium the SFTF will be defined as:

$$SFTF(k_x) = t cos\theta G^{1/2} e^{j\mathscr{R}(k_z')l} \qquad (2.25)$$

where G is the gain, t is the transmission coefficient, $cos\theta$ is proportional to the cross-sectional area and l is a desired distance inside the gain medium. The transmission coefficient t was previously defined in Equation (2.23). The refracted angle θ in the SFTF was also defined previously in Equation (2.24). The theta can be more thoroughly explained in Figure (2.4).
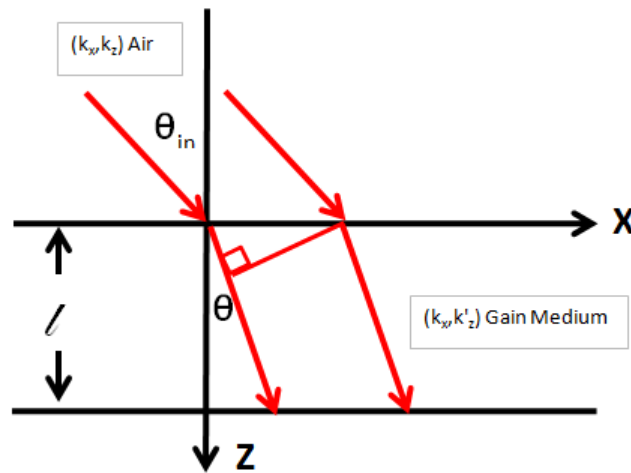
Figure 2.4: Cross-sectional Area

The l term in the exponential of the SFTF is a distance inside the gain medium shown in Figure (2.4. This figure also shows the importance of determining the θ of the transmitted portion of the beam. To determine the SFTF one must know the spatial information which can be characterized by the cross sectional area determined by θ. The retention of spatial information is the goal of evanescent wave conversion, and the SFTF allows for a method to simulate the anticipated results. Figure (2.5) gives the simulated results of the SFTF.
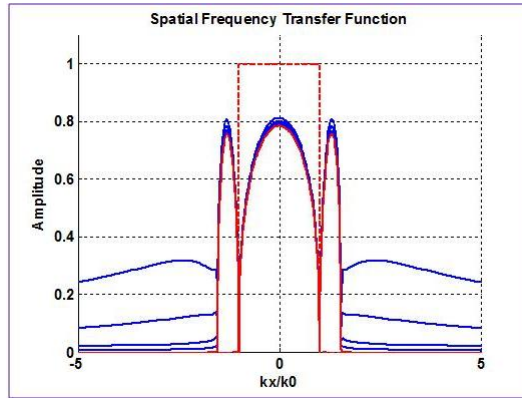
Figure 2.5: Spatial Frequency Transfer Function

In Figure (2.5) the red dashed square curve shows Abbe's limit of optical imaging. Without super-resolution, any spatial frequency content outside of the square window is lost. As one can see from the other transfer functions given for different optical gain levels shown by the different amplitudes, more of these high spatial frequencies are sustained. The gain levels for this simulation were realistic material gain coefficients ($< \frac{13}{mm}$ for 500 nm light). Also a Sub-Diffraction-Limit Point Spread Function can be gathered from the Spatial Frequency Domain Transfer Function. This point spread function is the 2-D inverse Fourier transform of the spatial frequency transfer function given by:

$$PSF(x,y) = \int_{\infty}^{\infty} \int_{\infty}^{\infty} SPSF(k_x,k_y)e^{j(k_x x + k_y y)} dk_x dk_y \qquad (2.26)$$

Figure (2.6) shows the point spread function given by Equation (2.26). Each different line in the point spread function plot represents different gain levels alongside of Abbe's limit.
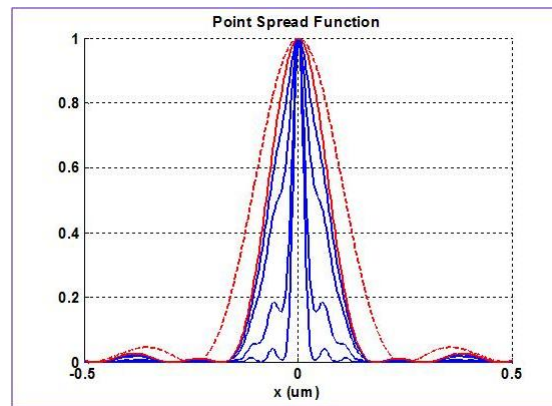
Figure 2.6: Point Spread Function

In Figure (2.6) the plot shows different gain levels with Abbe's limit. The narrower the point spread the better the resolution. The dashed red curve shows the resolution as dictated by Abbe's limit. The simulations show that using our method at various gain levels can surpass Abbe's diffraction limit. The units of the x-axis of Figure (2.6) are given in micro-meters. Thus theoretically the higher gain that is applied to the proposed system the narrower the point spread, and the more resolute the system.

CHAPTER 3: DESIGN PROCEDURE

The purpose of this thesis is to design an optical assembly capable of giving indications to whether or not our theory of evanescent wave conversion is correct. In our case the method of converting evanescent waves into non-uniform propagating waves will be by using an active objective lens. This lens will be illuminated with a signal laser and pumped with another laser. The pumping of the lens should provide some difference in spatial frequency information. This information will be examined by the comparison of two specific images. One image with the presence of pumping, and the other with the absence of pumping. This chapter discusses how this task was completed.

3.1   System Layout

In the design phase of the optical assembly several critical factors were defined. The first being the reproducibility needed so that the comparison of different images would be valid. This meant that the lens and pump laser needed to remain stable between different set-ups. The second factor that was deemed vital was the ability to make several fine adjustments, such as the changing of the incident angle of the pump beam. Figure(3.1) is a rough drawing that was made during the designing of the optical assembly. In this drawing all elements that were used are shown except for the tilt table. The mounting plate shown that the Ti:Sapphire lens is mounted to in the drawing, was later replaced with the tilt table. An optical assembly like the one in the drawing would allow for certain adjustments that should be made. This drawing demonstrates the aforementioned critical factors.
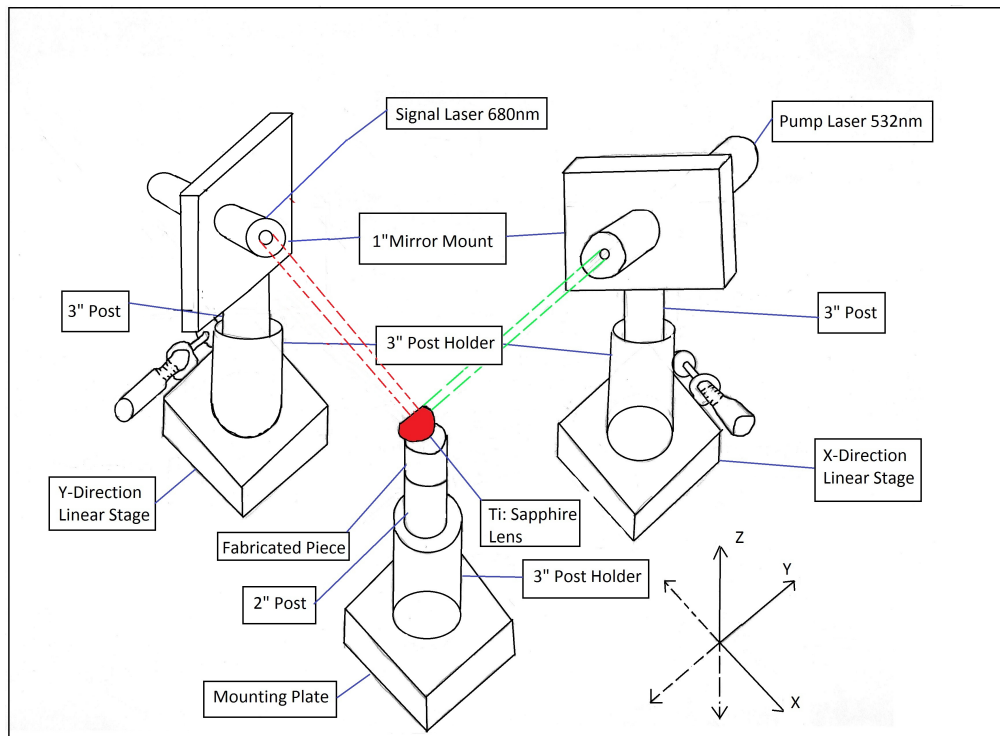
Figure 3.1: Optical Assembly Drawing

Both lasers were mounted into adapters manufactured by the mechanical track graduate students. These adapters were then mounted into mirror mounts, that have the ability to change the angle of the lasers in two different planes i.e.(xy plane, yz plane as illustrated in Figure(3.1)). The mirror mounts were attached to posts which were attached to linear transitions stages. The linear transition stage allows you to move the whole laser assembly back and forth in one dimension precisely. This ability to move the entire laser also allowed for the fine tuning of the lasers angle and position. The active objective lens proved to be a little more difficult to mount. One axis had to be sacrificed to mount the lens. The idea was to mount an additional piece to a post and adhere the lens to this piece. Originally the lens was adhered to a polymer piece that was somewhat translucent. This proved to ineffective because the polymer piece was absorbing some of the light and radi-

ating out affecting the images that were being taken. The solution was to put a small screw in the post and adhere the lens into the small dent in the end of the screw (like a golf ball and tee). The post and lens were then mounted to a tilt table. An image taken from above the system can be seen in Figure 3.2 showing the overall layout of the optical assembly.
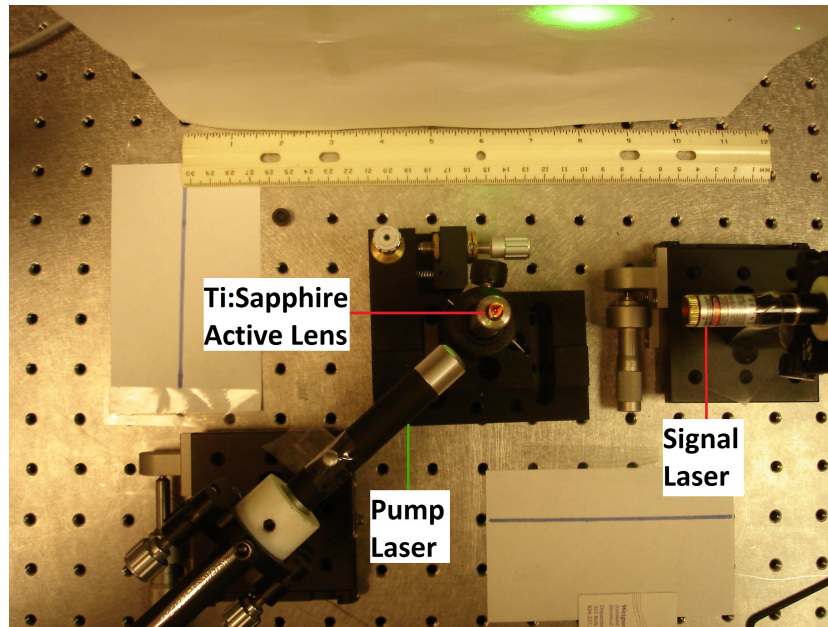
Figure 3.2: Optical Assembly Image

As can be seen, the majority of the items shown in the original design drawing made it to the final design. The pump laser is at a more appropriate angle in Figure (3.2) rather than the angle indicated by Figure(3.1). The ruler shown in the figure was used to determine approximate angle and distance measurements. The next few sections will go into more specific detail regarding the lens and lasers used in the optical assembly.

3.2 Active Objective Lens Assembly

An objective lens is an optical element which focuses light rays after collecting these rays from an object to be imaged. The active objective lens will come into contact with the small object to be imaged. This object needs to be present for the production of evanescent waves. The active objective lens will collect all the evanescent waves that have been converted into sustainable propagating waves, allowing for the retention of the information contained in high spatial frequencies. As can be seen from Figure (3.3) for the objective lens to function properly a signal laser and pump laser are needed. This pump laser is needed to amplify the evanescent waves created at the facet of the lens, allowing for the conversion into non-uniform propagating plane waves.
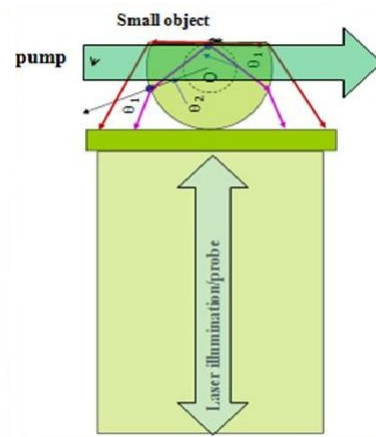
Figure 3.3: Active objective lens assembly

For our experimental set-up the additional lenses used for re-imaging were not implemented as given in Figure (3.3). The geometrical dimensions of the objective lens can be seen in Figure (3.4). The Ti:Sapphire lens that was implemented in the experiment has properties which make it useful for this purpose. The highest spatial frequency propagation wave that will exist parallel to the facet of the lens will be refracted as shown by the red arrows in Figure (3.4). Therefore, all propagating waves will be contained in the

propagation cone shown. Any spatial information that can be gathered outside this cone must be attributed to the conversion of evanescent waves into non-uniform propagating waves. This lens is constructed in a geometry which gives it specific properties conducive to applying optical gain and retaining converted evanescent waves. The distance from the face to the center of the lens is designed to be $d = \frac{r}{n}$, where d is the distance from face to center, r is the radius of the ball lens, and n is the index of refraction. For Ti:Sapphire crystal $n = 1.76$ so that for this lens $d = \frac{2.5mm}{1.76} = 1.42mm$.
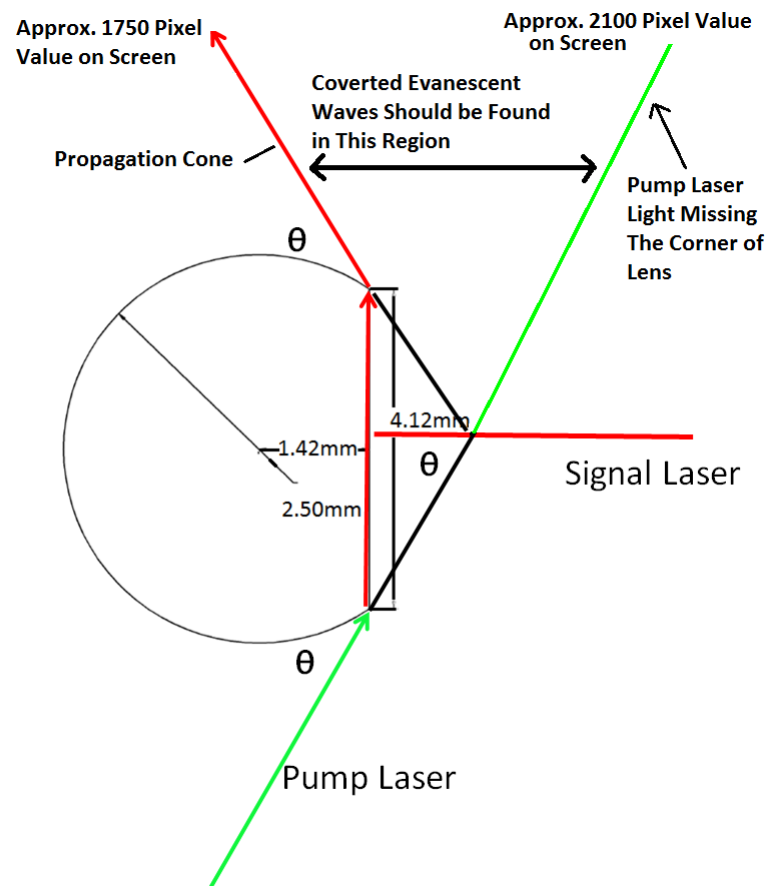
Figure 3.4: Lens Geometry

From Figure (3.4) the conditions which are ideal for evanescent wave conversion can be derived. More specifically the angle which the pump laser should be incident with

the tangent point of the lens can be derived.

$$r^2 = \sqrt{x^2 + \left(\frac{r}{n}\right)^2} \tag{3.1}$$

$$x = r\sqrt{1 - \left(\frac{1}{n^2}\right)} \tag{3.2}$$

$$\tan(\theta) = \frac{1}{\sqrt{n^2 - 1}} \tag{3.3}$$

$$\theta = 34.62° \tag{3.4}$$

The actual lens that was used for all of the experimentation is shown in Figure (3.5) mounted in the golf ball and tee fashion.

Figure 3.5: Actual Ti:Sapphire Lens

The manufacturer's specification for the Titanium Doped Sapphire lens shown in Figure (3.5), are given in Table (3.1).

Table 3.1: Specifications for Ti:Sapphire Active Objective Lens

Spec.		Spec.	
Ti_2O_3 concentration	0.06-0.5 wt%	Figure of Merit	100-300
Diameter	5mm	End configuration	flat/flat or Brewster/Brewster ends or custom specified
Orientation	Optical axis C normal to rod axis	α_{490}	1.0-7.5cm^{-1}
Flatness	$\frac{\lambda}{10}$ @633nm	Parallelism	10 arcsec
Surface Quality	10/5 scratch/dig	Wavefront distortion	4 per inch
Chemical formula	$Ti^{3+}:Al_2O_3$	Crystal structure	Hexagonal
Laser action	4-Level Vibronic	Fluorescence lifetime	$3.2\mu sec(T=300K)$
Tuning range	660-1050 nm	Absorption range	400-600 nm
Emission peak	795 nm	Absorption peak	488 nm
Refractive index	1.76 @ 800 nm		

For our experimentation it was assumed that the surface roughness of the Ti:sapphire lens, as given in Table (3.1), provides a sub-wavelength scaled object that would be capable of generating high spatial frequencies.

3.3   Signal and Pump Lasers

The pump laser is a 532nm 200mW laser that will amplify a signal wavelength provided by the signal laser of 680nm. The pump laser beam should be incident to a tangent point which is flush with the face of the objective lens. A rough estimate of this angle was determined to allow a starting point for experimentation. This was previously defined in Equations 3.1 through 3.4. This angle proved to be a general approximation. This is most likely due to the tolerance in the cut of the Ti:Sapphire lens. The angle was determined using ideal theoretical conditions, and it is likely that the geometry of the lens was not ideal. The signal laser was easier to align. The position of the signal laser was not as critical because the purpose of the signal laser was only to radiate inside the lens. When pumping a titanium doped sapphire lens with a 532 nm laser you will be able to amplify only the light which is at 680 nm. Thus the purpose of the signal laser. Figure (3.2) shows the set-up that was used for the proof-of-concept experimentations.

3.4 Data Retrieval

As stated, the objective of this thesis is to produce an optical assembly that can be used in proof-of-concept experiments. These experiments will be used to test our theory of optical gain assisted evanescent wave conversion. Therefore data needs to be captured to determine whether or not additional high frequency spatial information is retained. To obtain this information a digital camera was used to capture images of the light scattering from the objective lens. The experimentation process began by establishing what control factors would be varied while testing. Two control factors were established. The first was the angle that the pump laser was incident with the objective lens. The second control factor was the polarization of the signal laser. The pump angle was varied by using the linear transition stage, as well as, the mirror mount to make small, but distinguishable changes. There were four pump positions that were processed. The signal polarization was changed by rotating the signal laser. There were four signal polarizations that were tested. One being at at $0°$ and one at $90°$ and two polarizations in between 0 and 90. Images were taken at twelve different set-ups. Those twelve set-ups were four different signal polarizations for each of the three different pump beam angles. For each set-up a principal experimental data retrieval order was established. Six different images were to be recorded. The first was captured from above with both lasers and the room light on to observe what the pump beam angle was for the specific arrangement. The next image was taken with both lasers and the room light on from the stationary platform where the rest of the images were captured. The direction that the images were observed was chosen for several reasons. One reason being that one would expect if any evanescent waves were to be converted they would propagate towards a line parallel to the facet of the lens. This camera position was also chosen for the more obvious reasons so that you could have enough elevation to view the screen beyond the objective lens. Very much care was taken

to try and ensure that all the images were captured from the same position. The third image was captured at the normal camera platform with the room light off, both lasers on, and no filter. Next, was the exact same image as the previous but using the green filter. The fifth image was captured with the room light off, the signal laser only on, and with the green filter. Last was a filtered image and the only laser on was the pump laser. This image order for pump position A signal polarization A are inventoried in Table 3.2, the same image order was used for all other set-ups.

Table 3.2: Principal Data Retrieval Order

Pump Angle	A	Signal Polarization	A	
Room Light	Camera Location	Pump Laser	Signal Laser	Filter
On	Above	On	On	Off
On	Normal	On	On	Off
Off	Normal	On	On	Off
Off	Normal	On	On	On
Off	Normal	Off	On	On
Off	Normal	On	Off	On

This proved to be more difficult than originally anticipated. Due to the intense green light emitted from the pump laser, the camera was being saturated. This saturation was shown in the images as white light. Which in this situation proves to be highly problematic. White light is a combination of all of the colors in the color spectrum. To really determine whether any of the red evanescent waves had been retained the images were processed in Matlab using the imread function. When the green light was saturating the camera, an intense white spot was present in the center of the light from the pump beam. After separating the wavelengths with the RGB function this white spot contained red wavelengths which may not have been there. I researched several different camera modes to try to minimize this saturation. I implemented a camera mode which lessened the color intensity of the entire image. I also used a filter which eliminated the majority of the green light. Figures 3.6a and 3.6b show an example of the images before and after the

filter, and Figure (3.7) shows the optical density vs wavelength of the filter.
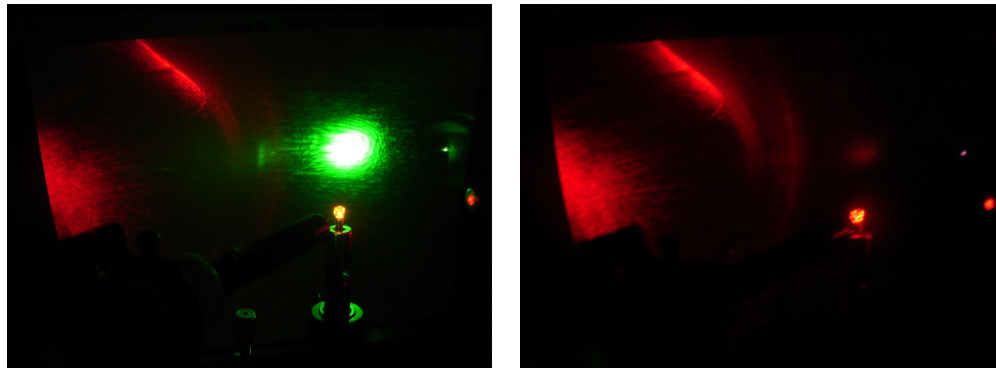
(a) Image Before Filter   (b) Image After Filter

Figure 3.6: Effects of Green Filter
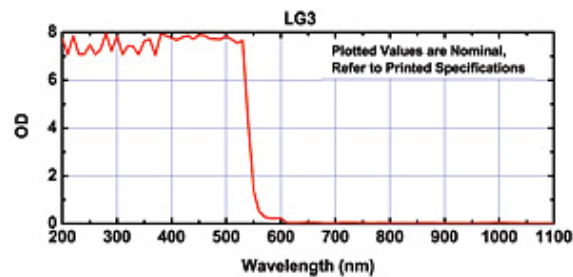
Figure 3.7: Optical Density vs Wavelength of Filter

By varying the pump beam angle we produce a very interesting comparison. This comparison derives from the fact that there exists an ideal situation that is required for our theory of evanescent wave conversion to completely work. Ideally all evanescent waves produced at the surface of the objective lens can be converted by using a gain medium. This will happen if the evanescent waves along the facet of the Ti:Sapphire lens are amplified. For these waves to be amplified the pump laser will have to refract parallel to the facet. Due to the geometry of the objective lens used in our experimentation this will happen

when the pump beam is tangent to the corner of the facet. In this ideal case the output angle of the propagating waves due to the pump beam will exit the lens at the same angle that the pump beam enters the lens. This ideal case is exemplified with pump angle A. The two set-ups that allowed for the greatest comparisons were pump angle A, and pump angle C. The reason that these set-ups allowed for the greatest comparisons were because of the intensity of the light due to the pump laser was similar in both, and the images were taken at virtually the same position (there was minimal shift in the images due to camera stability). Set-up pump angle B had a very low intensity of light due to the pump beam. This low intensity was due to a poor input angle that did not allow for the amplification of the evanescent waves. There are several conclusions which can be made because the angle of the refracted beam is further away from the facet in pump angle C. This means that the refracted angle θ_{iC} is smaller than the θ_{iA} in pump angle A. Subsequently, using snell's law one can infer that this means the output angle in case C will be smaller than the output angle in case A. Using this knowledge one can predict how the propagating waves should react in a normal case. The propagating waves in case C should be closer to a line parallel to the facet than the propagating waves in case A. This indicates that without any evanescent wave conversion you should expect to see more light close to the line parallel to the facet in case C rather than in case A. This is illustrated in Figure (3.8).

At this point in the experimentation process I now had a way to indicate the possibility of whether or not any evanescent waves had been converted. The comparison would be between the ideal case and non-ideal case. In the ideal scenario of pump angle A evanescent waves in theory could be converted into propagating waves. In the non-ideal case like pump angle C, there will be no increased amplitude spatial frequency components other than propagating waves. Accordingly, if pump angle A outperformed pump angle C, in terms of the intensities of light at or past a line parallel to the facet, we have
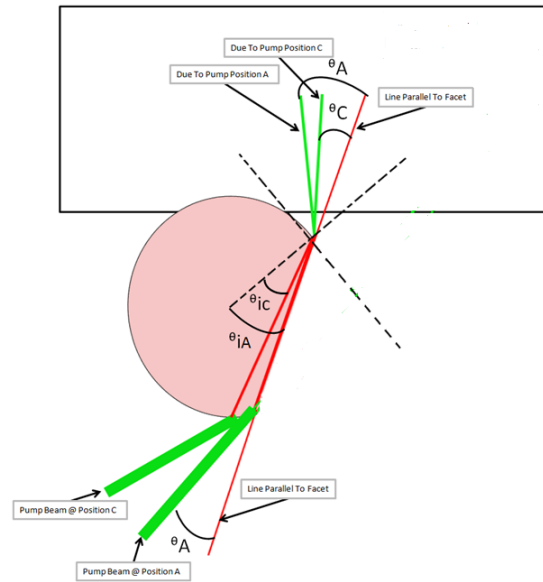
Figure 3.8: Angle Comparisons

a positive indication that increased amplitude spatial frequency components have resulted from the gain assisted evanescent wave conversion. These indications would derive from the fact that in order to outperform pump angle C, pump angle A would need additional spatial information not present in the original propagating waves. If the evanescent waves in air had not been converted into propagating waves in the gain medium, there is no way that pump angle A could outperform pump angle C. From this a hypothesis was made. The hypothesis states that pump angle A should have more far-field spatial frequency components beyond that of pump angle C. If this hypothesis is confirmed, we can conclude that evanescent waves have been converted with the optical gain as predicated by the theory. If the hypothesis is rejected then evanescent waves have not been converted. The following section will discuss the data that was retrieved and how it tests the hypothesis.

CHAPTER 4: EXPERIMENTAL RESULTS

This chapter presents the experimental results gathered after the implementation of the optical assembly. The purpose of these results is to test the hypothesis. The hypothesis is designed so that two situations will allow for a comparison that will indicate if optical gain assisted evanescent wave conversion is being provided using the experimental optical assembly. The first situation is Pump angle A position which should provide optical gain to help to convert the evanescent waves into non-uniform propagating waves. The second situation is Pump angle C position where the optical gain path misses the interface and should not possess the ability to convert evanescent waves. The comparison of these two situations produce results which are analysed below.

During the Design Procedure section of this thesis the optical assembly design was discussed, as well as, the manner in which data would be retrieved. A principal experimental data retrieval order was implemented for several different situations. This order is illustrated in Table (3.2) and was used for three different pump angle positions A - C. The data collection order was used for each pump angle position at four different signal polarizations A-D. For each separate case (i.e. Pump angle A Signal polarization A) six images were taken as outline in Table (3.2). Each of these images are inventoried in Tables (4.1-4.3).

Table 4.1: Image Inventory Pump Angle A

Pump Angle A, Signal Polarization A						
Room Light	Camera Location	Pump Laser	Signal Laser	Filter	File Name	Saved Under
On	Above	On	On	Off	DSC02386	A and A
On	Normal	On	On	Off	DSC02389	A and A
Off	Normal	On	On	Off	DSC02390	A and A
Off	Normal	On	On	On	DSC02392	A and A
Off	Normal	Off	On	On	DSC02397	A and A
Off	Normal	On	Off	On	DSC02394	A and A
Pump Angle A, Signal Polarization B						
Room Light	Camera Location	Pump Laser	Signal Laser	Filter	File Name	Saved Under
On	Above	On	On	Off	DSC02400	A and B
On	Normal	On	On	Off	DSC02407	A and B
Off	Normal	On	On	Off	DSC02408	A and B
Off	Normal	On	On	On	DSC02410	A and B
Off	Normal	Off	On	On	DSC02414	A and B
Off	Normal	On	Off	On	DSC02413	A and B
Pump Angle A, Signal Polarization C						
Room Light	Camera Location	Pump Laser	Signal Laser	Filter	File Name	Saved Under
On	Above	On	On	Off	DSC02421	A and C
On	Normal	On	On	Off	DSC02426	A and C
Off	Normal	On	On	Off	DSC02427	A and C
Off	Normal	On	On	On	DSC02429	A and C
Off	Normal	Off	On	On	DSC02432	A and C
Off	Normal	On	Off	On	DSC02434	A and C
Pump Angle A, Signal Polarization D						
Room Light	Camera Location	Pump Laser	Signal Laser	Filter	File Name	Saved Under
On	Above	On	On	Off	DSC02439	A and D
On	Normal	On	On	Off	DSC02441	A and D
Off	Normal	On	On	Off	DSC02445	A and D
Off	Normal	On	On	On	DSC02448	A and D
Off	Normal	Off	On	On	DSC02449	A and D
Off	Normal	On	Off	On	DSC02450	A and D

Table 4.2: Image Inventory Pump Angle B

Pump Angle B, Signal Polarization A						
Room Light	Camera Location	Pump Laser	Signal Laser	Filter	File Name	Saved Under
On	Above	On	On	Off	DSC02457	B and A
On	Normal	On	On	Off	DSC02487	B and A
Off	Normal	On	On	Off	DSC02488	B and A
Off	Normal	On	On	On	DSC02489	B and A
Off	Normal	Off	On	On	DSC02490	B and A
Off	Normal	On	Off	On	DSC02491	B and A
Pump Angle B, Signal Polarization B						
Room Light	Camera Location	Pump Laser	Signal Laser	Filter	File Name	Saved Under
On	Above	On	On	Off	DSC02457	B and B
On	Normal	On	On	Off	DSC02485	B and B
Off	Normal	On	On	Off	DSC02484	B and B
Off	Normal	On	On	On	DSC02481	B and B
Off	Normal	Off	On	On	DSC02483	B and B
Off	Normal	On	Off	On	DSC02482	B and B
Pump Angle B, Signal Polarization C						
Room Light	Camera Location	Pump Laser	Signal Laser	Filter	File Name	Saved Under
On	Above	On	On	Off	DSC02457	B and C
On	Normal	On	On	Off	DSC02466	B and C
Off	Normal	On	On	Off	DSC02467	B and C
Off	Normal	On	On	On	DSC02468	B and C
Off	Normal	Off	On	On	DSC02471	B and C
Off	Normal	On	Off	On	DSC02472	B and C
Pump Angle B, Signal Polarization D						
Room Light	Camera Location	Pump Laser	Signal Laser	Filter	File Name	Saved Under
On	Above	On	On	Off	DSC02457	B and D
On	Normal	On	On	Off	DSC02459	B and D
Off	Normal	On	On	Off	DSC02461	B and D
Off	Normal	On	On	On	DSC02462	B and D
Off	Normal	Off	On	On	DSC02465	B and D
Off	Normal	On	Off	On	DSC02463	B and D

Table 4.3: Image Inventory Pump Angle C

Pump Angle C, Signal Polarization A						
Room Light	Camera Location	Pump Laser	Signal Laser	Filter	File Name	Saved Under
On	Above	On	On	Off	DSC02507	C and A
On	Normal	On	On	Off	DSC02508	C and A
Off	Normal	On	On	Off	DSC02509	C and A
Off	Normal	On	On	On	DSC02511	C and A
Off	Normal	Off	On	On	DSC02512	C and A
Off	Normal	On	Off	On	DSC02513	C and A
Pump Angle C, Signal Polarization B						
Room Light	Camera Location	Pump Laser	Signal Laser	Filter	File Name	Saved Under
On	Above	On	On	Off	DSC02507	C and B
On	Normal	On	On	Off	DSC02514	C and B
Off	Normal	On	On	Off	DSC02515	C and B
Off	Normal	On	On	On	DSC02516	C and B
Off	Normal	Off	On	On	DSC02517	C and B
Off	Normal	On	Off	On	DSC02518	C and B
Pump Angle C, Signal Polarization C						
Room Light	Camera Location	Pump Laser	Signal Laser	Filter	File Name	Saved Under
On	Above	On	On	Off	DSC02507	C and C
On	Normal	On	On	Off	DSC02520	C and C
Off	Normal	On	On	Off	DSC02522	C and C
Off	Normal	On	On	On	DSC02524	C and C
Off	Normal	Off	On	On	DSC02525	C and C
Off	Normal	On	Off	On	DSC02526	C and C
Pump Angle C, Signal Polarization D						
Room Light	Camera Location	Pump Laser	Signal Laser	Filter	File Name	Saved Under
On	Above	On	On	Off	DSC02507	C and D
On	Normal	On	On	Off	DSC02527	C and D
Off	Normal	On	On	Off	DSC02528	C and D
Off	Normal	On	On	On	DSC02530	C and D
Off	Normal	Off	On	On	DSC02532	C and D
Off	Normal	On	Off	On	DSC02531	C and D

The objective of the experimentation is to make comparisons between the two specific cases, and to verify evanescent wave conversion via optical gain. The first of these cases is Pump angle position A and is shown in Figure (4.1).

In this situation there was a visible glowing line due to the Amplified Spontaneous Emissions caused by the pumping of the lens. This glowing region is close and parallel to the facet line in case A, and is the best indication we had that gain was being applied
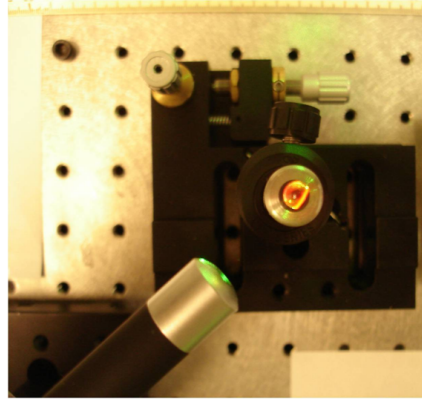
Figure 4.1: Pump Position A, Signal Polarization C

along the facet. The second case, Pump angle C position is shown in Figure (4.2) for the signal polarization C. This is the control case, and the pump angle for this case is shown in Figure (4.2). In this case the pump beam is not tangent to the corner of the lens. In fact the glowing line due to the pump beam does not shade the corner that the beam is incident with. This indicates that gain is not being applied along the facet and therefore will not convert the evanescent waves. The way that each situation should react without the conversion of evanescent waves was illustrated in Figure (3.8)
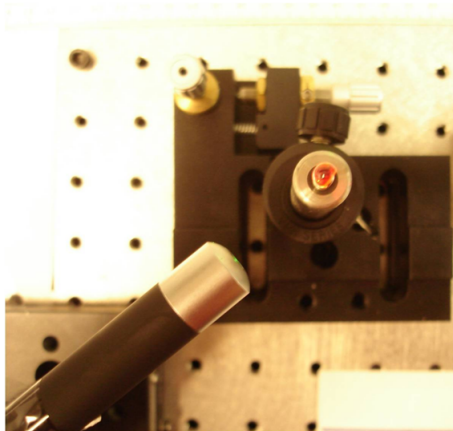

Figure 4.2: Pump Position C, Signal Polarization C

The set-up pictures for all other set-ups are available for review in the appendix. The raw data images were processed for each situation. The processing began with three different raw data images. The first of these three images was taken with only the signal laser active. The second image was taken with both the signal and pump lasers active, and the final image was taken with the pump laser only active. All of these images are shown in Figure (4.3) for Pump angle A position and Signal polarization C.

(a) Filtered Image Before Pumping   (b) Filtered Image After Pumping
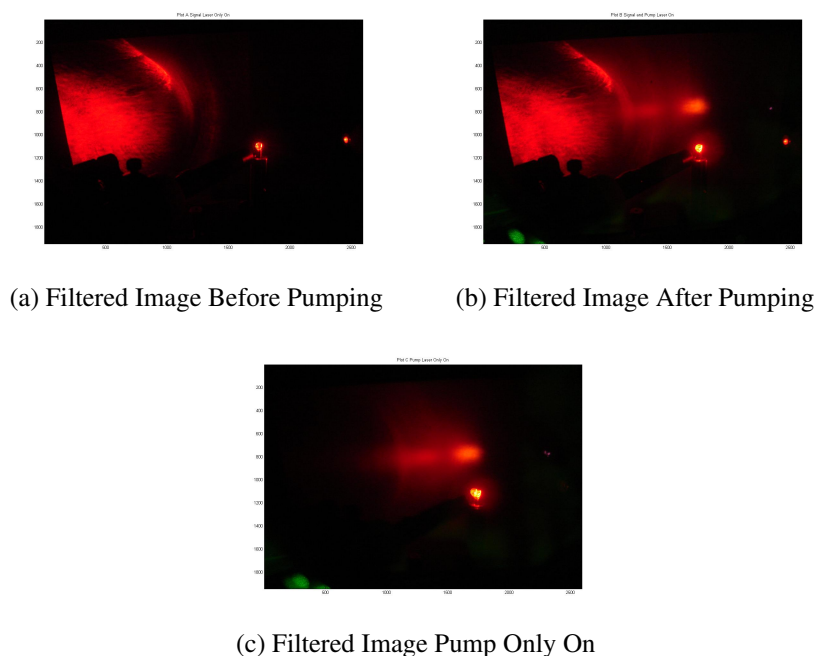

(c) Filtered Image Pump Only On

Figure 4.3: Pump Position A Signal Polarization C

Figure (4.3) shows the filtered images taken for case A and C. In Figure (4.12a) the system with only the signal laser on is shown. The image in Figure (4.12b) shows the image with both the pump and signal lasers on, and Figure (4.12c) shows the pump laser only. Each of these images were then processed to determine what the intensity of the red light was at various points in the image. The processing point at which I started for each set was at the peak intensity for each set-up. This point was chosen so that we could see how the intensity reacts the further from that point that you travel toward the facet line,

correlating to additional spatial frequencies. Figure (4.4) are the plots of the intensity at 1750 on the x-axis of the images in Figure (4.3). In Figure (4.4) Plot A is the plot of the image with only the signal laser on. Plot B is the plot of the image with both the signal and pump lasers on, and Plot C is the plot of just the pump laser on. Plots D and E are the differences due to the pump and signal lasers. Plot D is the subtraction of Plot A from Plot B. Plot E is the subtraction of Plot C from Plot B. Therefore:, Plot A=signal only, Plot B=Both, Plot C=pump only, Plot D=difference between pumped and non-pumped, Plot E=difference between signal and no signal. To clarify, the x-axis of the plot in Figure (4.4) is the y-axis at pixel 1750 along the x-axis in Figure (4.3).
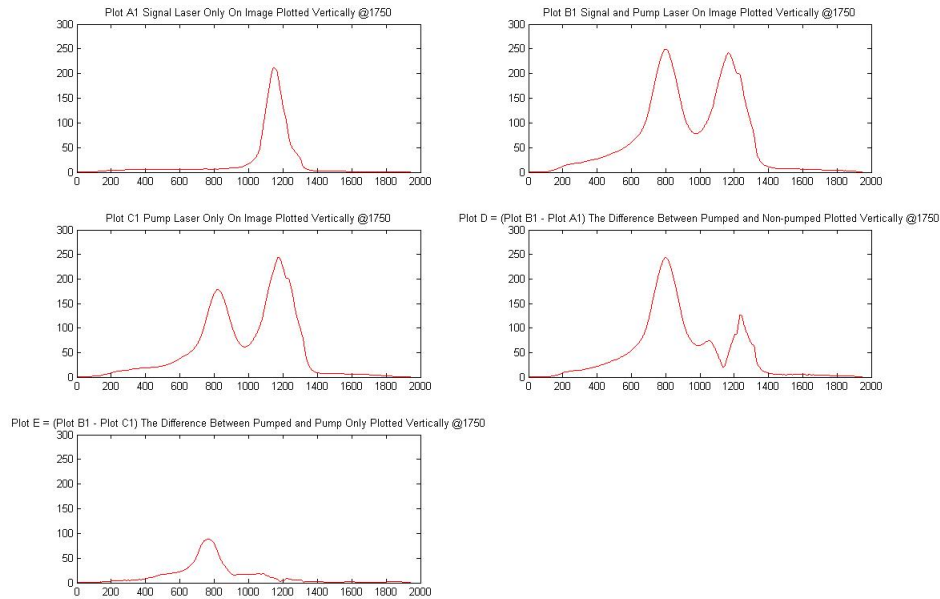

Figure 4.4: Pump Position A, Signal Polarization C at 1750

In Plot B of Figure (4.4) you will see two peaks. The first peak is the one that interests us most. The second peak is the peak due to the glowing of the Ti:Sapphire lens. Results were found in the same manner as in Figure (4.4) for points 50 pixels apart. So

therefore, results were found at 1800, 1850, 1900, ... 2100 for these images. A characterization of the drop-off of the intensity at higher spatial frequency angles can be determined from each of these different plots.
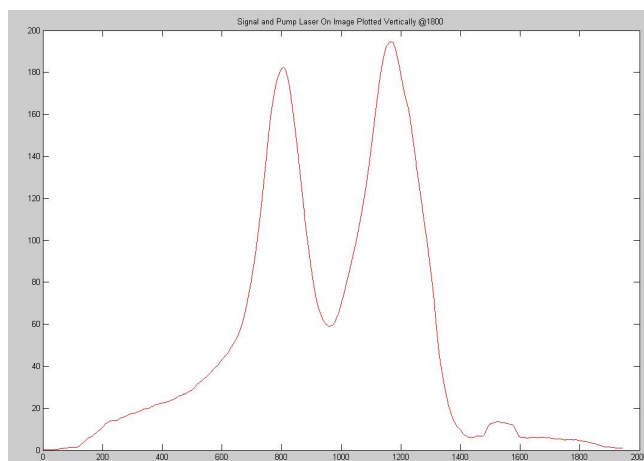

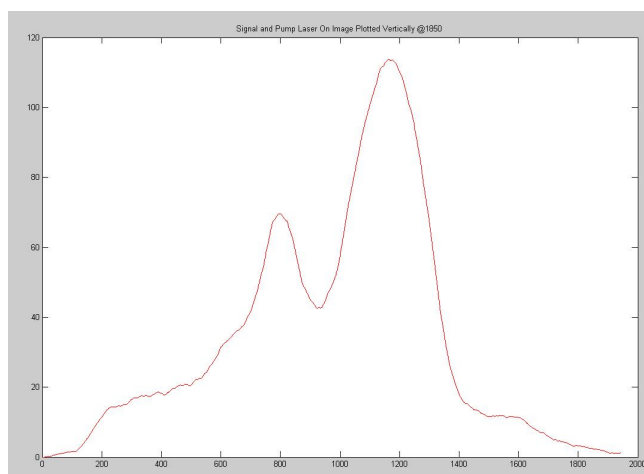Figure 4.5: Plot B1: Pump Position A, Signal Polarization C at 1800

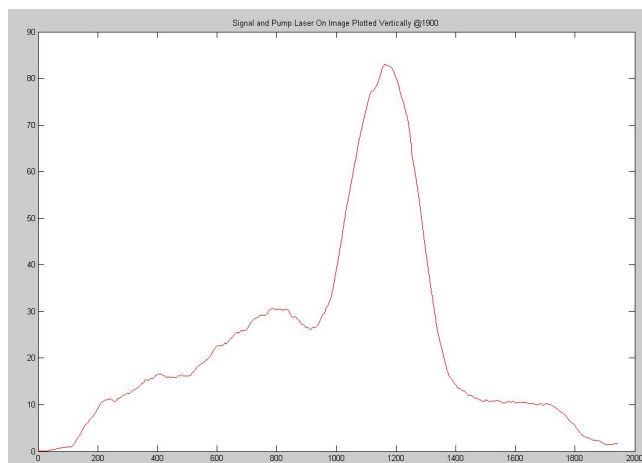Figure 4.6: Plot B1: Pump Position A, Signal Polarization C at 1850

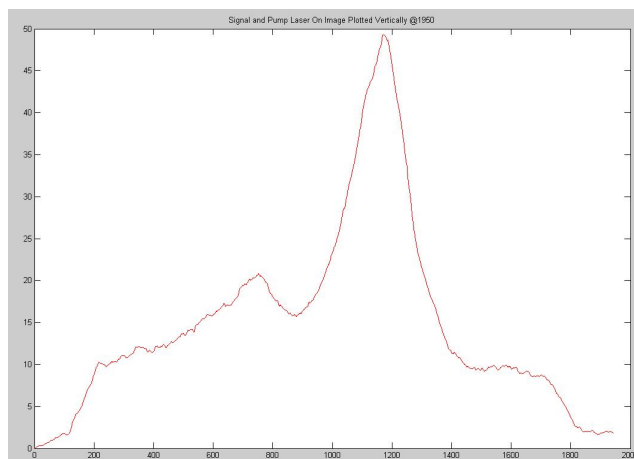Figure 4.7: Plot B1: Pump Position A, Signal Polarization C at 1900

Figure 4.8: Plot B1: Pump Position A, Signal Polarization C at 1950
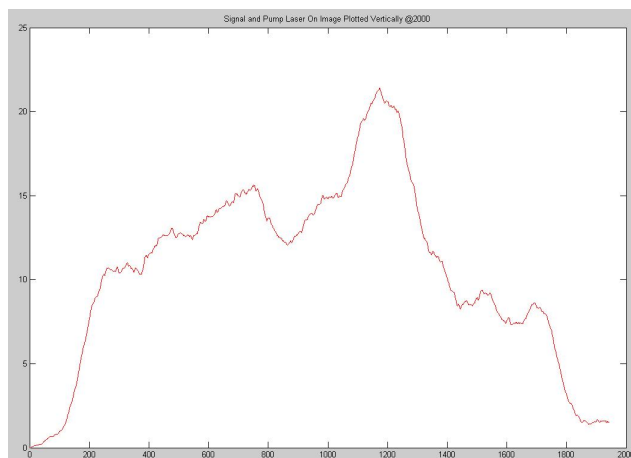
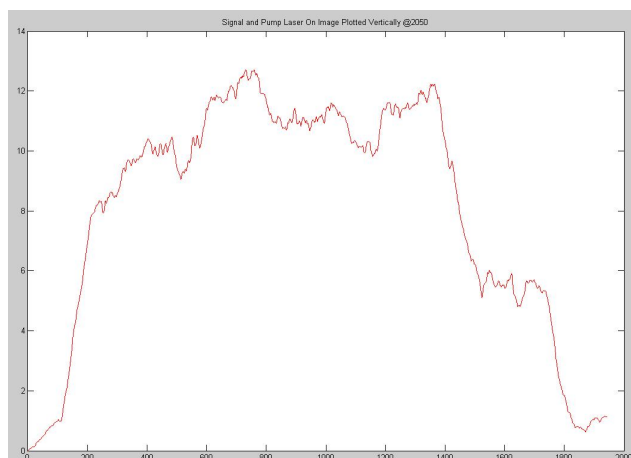Figure 4.9: Plot B1: Pump Position A, Signal Polarization C at 2000

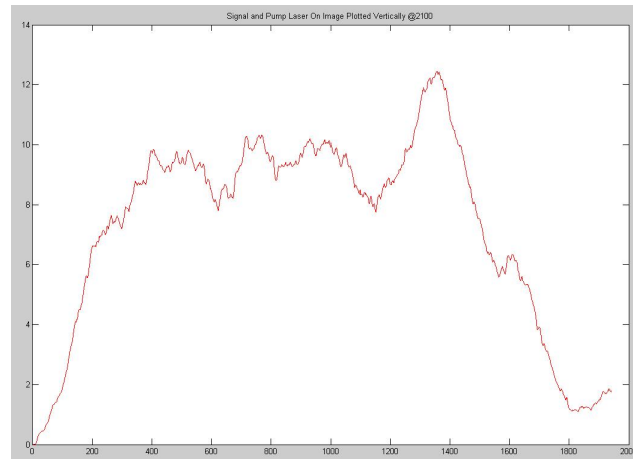Figure 4.10: Plot B1: Pump Position A, Signal Polarization C at 2050

Figure 4.11: Plot B1: Pump Position A, Signal Polarization C at 2100

As discussed earlier we want to know which case performs better. Therefore, we want to know which intensity drops to noise level first as you travel toward the facet line. At position 2000 for case A and C you can still make out what is left of the peak intensity. Knowing where the peak due to the pumping of the system dissipates will allow us to compare this to where the peak dissipates for the second case. As previously discussed the second set-up of interest is Pump angle C position set-up. The raw images for Signal polarization C of Pump angle C position, are given in Figure (4.12). Just as in case A and C results were processed at 1750, 1800, 1850, ... 2100. The results at 1750 are shown in Figure (4.13) and the results for 2000 shown in Figure (4.18).

(a) Filtered Image Before Pumping   (b) Filtered Image After Pumping

(c) Filtered Image Pump Only On

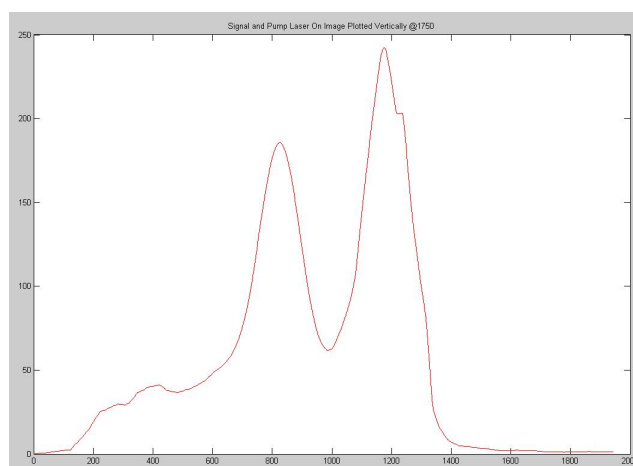Figure 4.12: Pump Position C Signal Polarization C

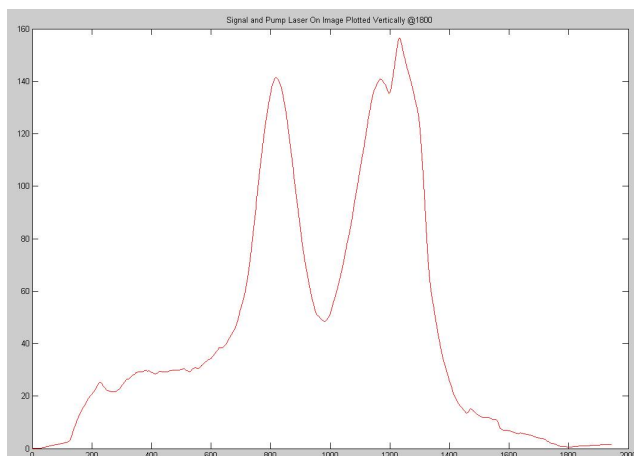Figure 4.13: Plot B1: Pump Position C, Signal Polarization C at 1750

Figure 4.14: Plot B1: Pump Position C, Signal Polarization C at 1800
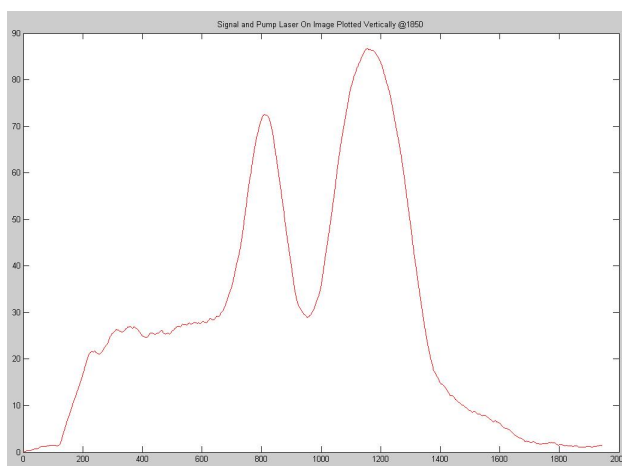

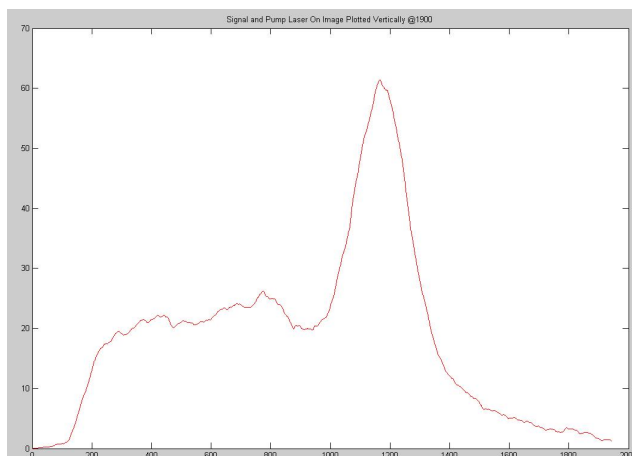Figure 4.15: Plot B1: Pump Position C, Signal Polarization C at 1850

Figure 4.16: Plot B1: Pump Position C, Signal Polarization C at 1900
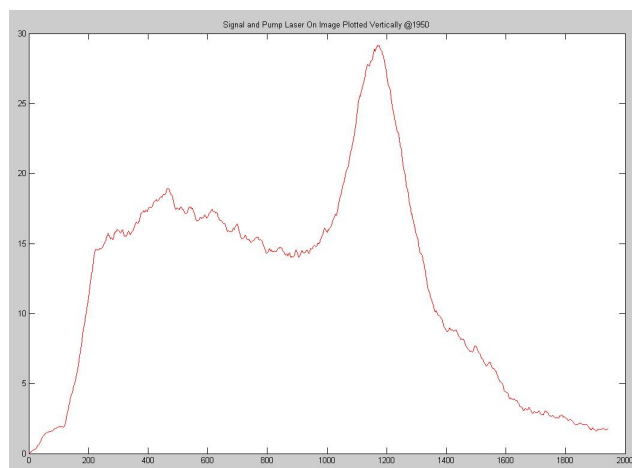

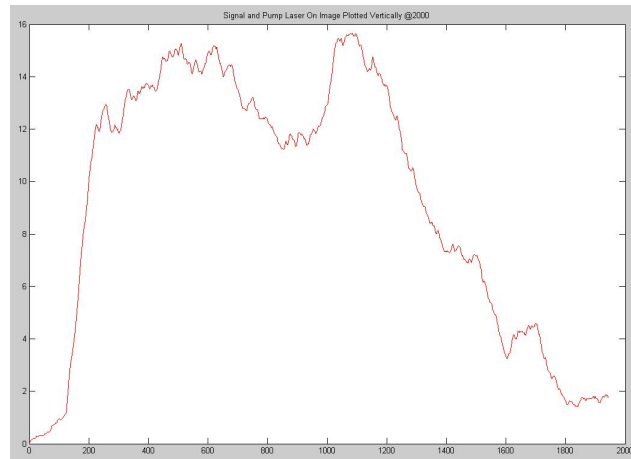Figure 4.17: Plot B1: Pump Position C, Signal Polarization C at 1950

Figure 4.18: Plot B1: Pump Position C, Signal Polarization C at 2000
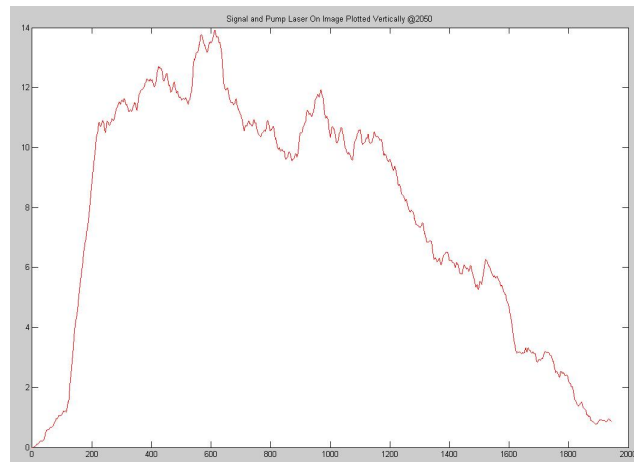

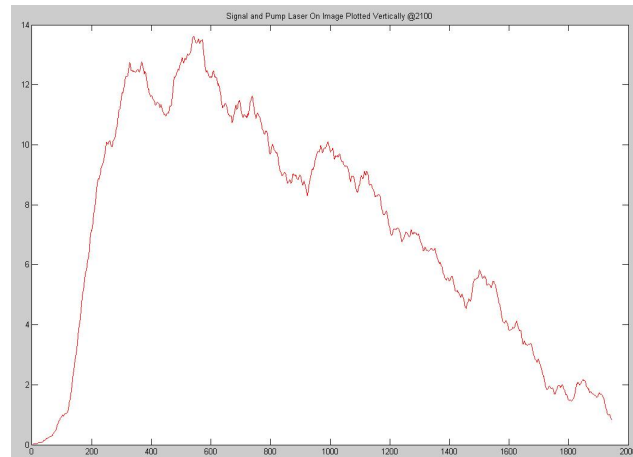Figure 4.19: Plot B1: Pump Position C, Signal Polarization C at 2050

Figure 4.20: Plot B1: Pump Position C, Signal Polarization C at 2100

If you observe the plot in Figure (4.18) you can see that the peak intensity has already dropped off to a noise level. This indicates that A and C has spatial frequencies beyond C and C even though the propagating waves are closer to the facet line in case C and C as illustrated in Figure (3.8). To show this in an easier platform the peak intensities were plotted at every 10 pixels for every different set-up. To allow for easier comparisons of how these plots are reacting we can make a pair-wise comparison between pump angles A and C, at the same signal polarizations. In Figure (4.21) a visual comparison can be made between pump angle A signal polarization A, and pump angle C signal polarization A. The plot in Figure (4.21) is found by first separating the red light from the original image with both lasers active. The red wavelength that has been separated is now narrowed down to the region in which the peak due to pumping is located. Next, the new plots of the red wavelength are generated every ten pixels from the peak intensity of the spot due to the pumping. The maximum value of this peak is now found for all pixel positions and is plotted in Figure (4.21). The maximum peak of this final plot is normalized for each case AA and CA to eliminate any variation due to the weaker pump laser intensity in case C.
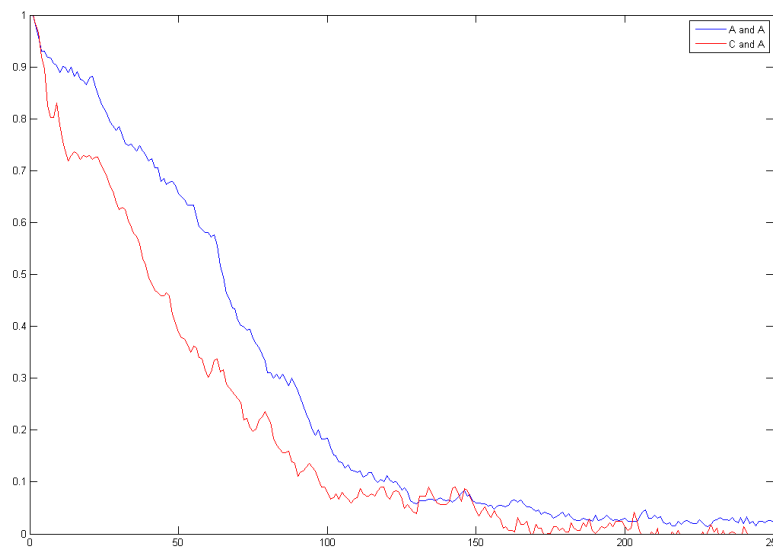
Figure 4.21: Intensity of A and A v. C and A

As you can see from Figure (4.21) the AA plot is wider than the CA plot until the intensities reach a noise level. This is also true for the other comparisons show in Figures (4.22) through (4.24).
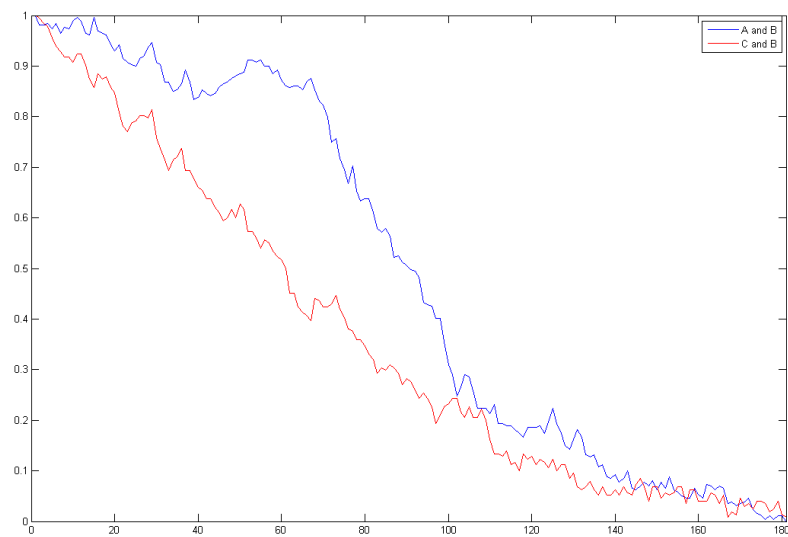
Figure 4.22: Intensity of A and B v. C and B

Figure 4.23: Intensity of A and C v. C and C

To illustrate the fact that the plot in pump angle A is indeed wider than in pump angle C a point of reference was found. The width of each plot was found by determining
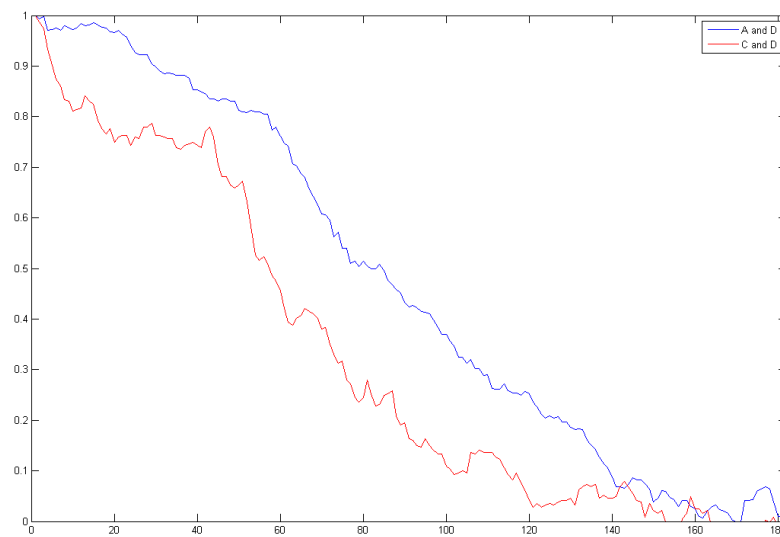
Figure 4.24: Intensity of A and D v. C and D

at what distance the plot was at $\frac{1}{2}$ the peak intensity. This plot is illustrated in Figure (4.25)
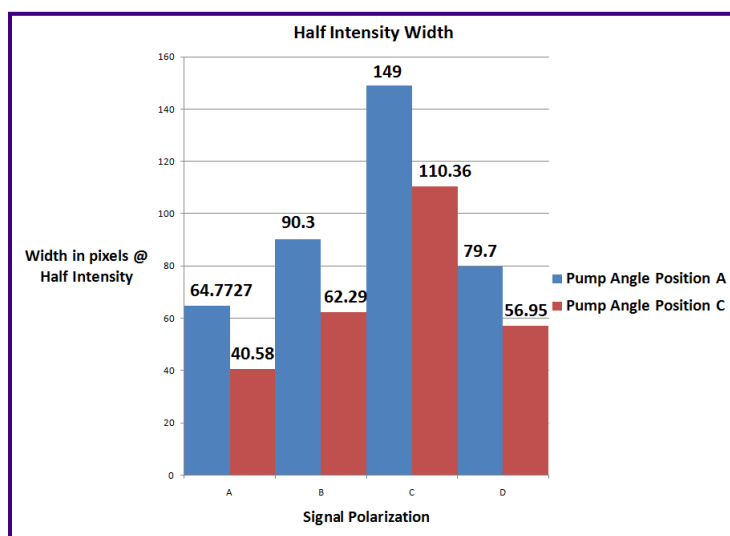
Figure 4.25: Half Intensity Width

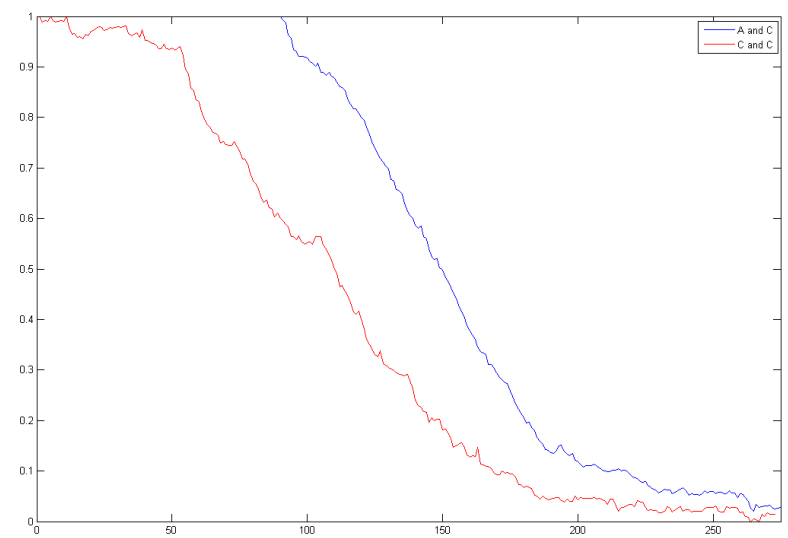In each of the four different signal polarizations Pump angle A position reached the half intensity mark at a position further away from the original peak intensity than Pump angle C position. This confirms that the Pump angle A position generated a larger spread in far-field spatial frequencies than the Pump angle C position. In all cases until you reach the noise level, pump angle A outperforms pump angle C in this respect. There has to be an explanation for this, and the explanation is that evanescent waves have been converted into non-uniform propagating waves.

CHAPTER 5: CONCLUSION AND FUTURE WORK

The purpose of this thesis was to construct an optical assembly capable of indicating whether or not evanescent waves could be converted into propagating waves via optical gain. The gain medium used in this case was Ti:Sapphire with peak gain around 800 nm with a bandwidth of 90 nm. The geometry of the ball lens allows us to establish a cone which should contain all propagating waves as shown in Figure (3.4). Knowing, this any spatial frequencies outside the propagation cone would have to be attributed to evanescent waves. Data was retrieved by taking far-field images to determine if any spatial frequencies were located outside the propagation cone. The drop-off of the peak intensity of the far-field beam profile was then observed at positions further away from the peak intensity. These distances correlate to different far-field angles and accordingly different spatial frequencies. Therefore the greater the pixel distance the further from the propagation cone. Pump angle C position's propagation cone should be at a greater pixel distance than Pump angle A position's as illustrated in Figure (3.8) if only propagating modes are considered. However, Pump angle A position provides the possibility of optical gain to the evanescent modes and, accordingly to our theory, will convert them into sustainable propagating waves that will be located outside the propagation cone in the far field. Accordingly, Pump angle A position produced more spatial frequencies than Pump angle C position did. This confirms the hypothesis and the theory of evanescent wave conversion via optical gain, providing the potential for far-field super-resolution.

5.1 Discussion

During the design phase of the optical assembly control factors were determined. The control factors were chosen to ensure the reproducibility of the experiments. Different components of the assembly were mounted in finely tunable apparatuses, allowing for exact adjustments. These apparatuses also ensured that each component should remain in its desired position. The digital camera was placed on a stand that was attached to the optics table. I made two marks on the camera so that when each image was captured it would be captured with the same perspective. There was some small variation in the position of image capture in a couple of the images. This variation was due to small shifts in the camera while manually pressing the shutter action. When analyzing the data this small shift was accounted for by normalizing different far-field profiles to the peak intensity of each configuration. So for example, if the peak intensity of Pump angle A position was at 1750 on the pixel map and the Pump angle C position's peak intensity was at 1700 each would then be normalized to zero. It is the extension of the far-field profile that provides the critical information on the spread of the spectral frequency, which is compared and used to draw our conclusions. Also, the peak power of the field profile was normalized to 1 to account for any difference in power output of the pump laser. An advantage of using a higher powered pump laser would be the increased angle of the spatial frequencies allowing for a more noticeable difference between Pump angle A position and Pump angle C position. A disadvantage would be the camera would more than likely become saturated. The camera was saturated using a 200mW pump laser, but by using certain camera modes and the filter the saturation was avoided for the most part.

5.2   Future Work

I have several suggestions that could be used in future research regarding this topic. Some of these are basic improvements that can be made with the experimental set-up. A more precise data retrieval system could be used to so that less image processing would be needed. The action of taking a picture with the camera did increase some small variation between different images. The change in these images caused a slight shift in the images. This shift was slight, and was mostly eliminated by normalizing the results to the peak intensity when comparing different set-ups. Another improvement that could be made to the assembly would be to use lasers with a constant power output. The constant power would help to reproduce the same conditions for each image. The amount of intensity change was not drastic and was again remedied by normalizing the peak intensities for different configurations. The pump laser used for the experimentation was a 200mW laser. If a higher powered laser had been used it is my belief that one would see more spatial frequencies, at greater angles from the lens. This could cause some issues if the experiment were done using a basic digital camera as I did in this case. The camera that I used was very easily saturated with the high intensity light. An improved digital camera with a larger dynamic range would be helpful to address this issue. Also, a card-mounted diffraction grating could be used to generate more evanescent waves. The more evanescent waves that are produced the more spatial frequencies that could be retained by converting the evanescent waves into non-uniform propagating waves.

BIBLIOGRAPHY

[1] Frank L. Pedrotti and Leno S. Pedrotti, *Introduction to Optics*, Prentice Hall, 1993.

[2] W. Yang, "Optical assembly of far-field super-resolution imaging via optical gain," Tech. Rep., Western Carolina University, 2010.

[3] J. B. Pendry, "Negative refraction makes a perfect lens," *Phys. Rev. Lett.*, vol. 85, no. 18, pp. 3966–3969, Oct 2000.

[4] L. Alekseyev, E. Narimanov, and J. Khurgin, "Super-resolution imaging using spatial fourier transform infrared spectroscopy," in *Lasers and Electro-Optics, 2009 and 2009 Conference on Quantum electronics and Laser Science Conference. CLEO/QELS 2009. Conference on*, 2009, pp. 1 –2.

[5] Andreas Zumbusch, Gary R. Holtom, and X. Sunney Xie, "Three-dimensional vibrational imaging by coherent anti-stokes raman scattering," *Phys. Rev. Lett.*, vol. 82, no. 20, pp. 4142–4145, May 1999.

[6] "Structured light illumination for extended resolution in fluorescence microscopy," *Optics and Lasers in Engineering*, vol. 43, no. 3-5, pp. 403 – 414, 2005, Optics in Switzerland.

[7] Viktor A. Podolskiy and Evgenii E. Narimanov, "Near-sighted superlens," *Optics Letters*, 2005.

[8] N.Fang, "Sub-diffraction-limited optical imaging with a silver superlens," *Science*, 2005.

[9] S. Anantha Ramakrishna and J.B. Pendry, "Refining the perfect lens: Layered media and optical gain," in *Microwave Conference, 2002. 32nd European*, sept. 2002, pp. 1 –4.

[10] Weiguo Yang, J.O. Schenk, and M.A. Fiddy, "Revisiting the perfect lens with loss," in *IEEE SoutheastCon 2010 (SoutheastCon), Proceedings of the*, march 2010, pp. 302 –304.

[11] Weiguo Yang, John O. Schenk, and Michael A. Fiddy, "Optical gain-assisted far-field sub-wavelength imaging," *None*.

[12] A. Alu and Nader Engheta, "Physical insight into the growing evanescent fields of double-negative metamaterial lenses using their circuit equivalence," *Antennas and Propagation, IEEE Transactions on*, vol. 54, no. 1, pp. 268 – 272, 2006.

[13] C. Caloz, Cheng-Jung Lee, D.R. Smith, J.B. Pendry, and T. Itoh, "Existence and properties of microwave surface plasmons at the interface between a right-handed and a left-handed media," in *Antennas and Propagation Society International Symposium, 2004. IEEE*, 2004, vol. 3, pp. 3151 – 3154 Vol.3.

[14] Jyh-Long Chern, Yu-Sheng Wang, Min-Chou Lu, Jiann-Shing Lih, Ming-Chang Chen, Yen-Chun Huang, and Kuan-Hung Chen, "Breaking diffraction limit with meta-materials," in *Quantum Electronics and Laser Science, 2003. QELS. Postconference Digest*, 2003, p. 2 pp.

[15] V. G. Veselago, "The electrodynamics of substances with simultaneously negative values of e and ," *Physics-Uspekhi*, vol. 10, no. 4, pp. 509–514, 1968.

[16] Dejan Karadaglic and Tony Wilson, "Image formation in structured illumination wide-field fluorescence microscopy," *Micron*, vol. 39, no. 7, pp. 808 – 818, 2008.

Appendices

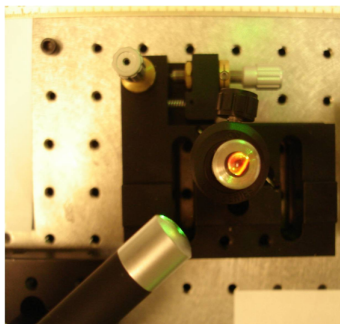# APPENDIX A: COLLECTED DATA

Figure A.1: Pump Position A

(a) Filtered Image Before Pumping

(b) Filtered Image After Pumping

(c) Filtered Image Pump Only On

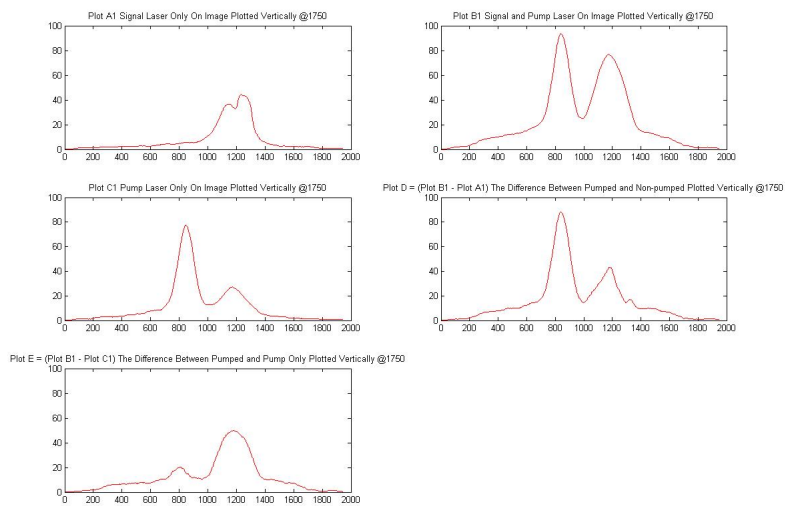Figure A.2: Pump Position A Signal Polarization A

Plot A1 Signal Laser Only On Image Plotted Vertically @1750

Plot B1 Signal and Pump Laser On Image Plotted Vertically @1750

Plot C1 Pump Laser Only On Image Plotted Vertically @1750

Plot D = (Plot B1 - Plot A1) The Difference Between Pumped and Non-pumped Plotted Vertically @1750

Plot E = (Plot B1 - Plot C1) The Difference Between Pumped and Pump Only Plotted Vertically @1750

Figure A.3: Pump Position A, Signal Polarization A at 1750

Plot A1 Signal Laser Only On Image Plotted Vertically @1800

Plot B1 Signal and Pump Laser On Image Plotted Vertically @1800

Plot C1 Pump Laser Only On Image Plotted Vertically @1800

Plot D = (Plot B1 - Plot A1) The Difference Between Pumped and Non-pumped Plotted Vertically @1800

Plot E = (Plot B1 - Plot C1) The Difference Between Pumped and Pump Only Plotted Vertically @1800
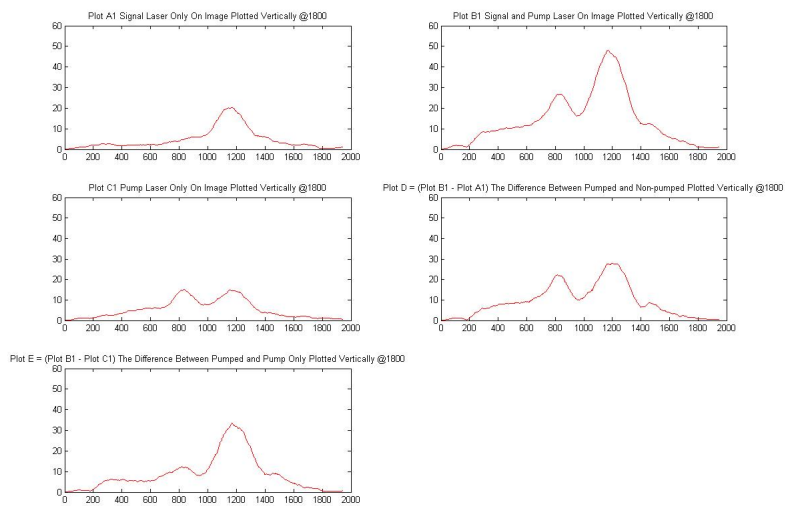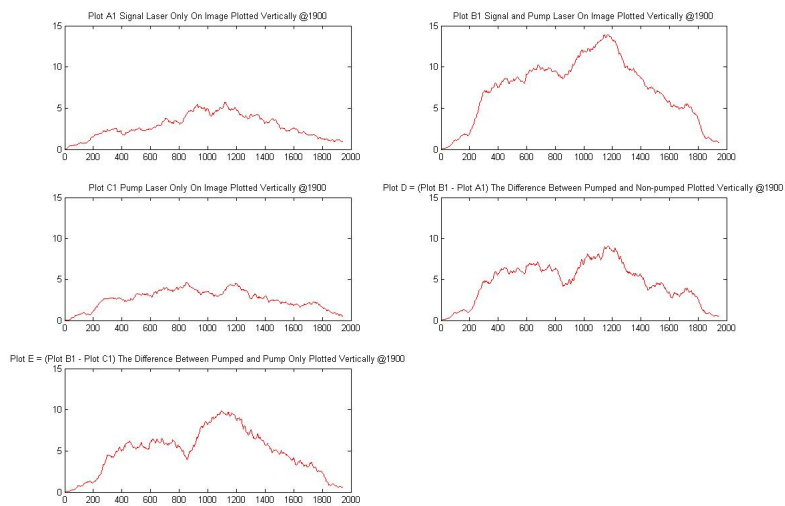
Figure A.4: Pump Position A, Signal Polarization A at 1800
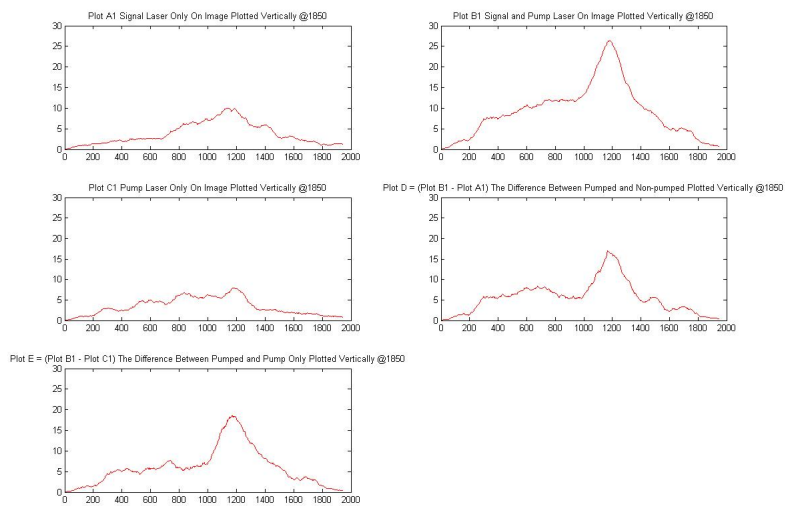
Figure A.5: Pump Position A, Signal Polarization A at 1850

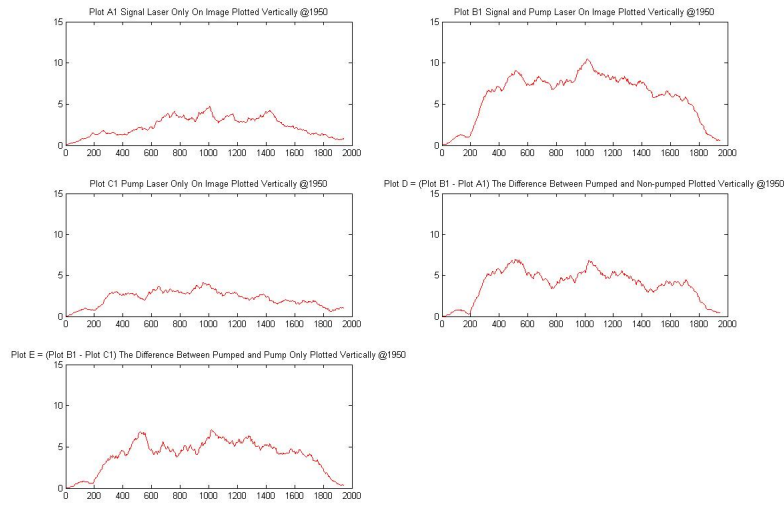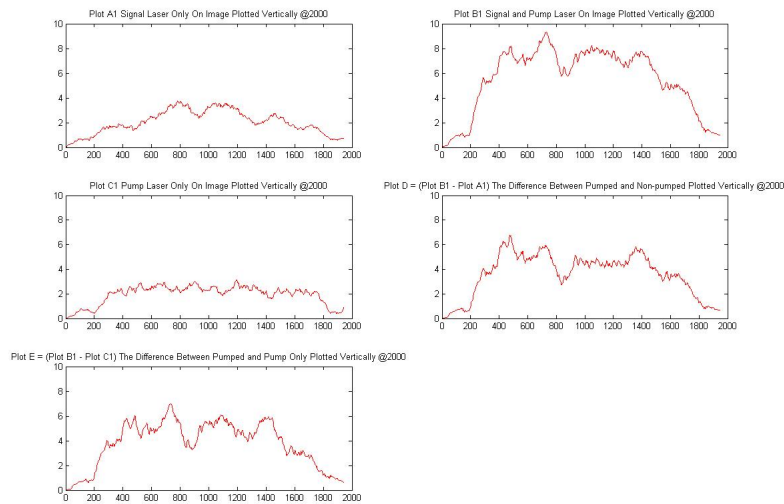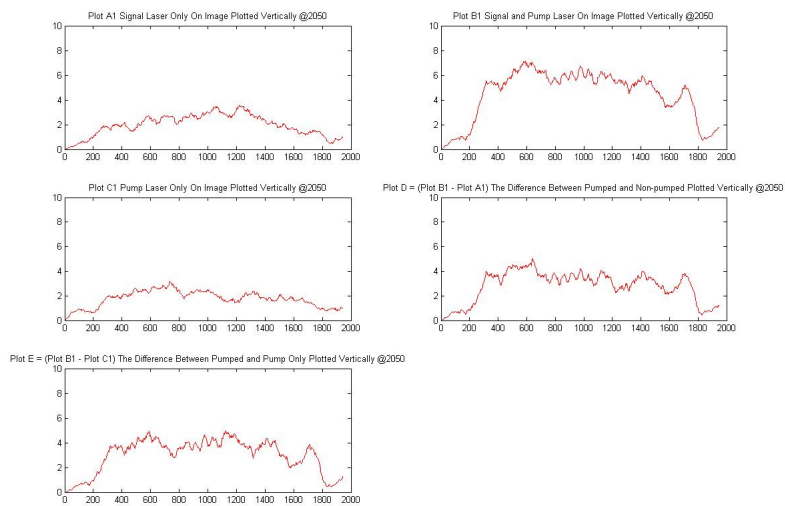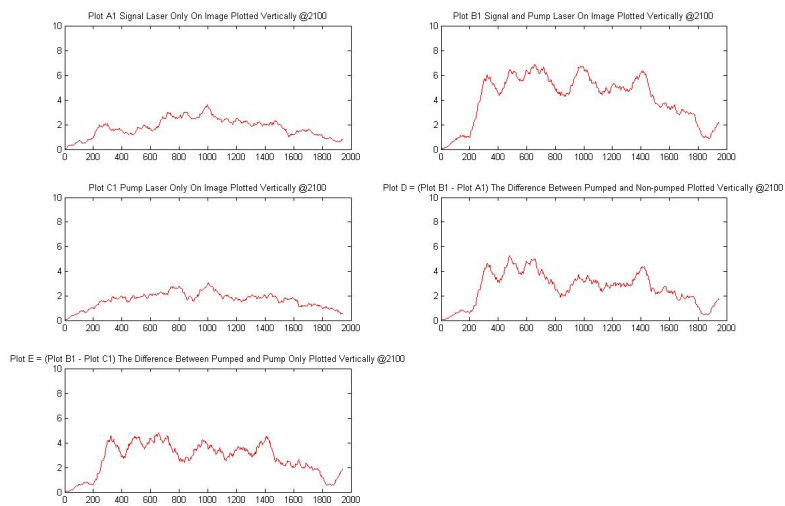Figure A.6: Pump Position A, Signal Polarization A at 1900

Plot A1 Signal Laser Only On Image Plotted Vertically @1950

Plot B1 Signal and Pump Laser On Image Plotted Vertically @1950

Plot C1 Pump Laser Only On Image Plotted Vertically @1950

Plot D = (Plot B1 - Plot A1) The Difference Between Pumped and Non-pumped Plotted Vertically @1950

Plot E = (Plot B1 - Plot C1) The Difference Between Pumped and Pump Only Plotted Vertically @1950

Figure A.7: Pump Position A, Signal Polarization A at 1950

Plot A1 Signal Laser Only On Image Plotted Vertically @2000

Plot B1 Signal and Pump Laser On Image Plotted Vertically @2000

Plot C1 Pump Laser Only On Image Plotted Vertically @2000

Plot D = (Plot B1 - Plot A1) The Difference Between Pumped and Non-pumped Plotted Vertically @2000

Plot E = (Plot B1 - Plot C1) The Difference Between Pumped and Pump Only Plotted Vertically @2000

Figure A.8: Pump Position A, Signal Polarization A at 2000

Figure A.9: Pump Position A, Signal Polarization A at 2050

Figure A.10: Pump Position A, Signal Polarization A at 2100

(a) Filtered Image Before Pumping
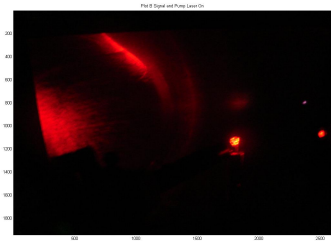
(b) Filtered Image After Pumping

(c) Filtered Image Pump Only On

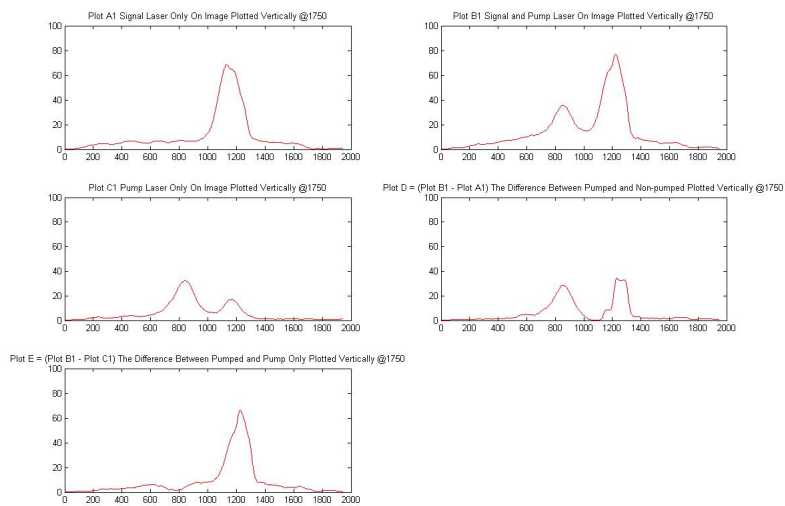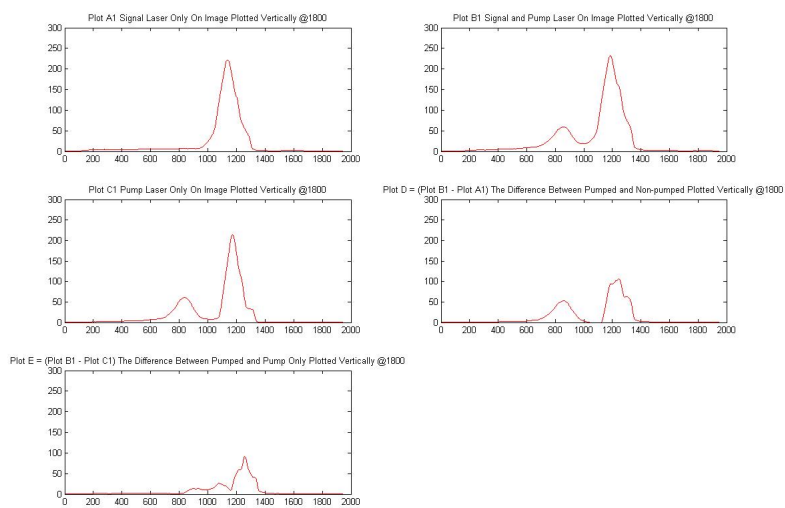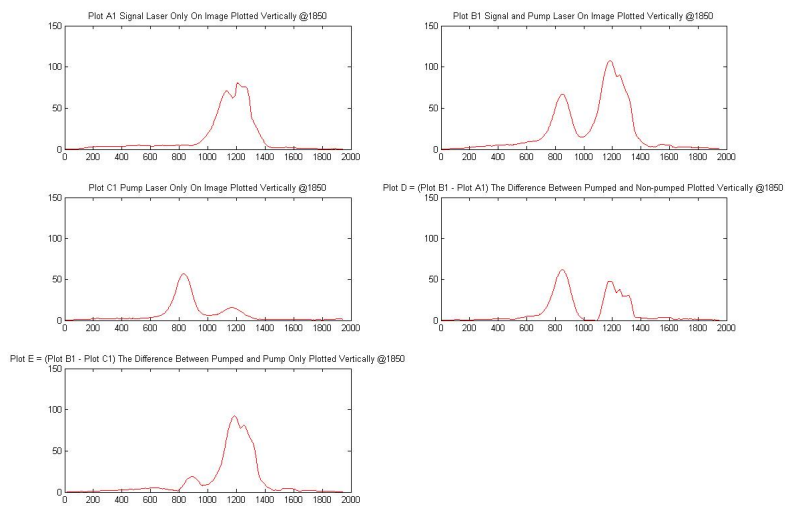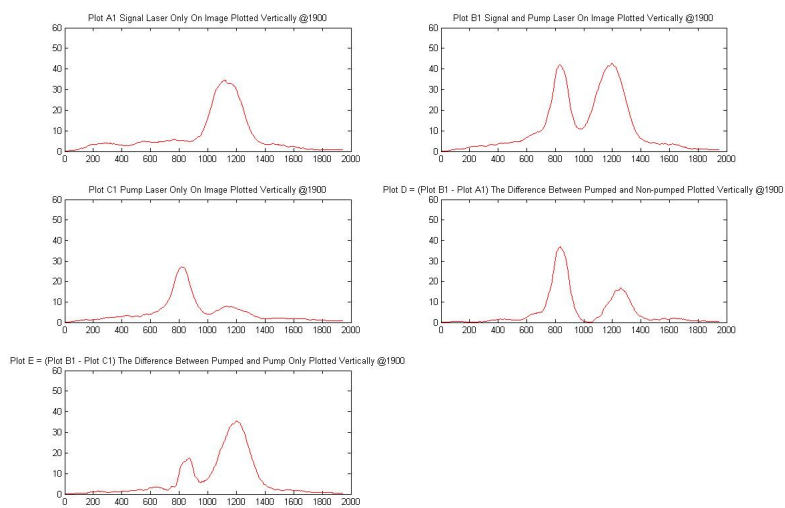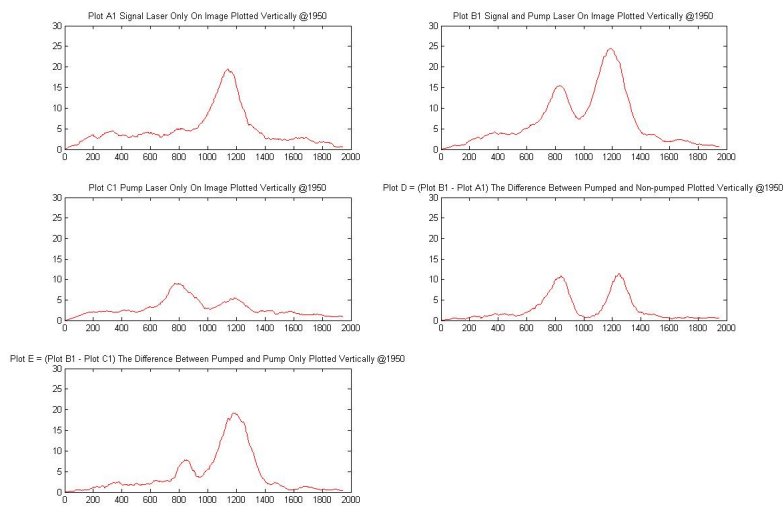Figure A.11: Pump Position A Signal Polarization B

Plot A1 Signal Laser Only On Image Plotted Vertically @1750

Plot B1 Signal and Pump Laser On Image Plotted Vertically @1750

Plot C1 Pump Laser Only On Image Plotted Vertically @1750

Plot D = (Plot B1 - Plot A1) The Difference Between Pumped and Non-pumped Plotted Vertically @1750

Plot E = (Plot B1 - Plot C1) The Difference Between Pumped and Pump Only Plotted Vertically @1750

Figure A.12: Pump Position A, Signal Polarization B at 1750

Plot A1 Signal Laser Only On Image Plotted Vertically @1800

Plot B1 Signal and Pump Laser On Image Plotted Vertically @1800

Plot C1 Pump Laser Only On Image Plotted Vertically @1800

Plot D = (Plot B1 - Plot A1) The Difference Between Pumped and Non-pumped Plotted Vertically @1800

Plot E = (Plot B1 - Plot C1) The Difference Between Pumped and Pump Only Plotted Vertically @1800

Figure A.13: Pump Position A, Signal Polarization B at 1800

Figure A.14: Pump Position A, Signal Polarization B at 1850

Figure A.15: Pump Position A, Signal Polarization B at 1900

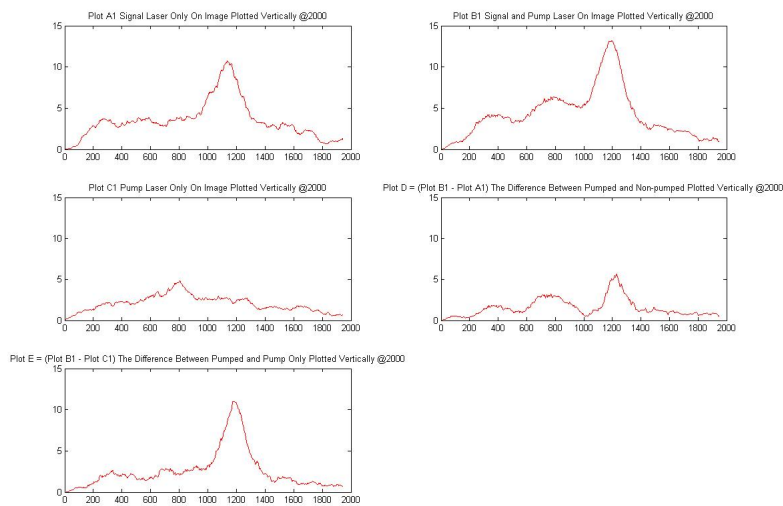Figure A.16: Pump Position A, Signal Polarization B at 1950

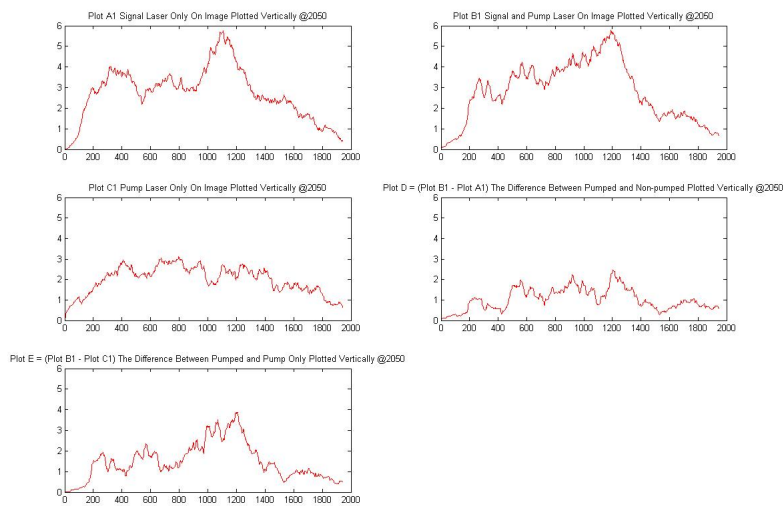Figure A.17: Pump Position A, Signal Polarization B at 2000

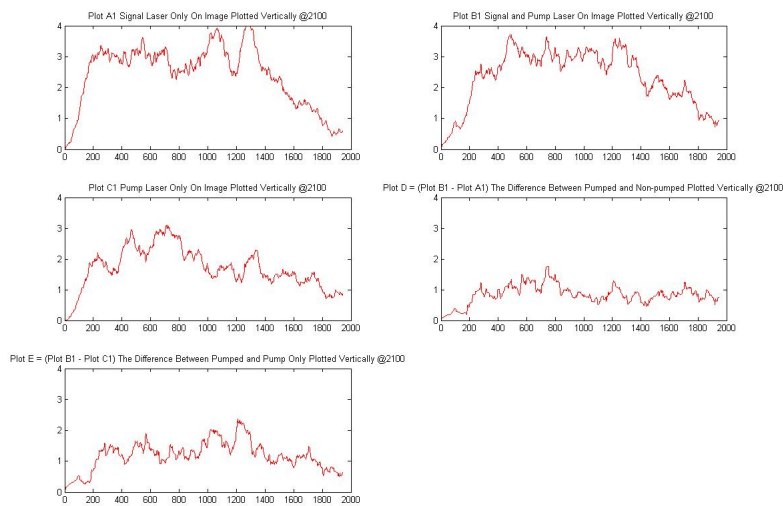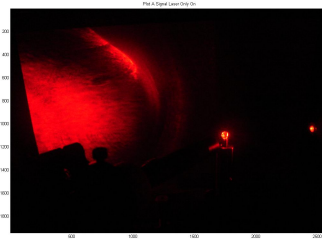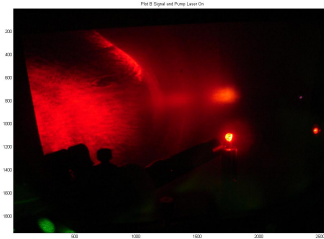Figure A.18: Pump Position A, Signal Polarization B at 2050

Figure A.19: Pump Position A, Signal Polarization B at 2100

(a) Filtered Image Before Pumping

(b) Filtered Image After Pumping

(c) Filtered Image Pump Only On
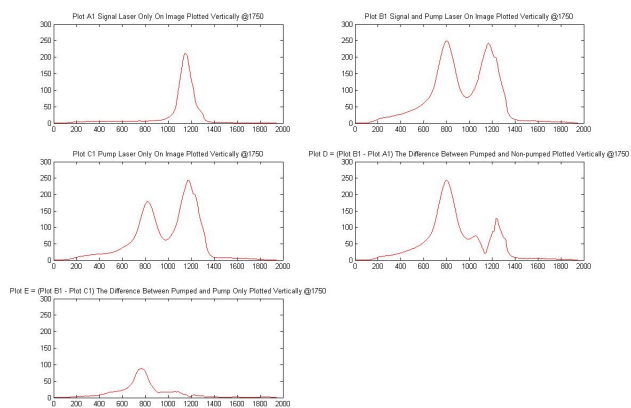
Figure A.20: Pump Position A Signal Polarization C

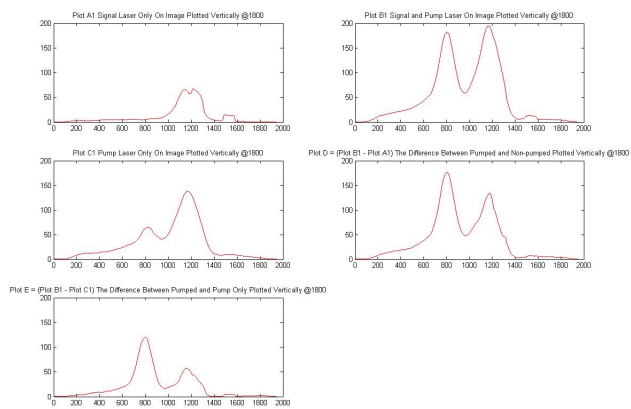Figure A.21: Pump Position A, Signal Polarization C at 1750

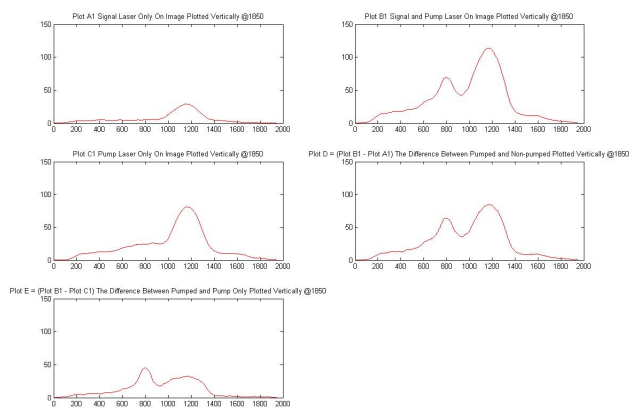Figure A.22: Pump Position A, Signal Polarization C at 1800

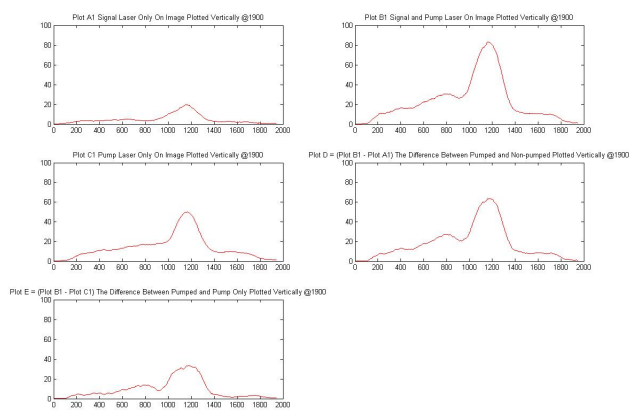Figure A.23: Pump Position A, Signal Polarization C at 1850

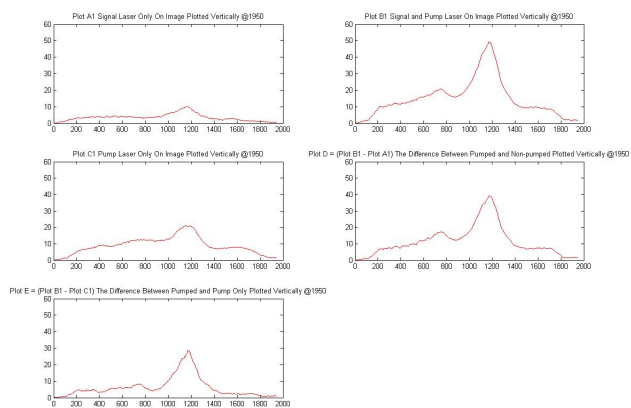Figure A.24: Pump Position A, Signal Polarization C at 1900

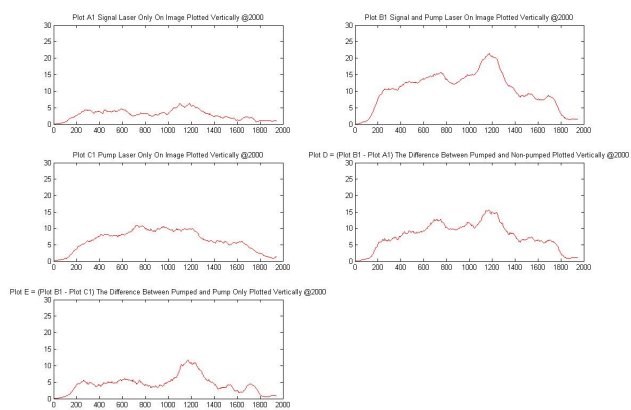Figure A.25: Pump Position A, Signal Polarization C at 1950

Figure A.26: Pump Position A, Signal Polarization C at 2000
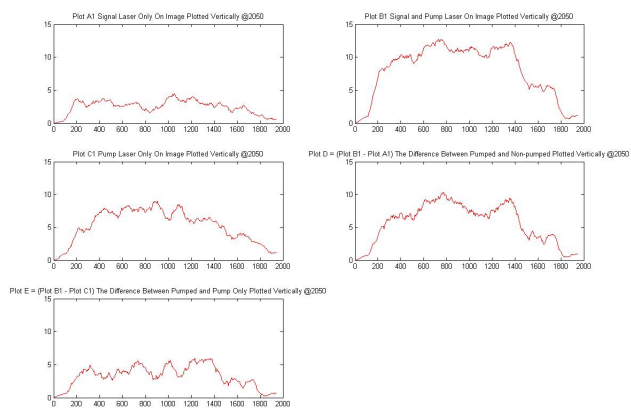
Figure A.27: Pump Position A, Signal Polarization C at 2050
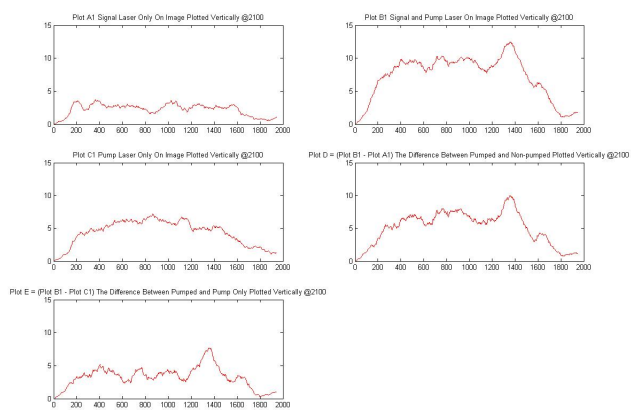

Figure A.28: Pump Position A, Signal Polarization C at 2100

(a) Filtered Image Before Pumping

(b) Filtered Image After Pumping

(c) Filtered Image Pump Only On

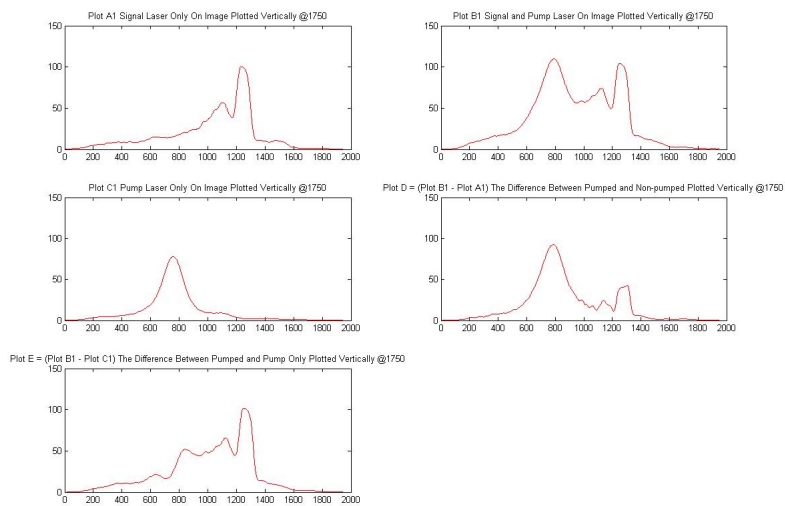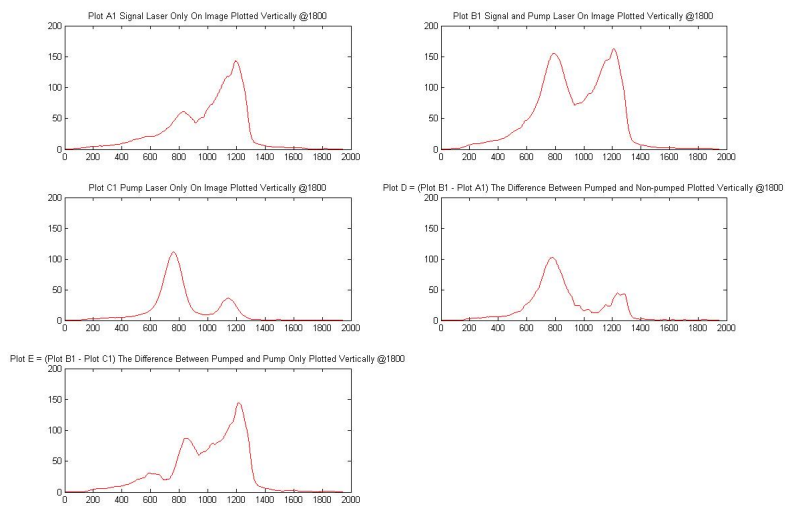Figure A.29: Pump Position A Signal Polarization D

Plot A1 Signal Laser Only On Image Plotted Vertically @1750

Plot B1 Signal and Pump Laser On Image Plotted Vertically @1750

Plot C1 Pump Laser Only On Image Plotted Vertically @1750

Plot D = (Plot B1 - Plot A1) The Difference Between Pumped and Non-pumped Plotted Vertically @1750

Plot E = (Plot B1 - Plot C1) The Difference Between Pumped and Pump Only Plotted Vertically @1750

Figure A.30: Pump Position A, Signal Polarization D at 1750

Plot A1 Signal Laser Only On Image Plotted Vertically @1800

Plot B1 Signal and Pump Laser On Image Plotted Vertically @1800

Plot C1 Pump Laser Only On Image Plotted Vertically @1800

Plot D = (Plot B1 - Plot A1) The Difference Between Pumped and Non-pumped Plotted Vertically @1800

Plot E = (Plot B1 - Plot C1) The Difference Between Pumped and Pump Only Plotted Vertically @1800

Figure A.31: Pump Position A, Signal Polarization D at 1800

Plot A1 Signal Laser Only On Image Plotted Vertically @1850

Plot B1 Signal and Pump Laser On Image Plotted Vertically @1850

Plot C1 Pump Laser Only On Image Plotted Vertically @1850

Plot D = (Plot B1 - Plot A1) The Difference Between Pumped and Non-pumped Plotted Vertically @1850

Plot E = (Plot B1 - Plot C1) The Difference Between Pumped and Pump Only Plotted Vertically @1850

Figure A.32: Pump Position A, Signal Polarization D at 1850

Plot A1 Signal Laser Only On Image Plotted Vertically @1900

Plot B1 Signal and Pump Laser On Image Plotted Vertically @1900

Plot C1 Pump Laser Only On Image Plotted Vertically @1900

Plot D = (Plot B1 - Plot A1) The Difference Between Pumped and Non-pumped Plotted Vertically @1900

Plot E = (Plot B1 - Plot C1) The Difference Between Pumped and Pump Only Plotted Vertically @1900
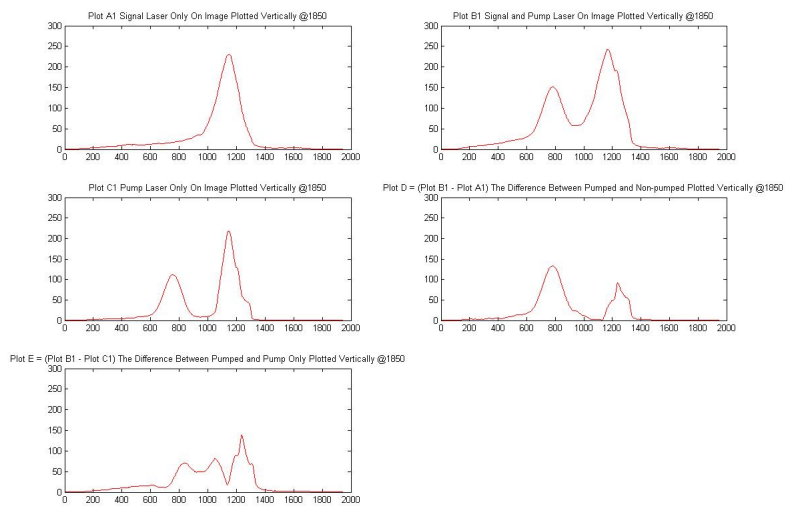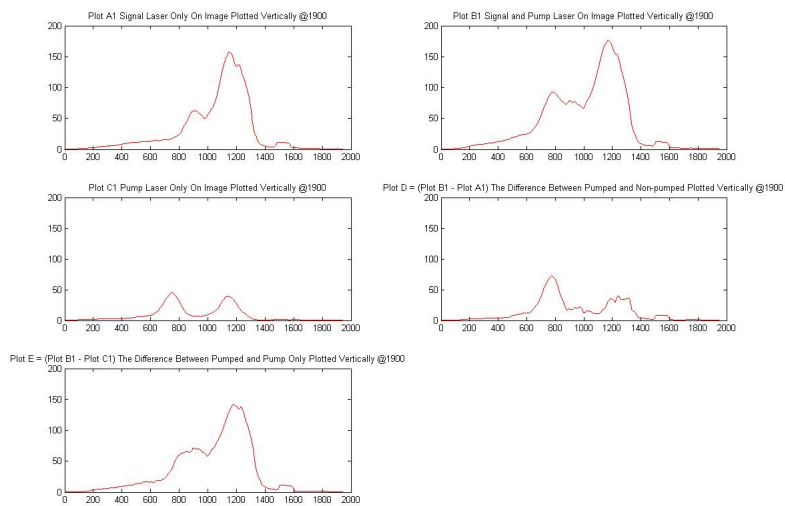
Figure A.33: Pump Position A, Signal Polarization D at 1900

Figure A.34: Pump Position A, Signal Polarization D at 1950

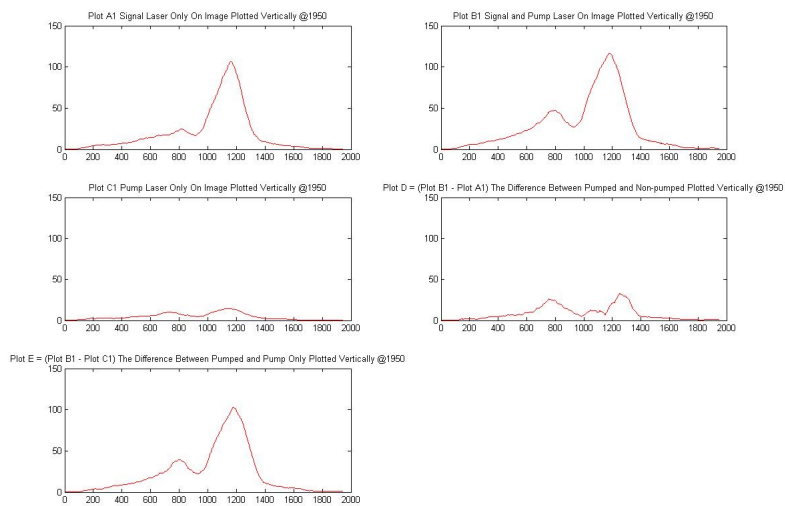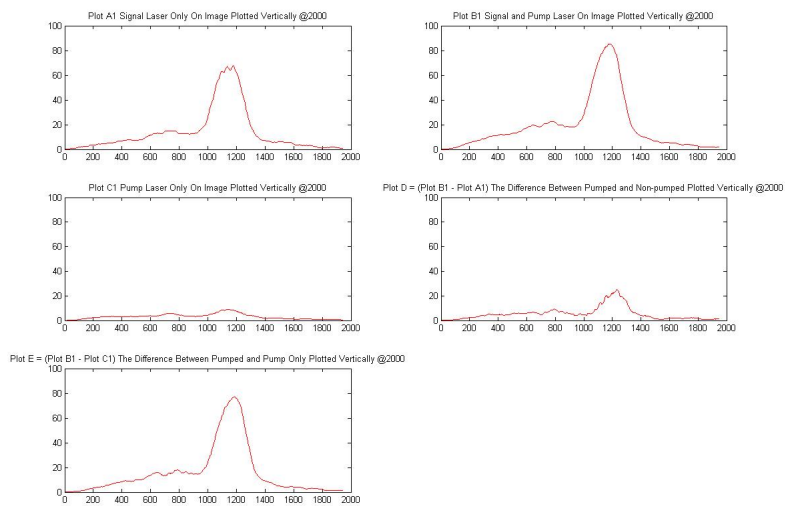
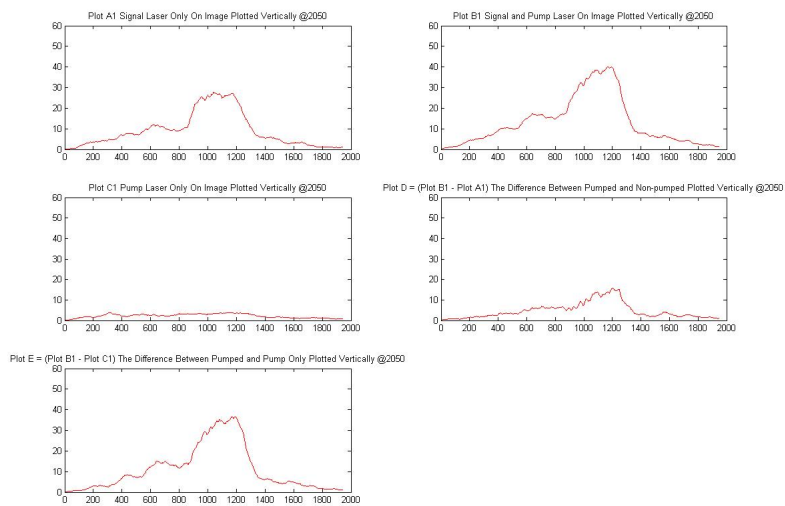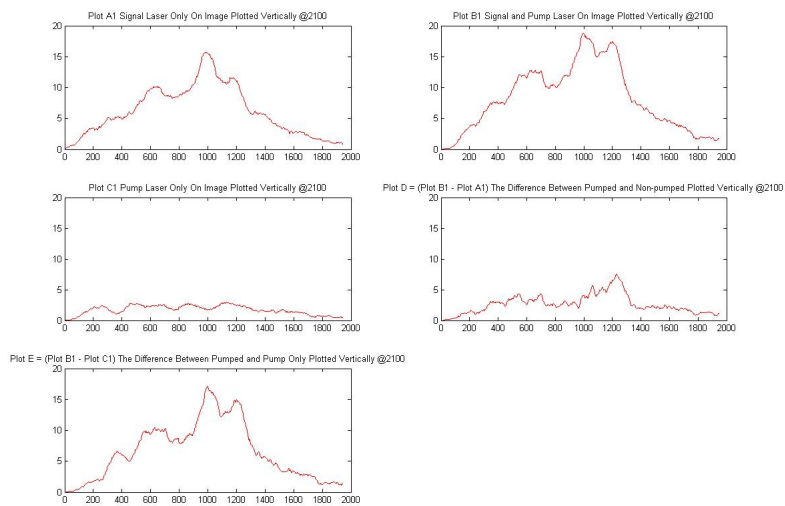Figure A.35: Pump Position A, Signal Polarization D at 2000

Plot A1 Signal Laser Only On Image Plotted Vertically @2050

Plot B1 Signal and Pump Laser On Image Plotted Vertically @2050

Plot C1 Pump Laser Only On Image Plotted Vertically @2050

Plot D = (Plot B1 - Plot A1) The Difference Between Pumped and Non-pumped Plotted Vertically @2050

Plot E = (Plot B1 - Plot C1) The Difference Between Pumped and Pump Only Plotted Vertically @2050

Figure A.36: Pump Position A, Signal Polarization D at 2050

Plot A1 Signal Laser Only On Image Plotted Vertically @2100

Plot B1 Signal and Pump Laser On Image Plotted Vertically @2100

Plot C1 Pump Laser Only On Image Plotted Vertically @2100

Plot D = (Plot B1 - Plot A1) The Difference Between Pumped and Non-pumped Plotted Vertically @2100

Plot E = (Plot B1 - Plot C1) The Difference Between Pumped and Pump Only Plotted Vertically @2100

Figure A.37: Pump Position A, Signal Polarization D at 2100
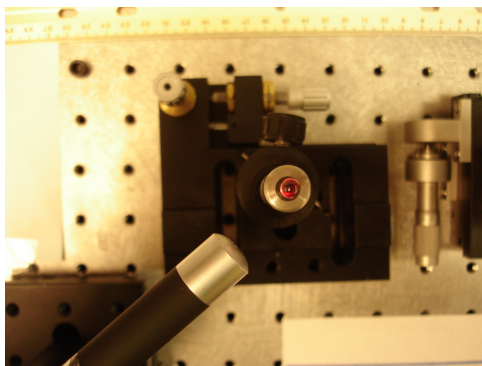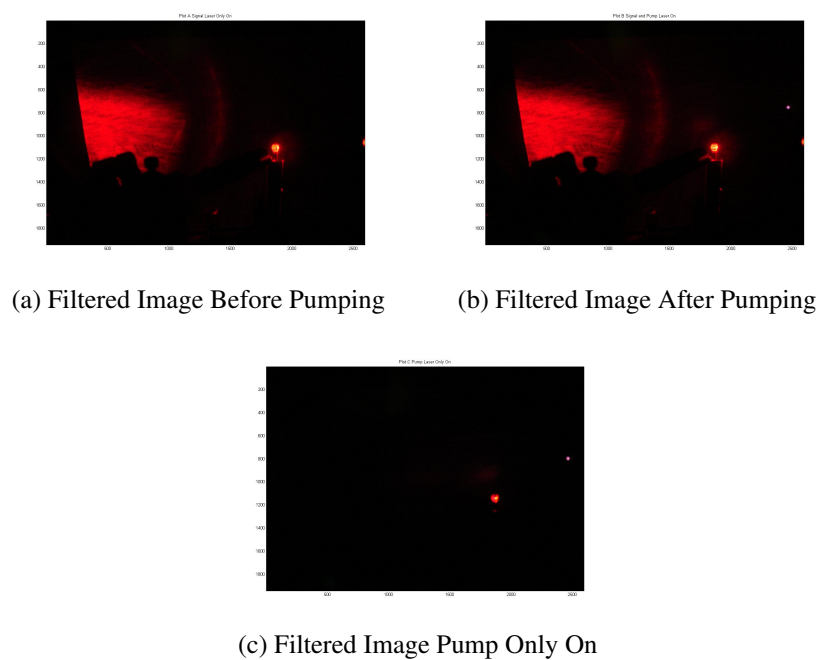
Figure A.38: Pump Position B

(a) Filtered Image Before Pumping

(b) Filtered Image After Pumping

(c) Filtered Image Pump Only On

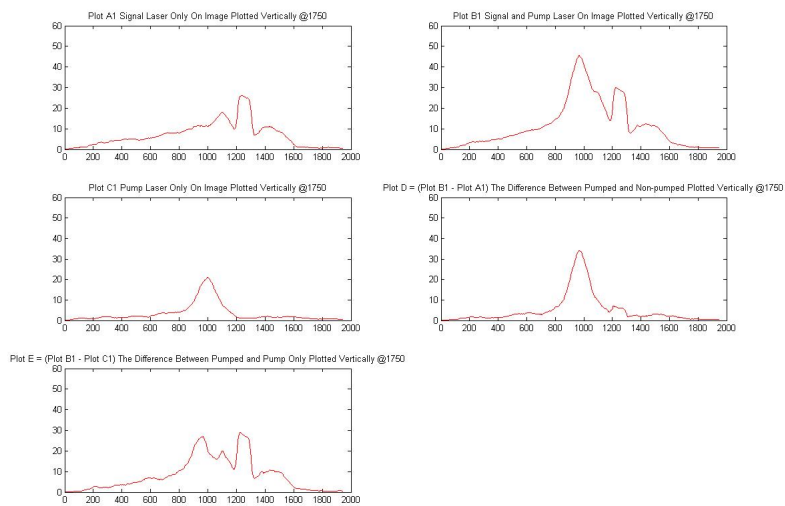Figure A.39: Pump Position B, Signal Polarization A

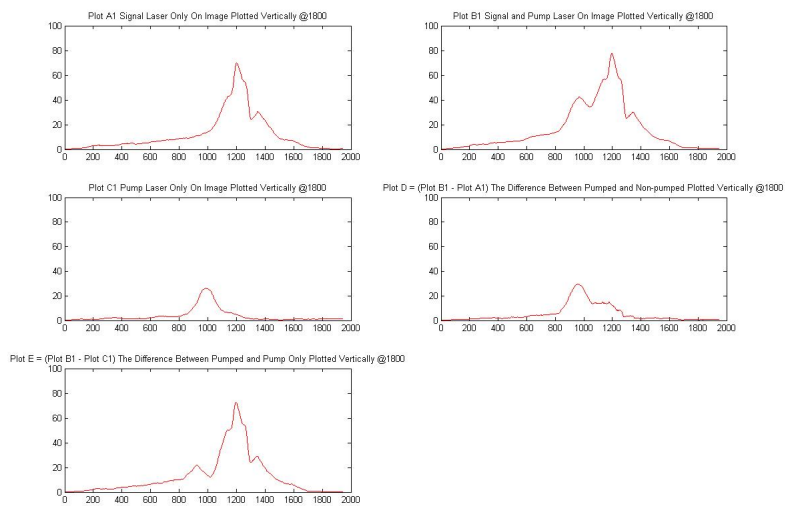Figure A.40: Pump Position B, Signal Polarization A at 1750

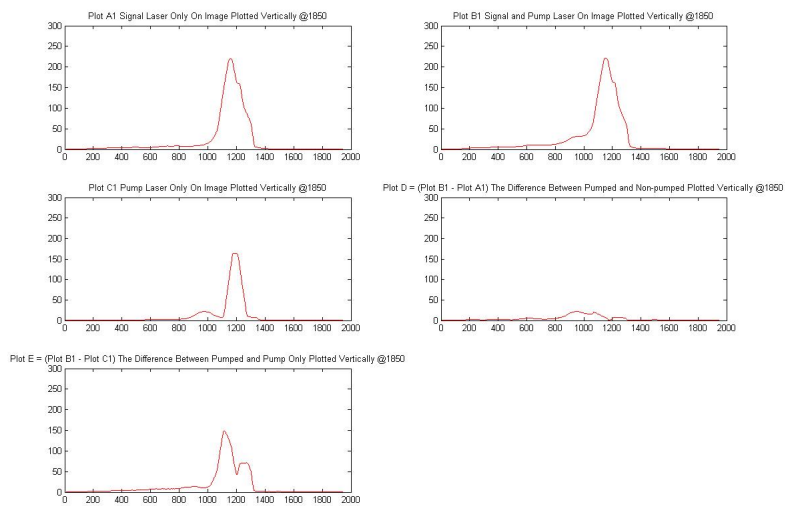Figure A.41: Pump Position B, Signal Polarization A at 1800

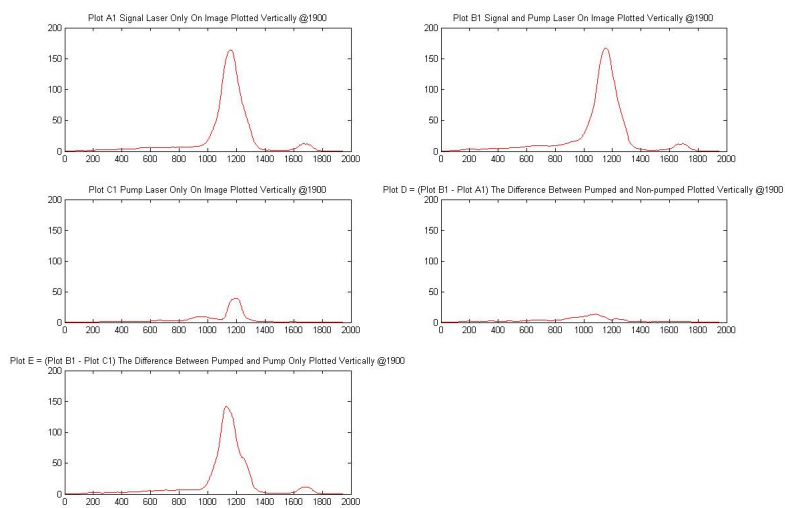Figure A.42: Pump Position B, Signal Polarization A at 1850

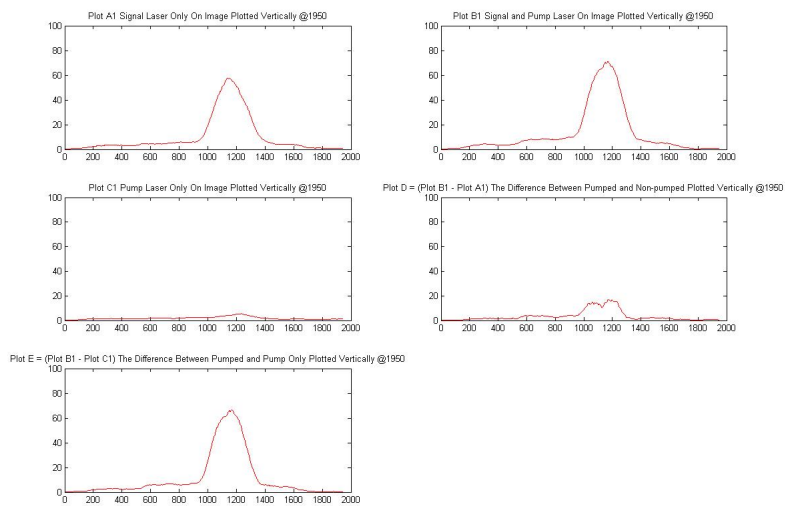Figure A.43: Pump Position B, Signal Polarization A at 1900

Plot A1 Signal Laser Only On Image Plotted Vertically @1950

Plot B1 Signal and Pump Laser On Image Plotted Vertically @1950

Plot C1 Pump Laser Only On Image Plotted Vertically @1950

Plot D = (Plot B1 - Plot A1) The Difference Between Pumped and Non-pumped Plotted Vertically @1950

Plot E = (Plot B1 - Plot C1) The Difference Between Pumped and Pump Only Plotted Vertically @1950

Figure A.44: Pump Position B, Signal Polarization A at 1950

Plot A1 Signal Laser Only On Image Plotted Vertically @2000

Plot B1 Signal and Pump Laser On Image Plotted Vertically @2000

Plot C1 Pump Laser Only On Image Plotted Vertically @2000

Plot D = (Plot B1 - Plot A1) The Difference Between Pumped and Non-pumped Plotted Vertically @2000

Plot E = (Plot B1 - Plot C1) The Difference Between Pumped and Pump Only Plotted Vertically @2000
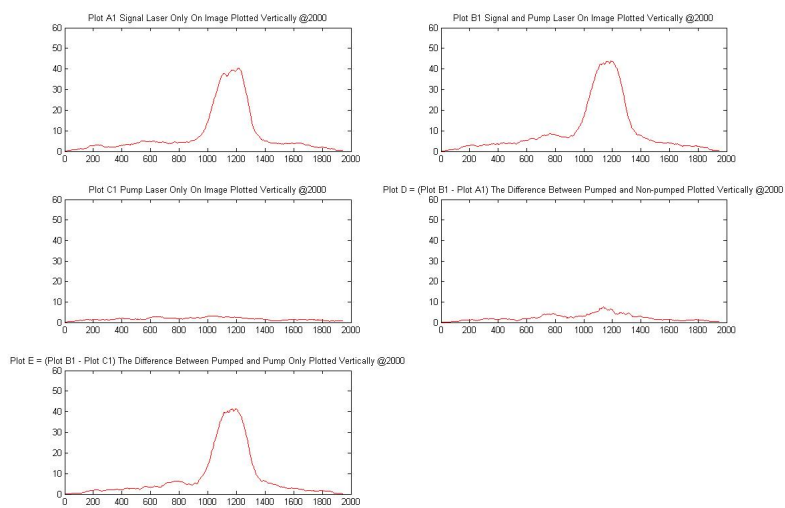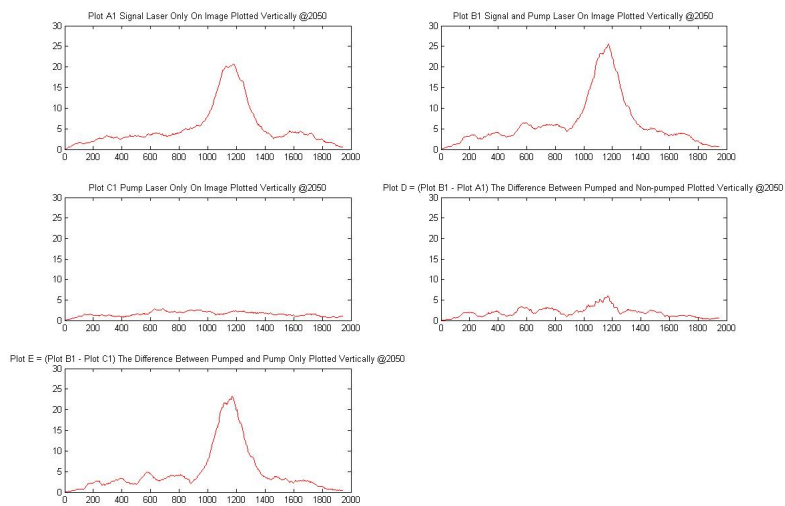
Figure A.45: Pump Position B, Signal Polarization A at 2000

Figure A.46: Pump Position B, Signal Polarization A at 2050

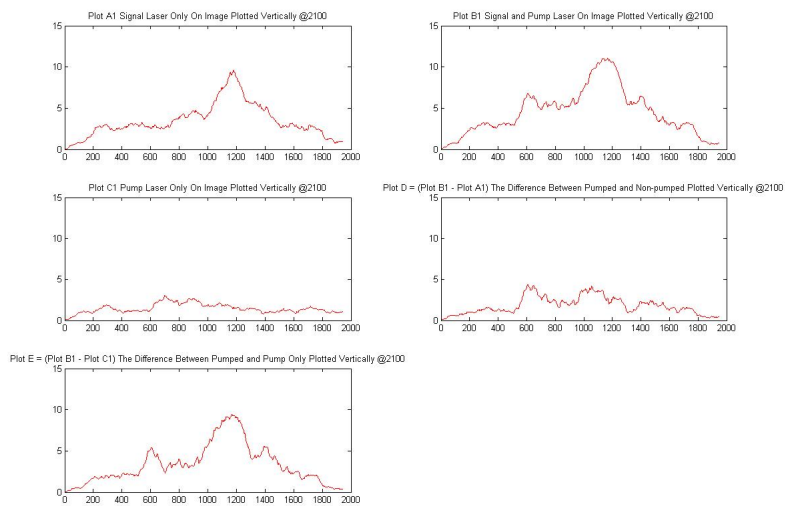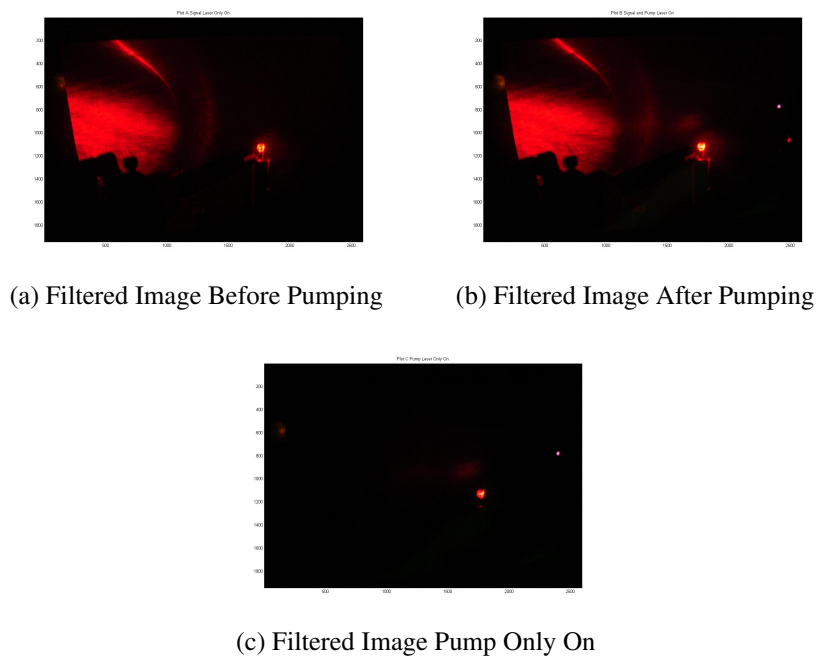Figure A.47: Pump Position B, Signal Polarization A at 2100
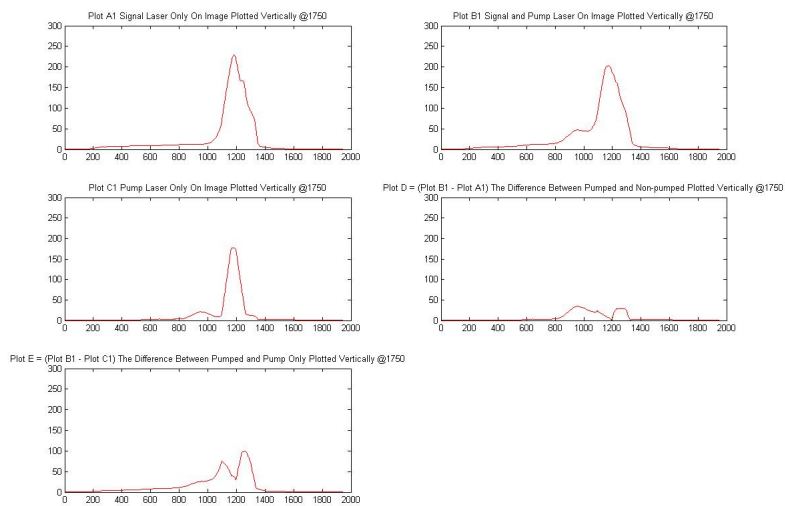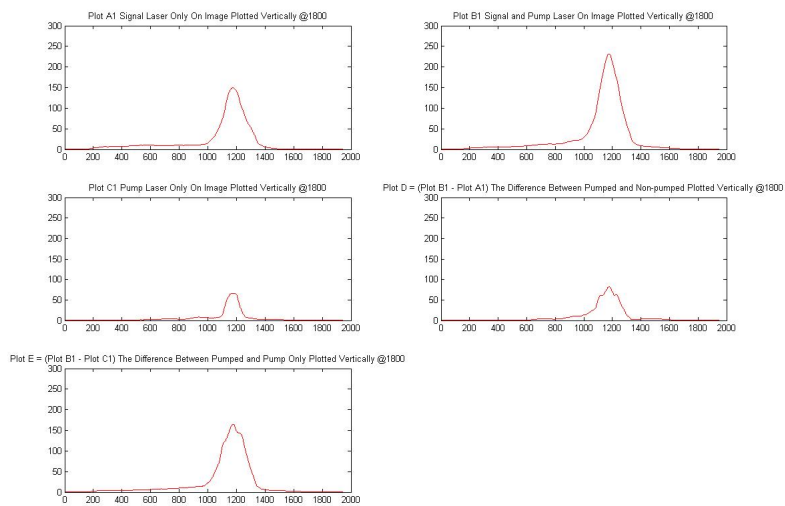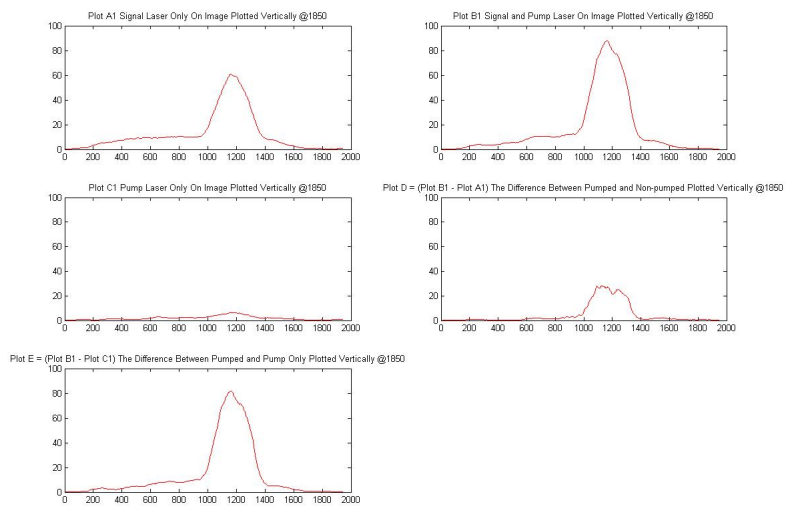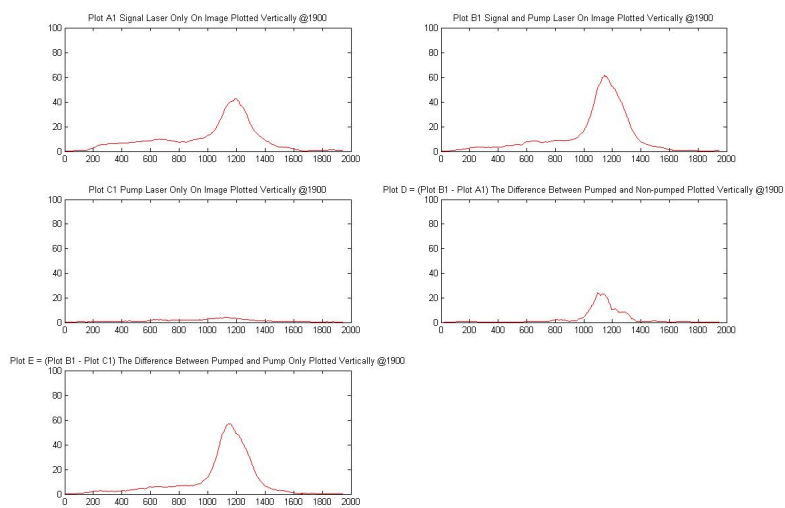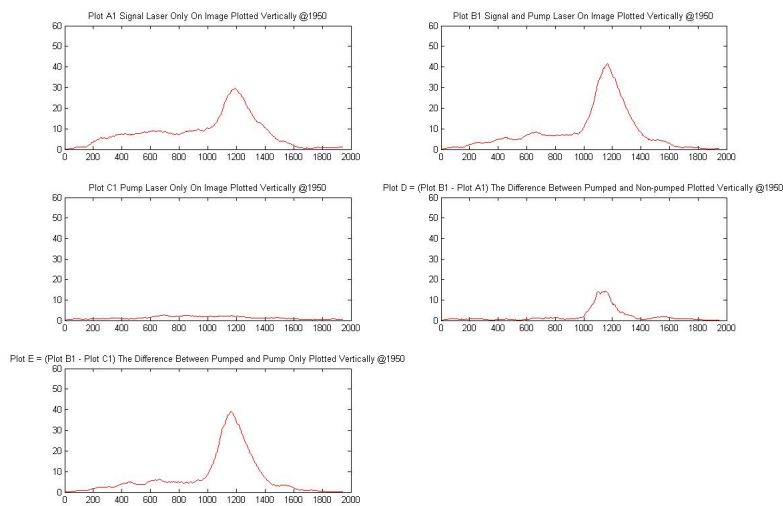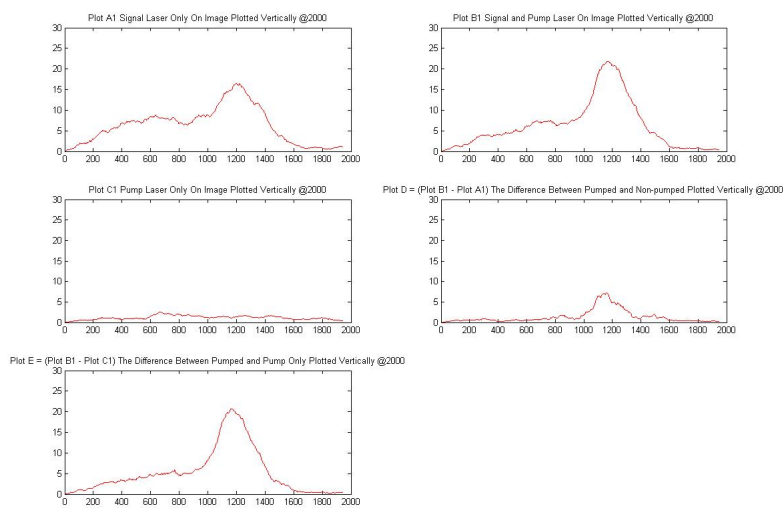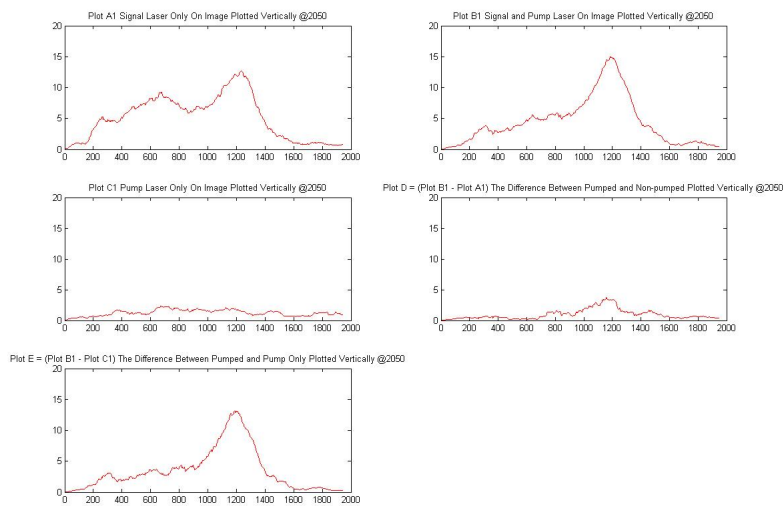
(a) Filtered Image Before Pumping

(b) Filtered Image After Pumping

(c) Filtered Image Pump Only On

Figure A.48: Pump Position B, Signal Polarization B

93

Plot A1 Signal Laser Only On Image Plotted Vertically @1750

Plot B1 Signal and Pump Laser On Image Plotted Vertically @1750

Plot C1 Pump Laser Only On Image Plotted Vertically @1750

Plot D = (Plot B1 - Plot A1) The Difference Between Pumped and Non-pumped Plotted Vertically @1750

Plot E = (Plot B1 - Plot C1) The Difference Between Pumped and Pump Only Plotted Vertically @1750

Figure A.49: Pump Position B, Signal Polarization B at 1750

Plot A1 Signal Laser Only On Image Plotted Vertically @1800

Plot B1 Signal and Pump Laser On Image Plotted Vertically @1800

Plot C1 Pump Laser Only On Image Plotted Vertically @1800

Plot D = (Plot B1 - Plot A1) The Difference Between Pumped and Non-pumped Plotted Vertically @1800

Plot E = (Plot B1 - Plot C1) The Difference Between Pumped and Pump Only Plotted Vertically @1800

Figure A.50: Pump Position B, Signal Polarization B at 1800

Plot A1 Signal Laser Only On Image Plotted Vertically @1850

Plot B1 Signal and Pump Laser On Image Plotted Vertically @1850

Plot C1 Pump Laser Only On Image Plotted Vertically @1850

Plot D = (Plot B1 - Plot A1) The Difference Between Pumped and Non-pumped Plotted Vertically @1850

Plot E = (Plot B1 - Plot C1) The Difference Between Pumped and Pump Only Plotted Vertically @1850

Figure A.51: Pump Position B, Signal Polarization B at 1850

Plot A1 Signal Laser Only On Image Plotted Vertically @1900

Plot B1 Signal and Pump Laser On Image Plotted Vertically @1900

Plot C1 Pump Laser Only On Image Plotted Vertically @1900

Plot D = (Plot B1 - Plot A1) The Difference Between Pumped and Non-pumped Plotted Vertically @1900

Plot E = (Plot B1 - Plot C1) The Difference Between Pumped and Pump Only Plotted Vertically @1900

Figure A.52: Pump Position B, Signal Polarization B at 1900

95

Figure A.53: Pump Position B, Signal Polarization B at 1950

Figure A.54: Pump Position B, Signal Polarization B at 2000

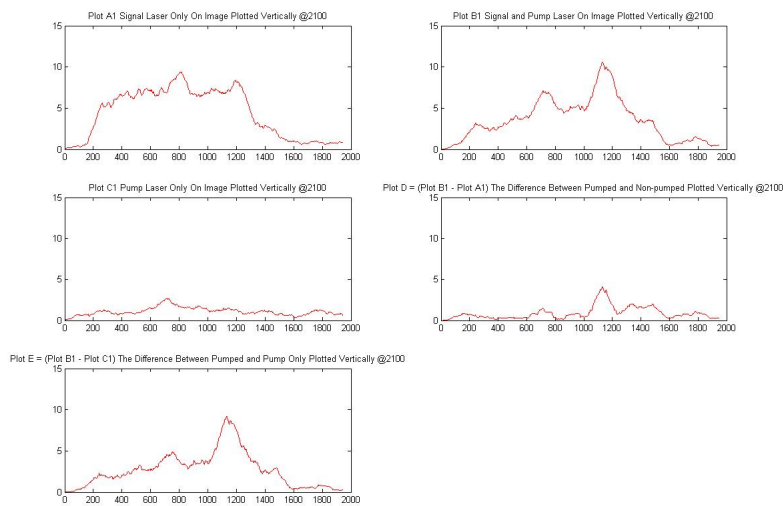Figure A.55: Pump Position B, Signal Polarization B at 2050

Figure A.56: Pump Position B, Signal Polarization B at 2100

(a) Filtered Image Before Pumping

(b) Filtered Image After Pumping

(c) Filtered Image Pump Only On

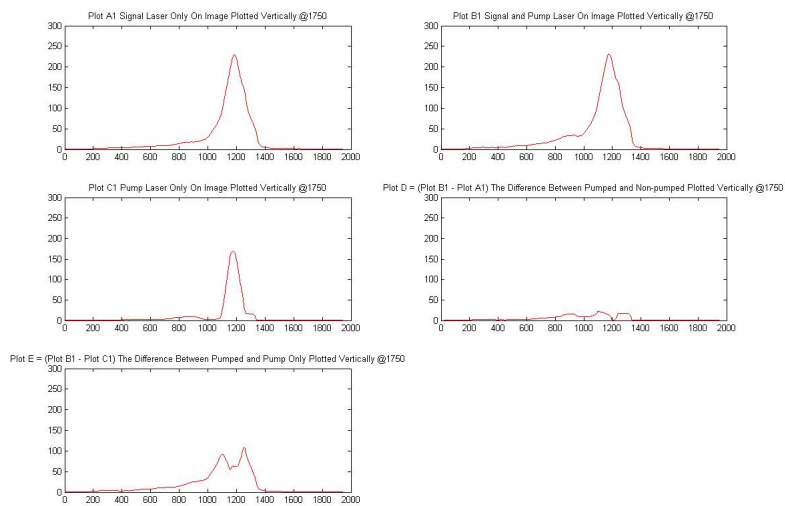Figure A.57: Pump Position B, Signal Polarization C

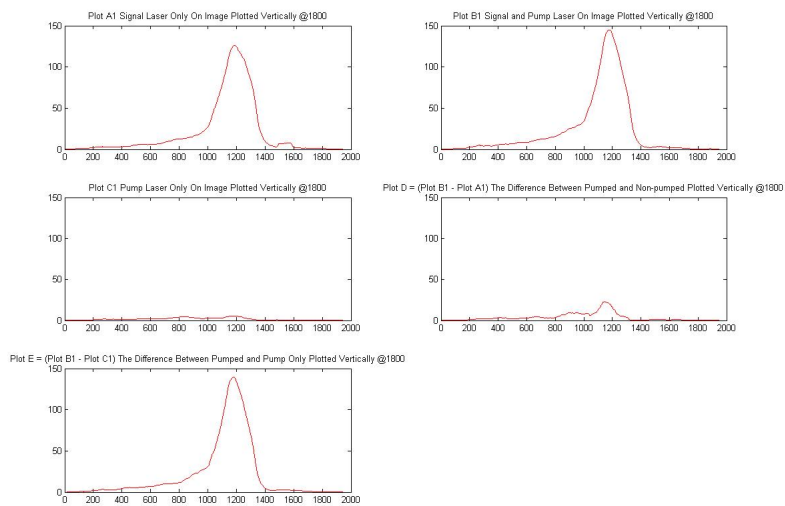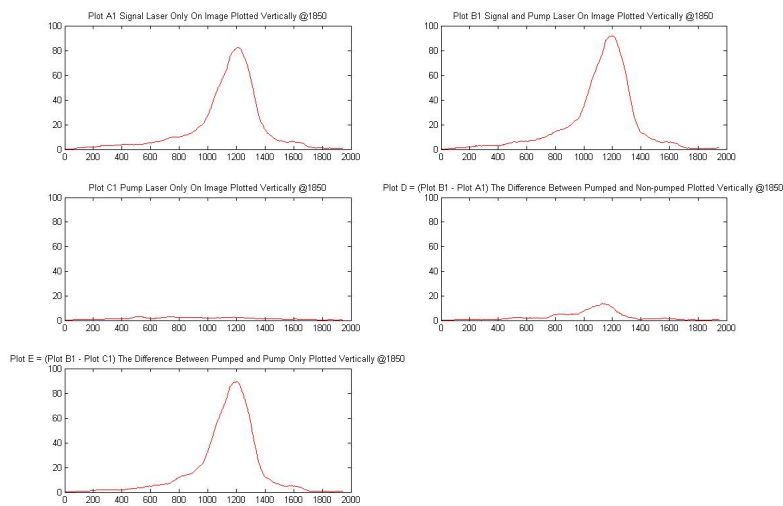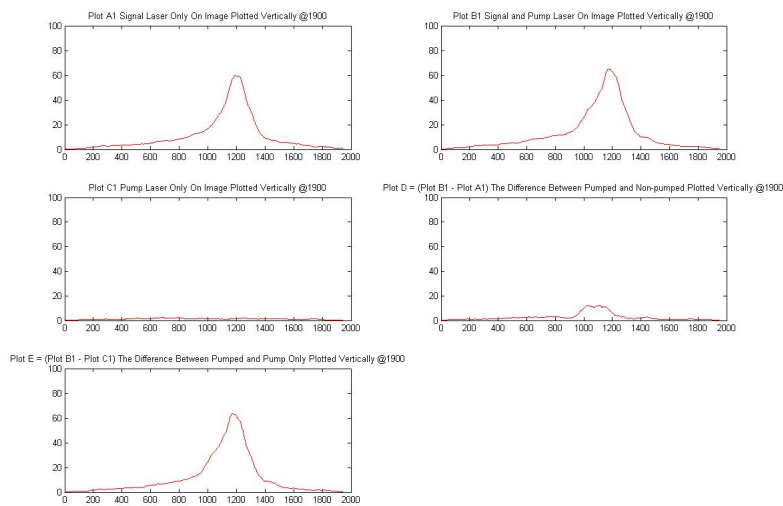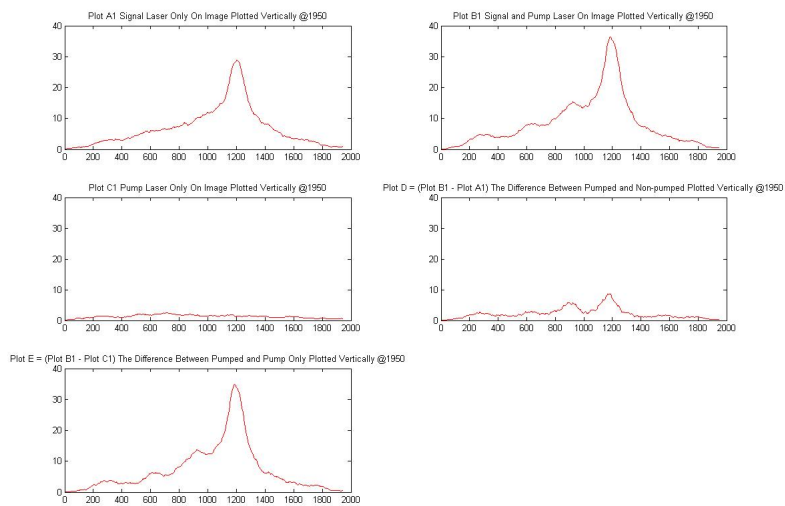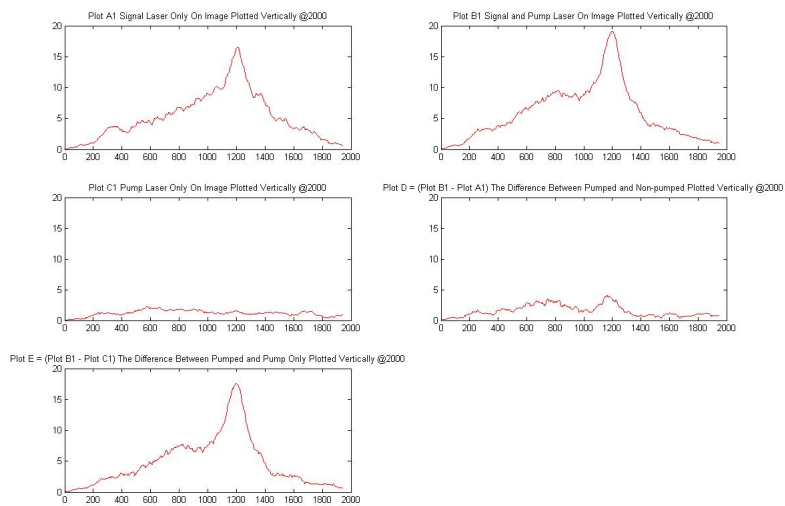Figure A.58: Pump Position B, Signal Polarization C at 1750

Figure A.59: Pump Position B, Signal Polarization C at 1800

Plot A1 Signal Laser Only On Image Plotted Vertically @1850

Plot B1 Signal and Pump Laser On Image Plotted Vertically @1850

Plot C1 Pump Laser Only On Image Plotted Vertically @1850

Plot D = (Plot B1 - Plot A1) The Difference Between Pumped and Non-pumped Plotted Vertically @1850

Plot E = (Plot B1 - Plot C1) The Difference Between Pumped and Pump Only Plotted Vertically @1850

Figure A.60: Pump Position B, Signal Polarization C at 1850

Plot A1 Signal Laser Only On Image Plotted Vertically @1900

Plot B1 Signal and Pump Laser On Image Plotted Vertically @1900

Plot C1 Pump Laser Only On Image Plotted Vertically @1900

Plot D = (Plot B1 - Plot A1) The Difference Between Pumped and Non-pumped Plotted Vertically @1900

Plot E = (Plot B1 - Plot C1) The Difference Between Pumped and Pump Only Plotted Vertically @1900

Figure A.61: Pump Position B, Signal Polarization C at 1900

Figure A.62: Pump Position B, Signal Polarization C at 1950

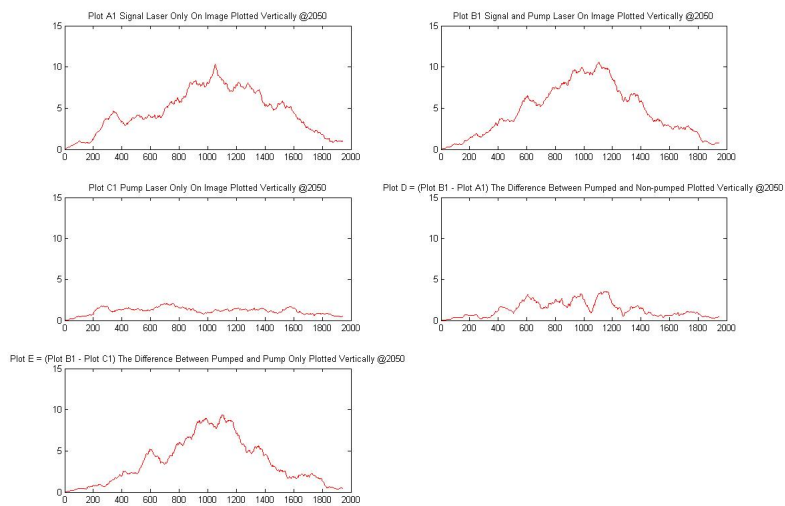Figure A.63: Pump Position B, Signal Polarization C at 2000

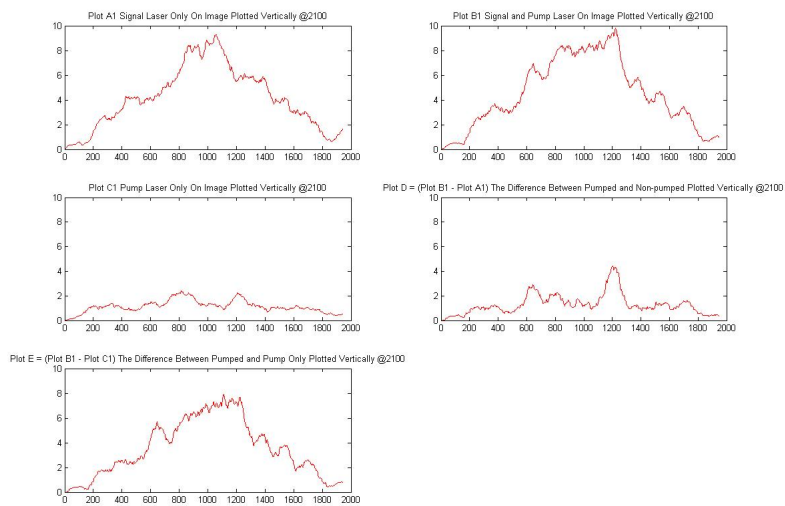Figure A.64: Pump Position B, Signal Polarization C at 2050

Figure A.65: Pump Position B, Signal Polarization C at 2100

(a) Filtered Image Before Pumping

(b) Filtered Image After Pumping

(c) Filtered Image Pump Only On

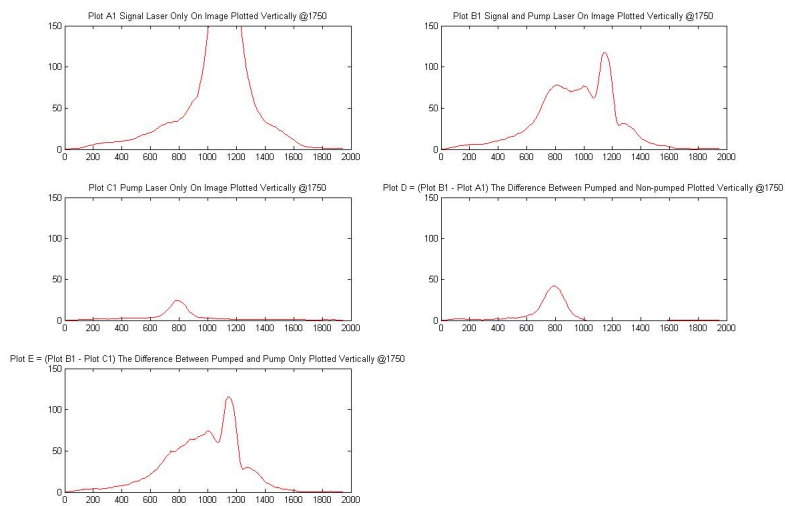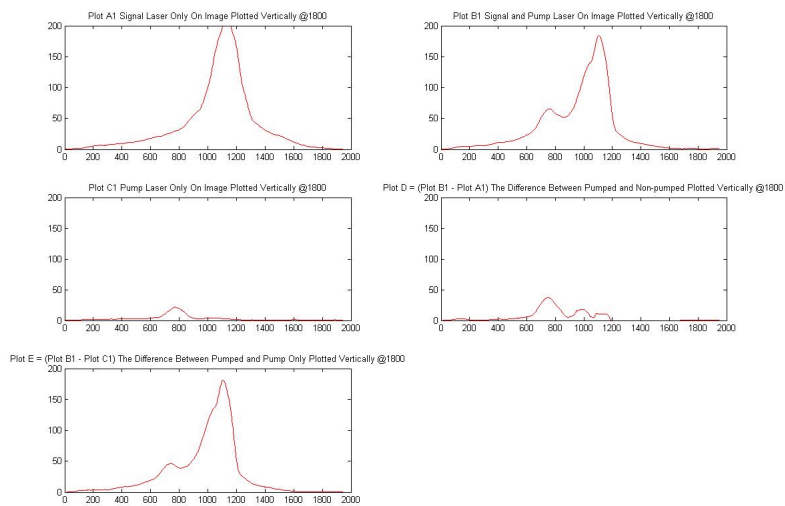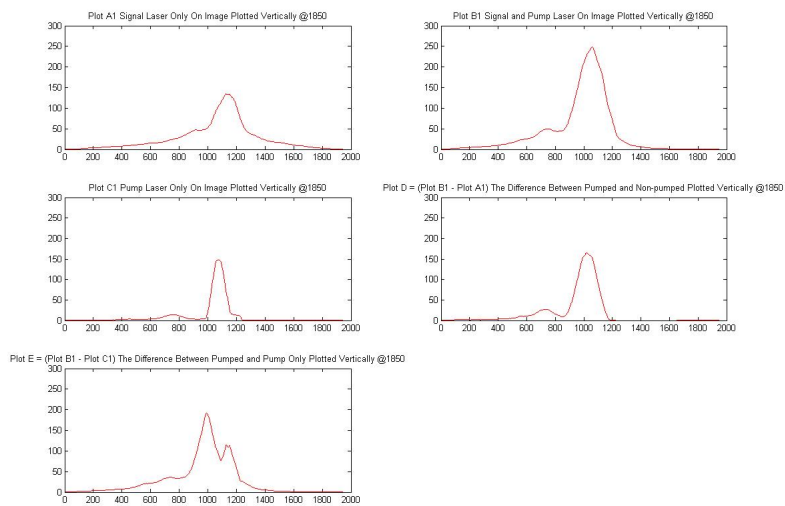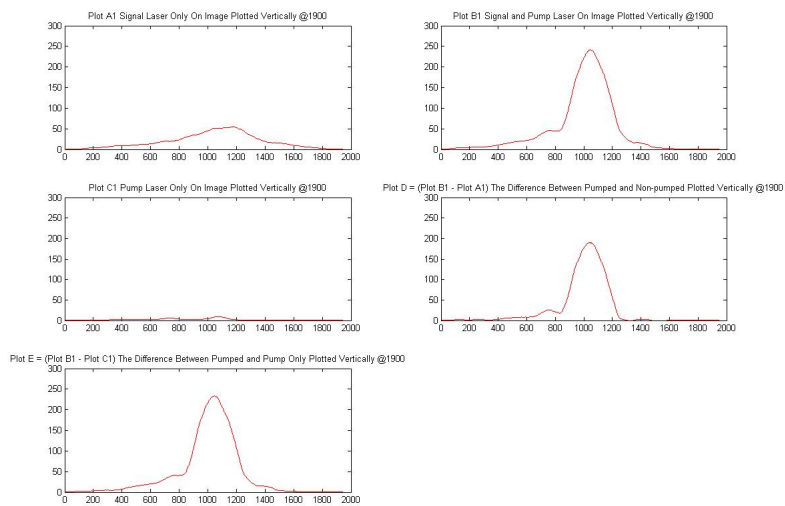Figure A.66: Pump Position B, Signal Polarization D

Plot A1 Signal Laser Only On Image Plotted Vertically @1750

Plot B1 Signal and Pump Laser On Image Plotted Vertically @1750

Plot C1 Pump Laser Only On Image Plotted Vertically @1750

Plot D = (Plot B1 - Plot A1) The Difference Between Pumped and Non-pumped Plotted Vertically @1750

Plot E = (Plot B1 - Plot C1) The Difference Between Pumped and Pump Only Plotted Vertically @1750

Figure A.67: Pump Position B, Signal Polarization D at 1750

Plot A1 Signal Laser Only On Image Plotted Vertically @1800

Plot B1 Signal and Pump Laser On Image Plotted Vertically @1800

Plot C1 Pump Laser Only On Image Plotted Vertically @1800

Plot D = (Plot B1 - Plot A1) The Difference Between Pumped and Non-pumped Plotted Vertically @1800

Plot E = (Plot B1 - Plot C1) The Difference Between Pumped and Pump Only Plotted Vertically @1800

Figure A.68: Pump Position B, Signal Polarization D at 1800

Figure A.69: Pump Position B, Signal Polarization D at 1850

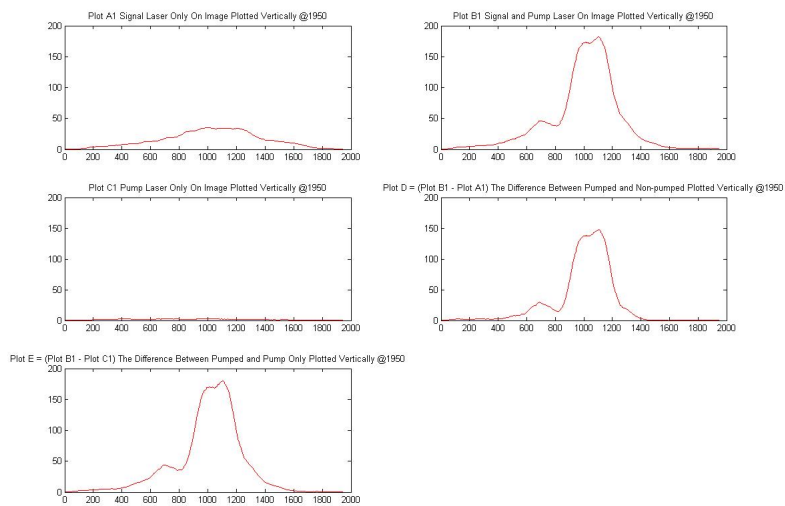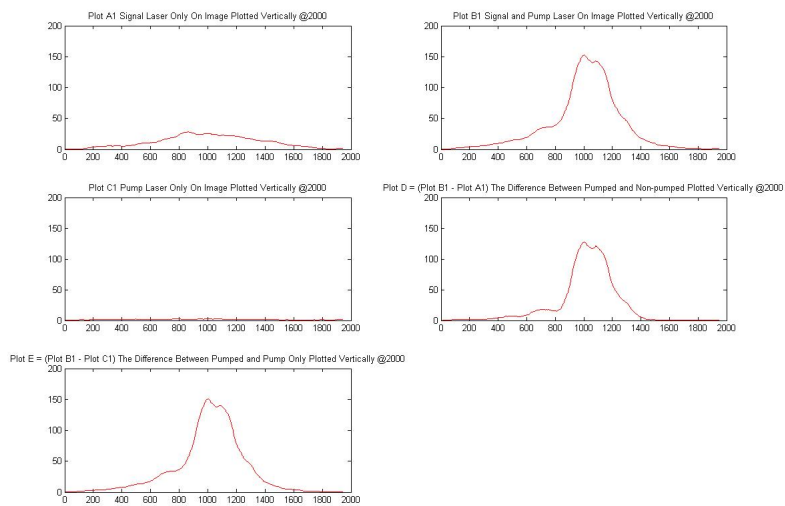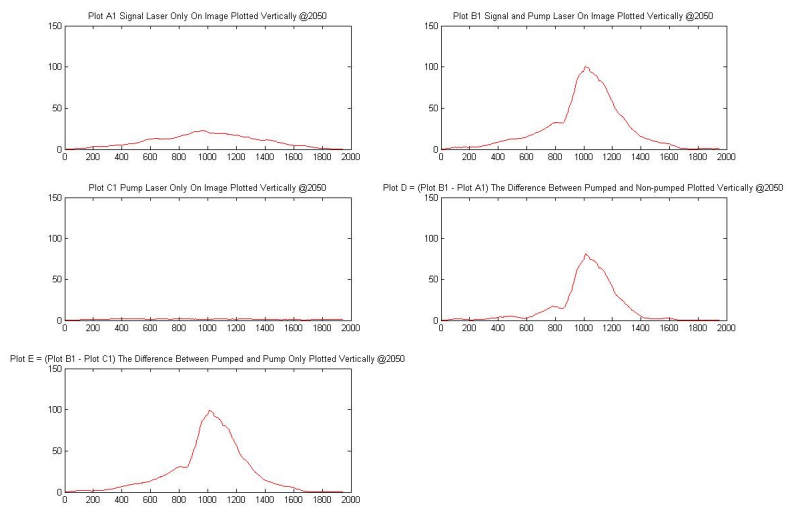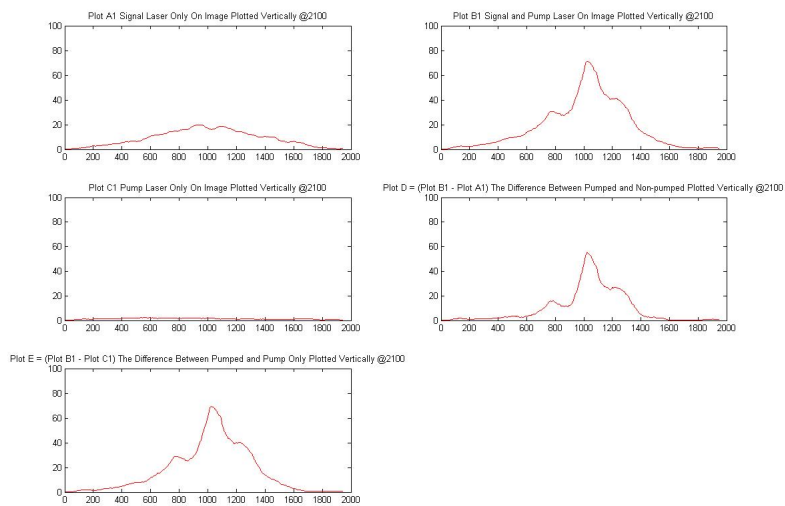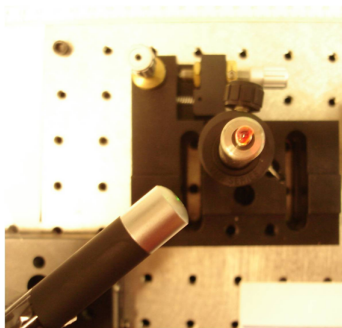Figure A.70: Pump Position B, Signal Polarization D at 1900

Plot A1 Signal Laser Only On Image Plotted Vertically @1950

Plot B1 Signal and Pump Laser On Image Plotted Vertically @1950

Plot C1 Pump Laser Only On Image Plotted Vertically @1950

Plot D = (Plot B1 - Plot A1) The Difference Between Pumped and Non-pumped Plotted Vertically @1950

Plot E = (Plot B1 - Plot C1) The Difference Between Pumped and Pump Only Plotted Vertically @1950

Figure A.71: Pump Position B, Signal Polarization D at 1950

Plot A1 Signal Laser Only On Image Plotted Vertically @2000

Plot B1 Signal and Pump Laser On Image Plotted Vertically @2000

Plot C1 Pump Laser Only On Image Plotted Vertically @2000

Plot D = (Plot B1 - Plot A1) The Difference Between Pumped and Non-pumped Plotted Vertically @2000

Plot E = (Plot B1 - Plot C1) The Difference Between Pumped and Pump Only Plotted Vertically @2000

Figure A.72: Pump Position B, Signal Polarization D at 2000

Figure A.73: Pump Position B, Signal Polarization D at 2050

Figure A.74: Pump Position B, Signal Polarization D at 2100

Figure A.75: Pump Position C

(a) Filtered Image Before Pumping

(b) Filtered Image After Pumping

(c) Filtered Image Pump Only On

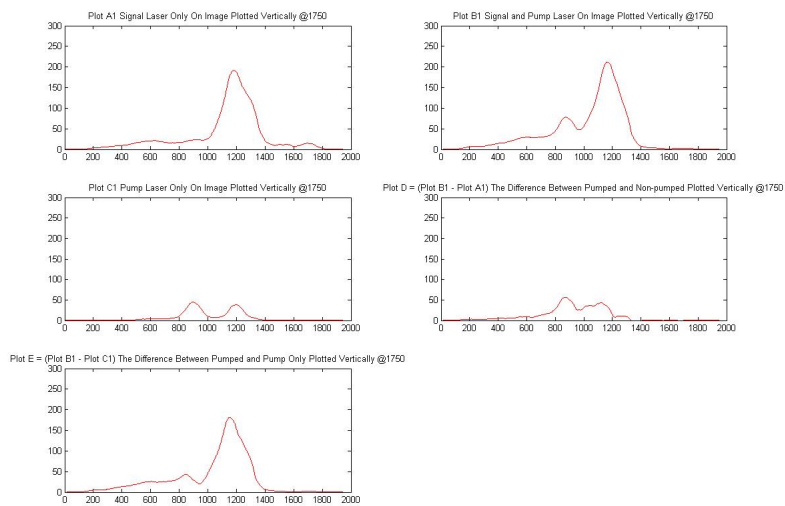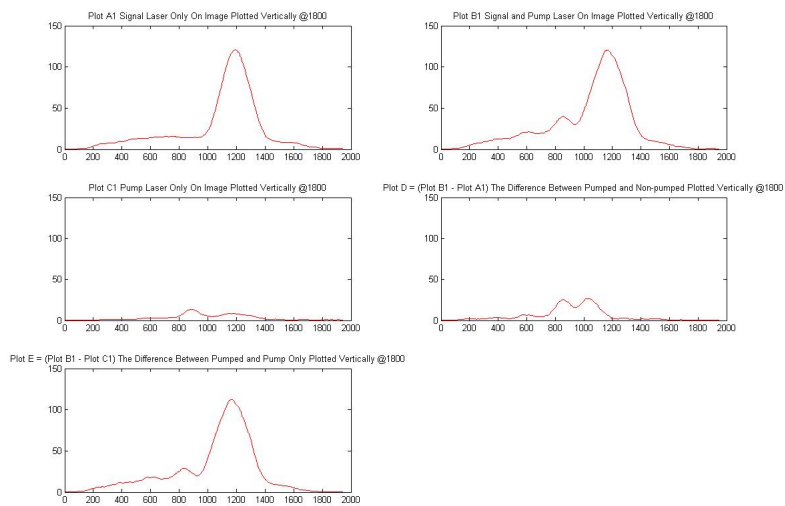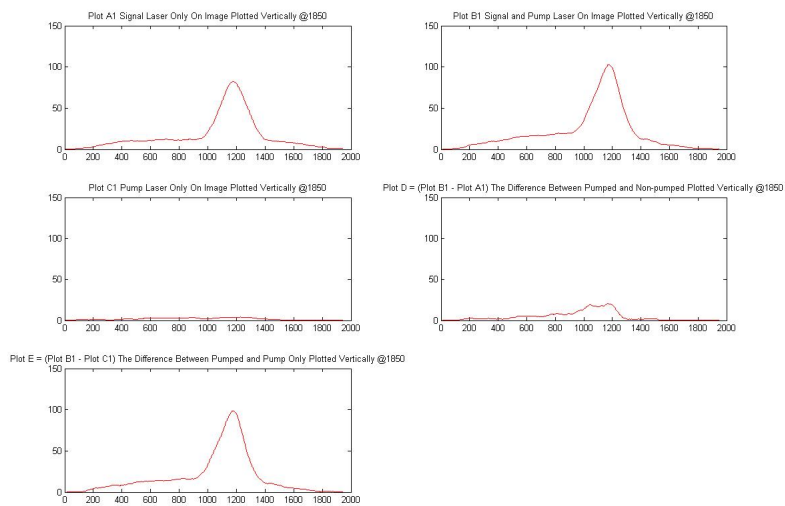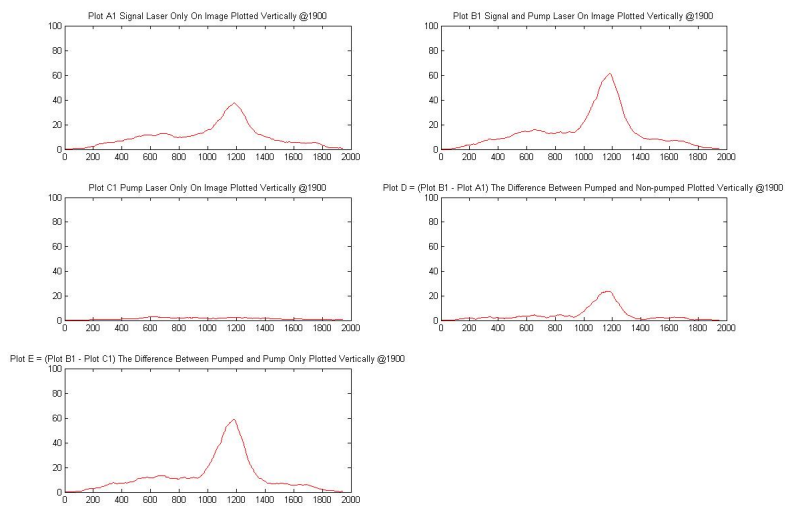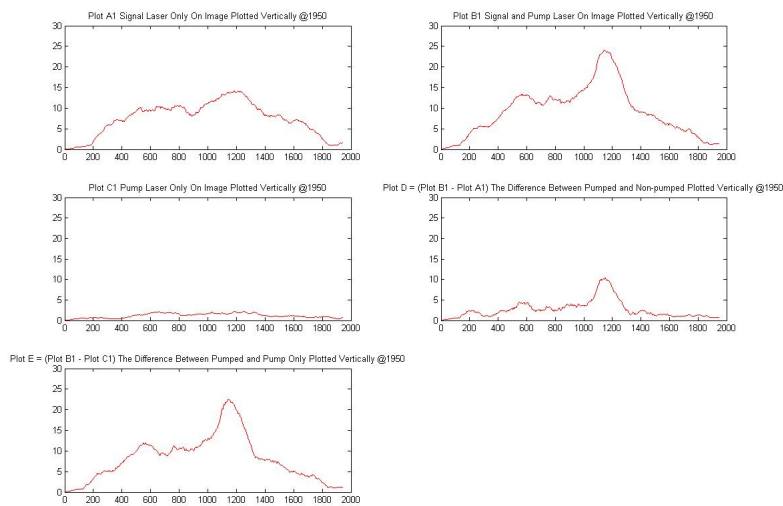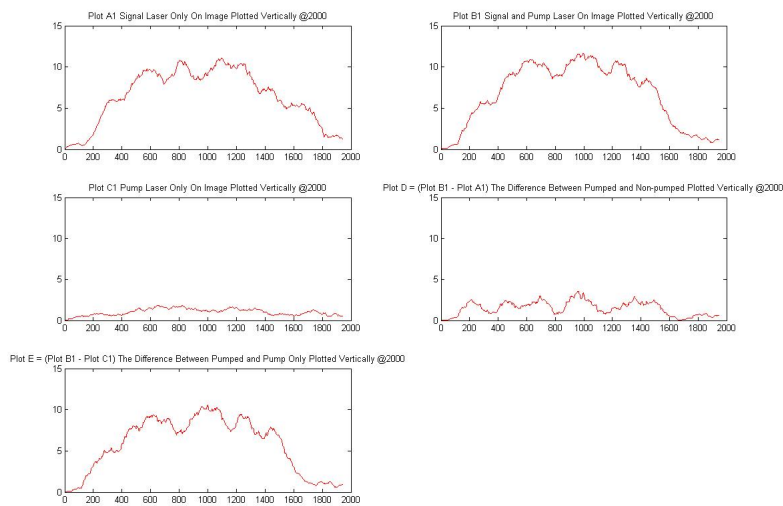Figure A.76: Pump Position C, Signal Polarization A

Plot A1 Signal Laser Only On Image Plotted Vertically @1750

Plot B1 Signal and Pump Laser On Image Plotted Vertically @1750

Plot C1 Pump Laser Only On Image Plotted Vertically @1750

Plot D = (Plot B1 - Plot A1) The Difference Between Pumped and Non-pumped Plotted Vertically @1750

Plot E = (Plot B1 - Plot C1) The Difference Between Pumped and Pump Only Plotted Vertically @1750

Figure A.77: Pump Position C, Signal Polarization A at 1750

Plot A1 Signal Laser Only On Image Plotted Vertically @1800

Plot B1 Signal and Pump Laser On Image Plotted Vertically @1800

Plot C1 Pump Laser Only On Image Plotted Vertically @1800

Plot D = (Plot B1 - Plot A1) The Difference Between Pumped and Non-pumped Plotted Vertically @1800

Plot E = (Plot B1 - Plot C1) The Difference Between Pumped and Pump Only Plotted Vertically @1800

Figure A.78: Pump Position C, Signal Polarization A at 1800

Figure A.79: Pump Position C, Signal Polarization A at 1850

Figure A.80: Pump Position C, Signal Polarization A at 1900

Figure A.81: Pump Position C, Signal Polarization A at 1950

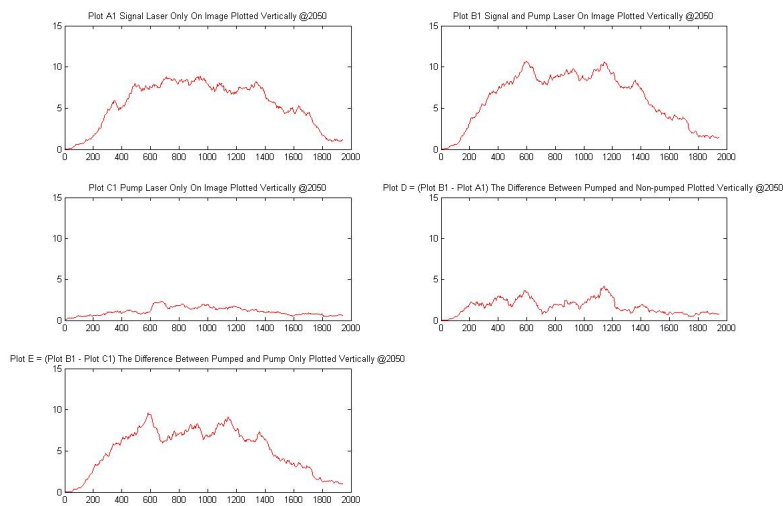Figure A.82: Pump Position C, Signal Polarization A at 2000

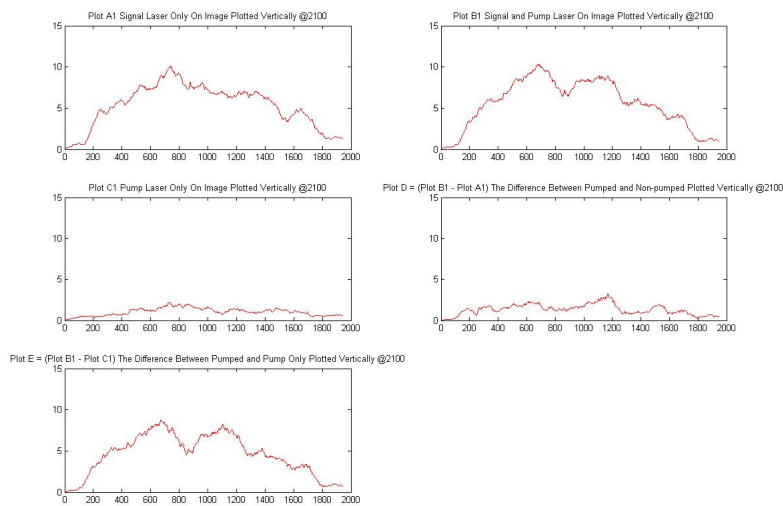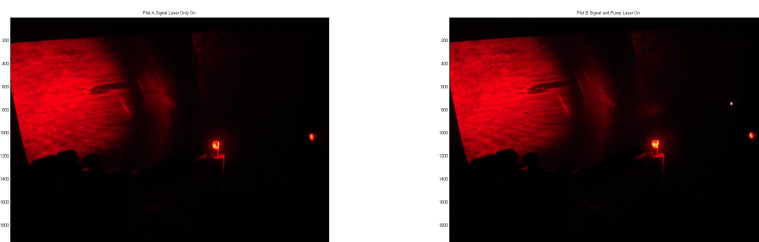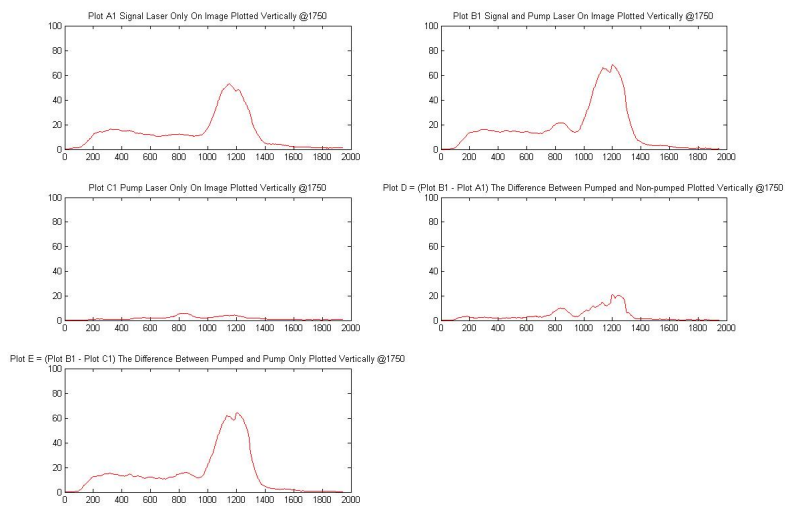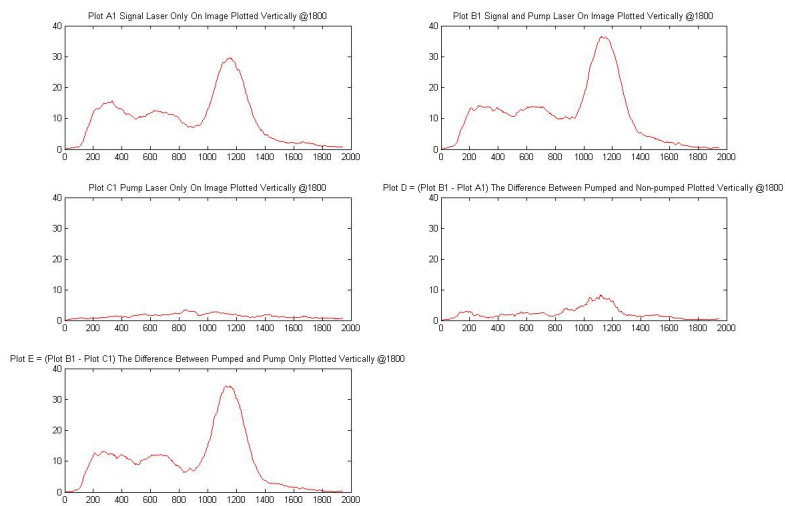Figure A.83: Pump Position C, Signal Polarization A at 2050

Figure A.84: Pump Position C, Signal Polarization A at 2100

(a) Filtered Image Before Pumping

(b) Filtered Image After Pumping

(c) Filtered Image Pump Only On

Figure A.85: Pump Position C, Signal Polarization B

Figure A.86: Pump Position C, Signal Polarization B at 1750

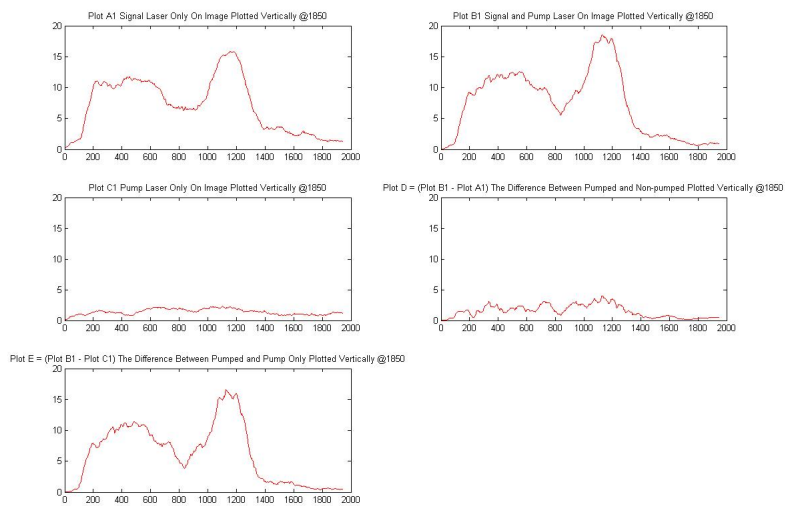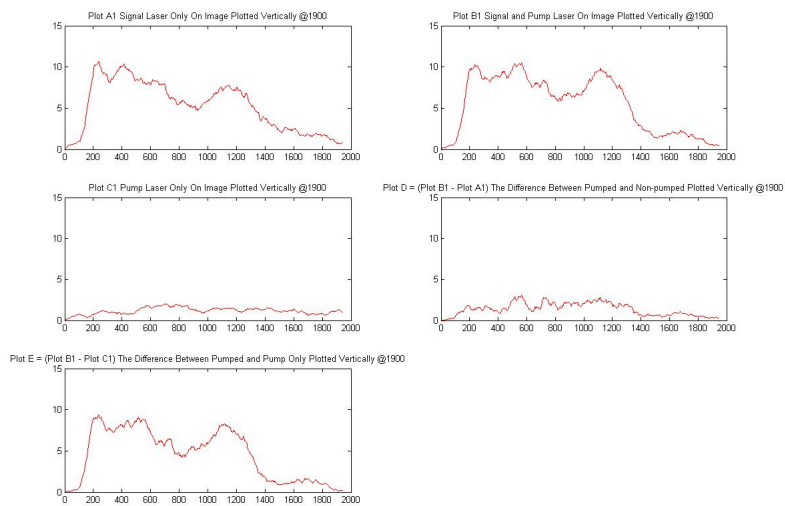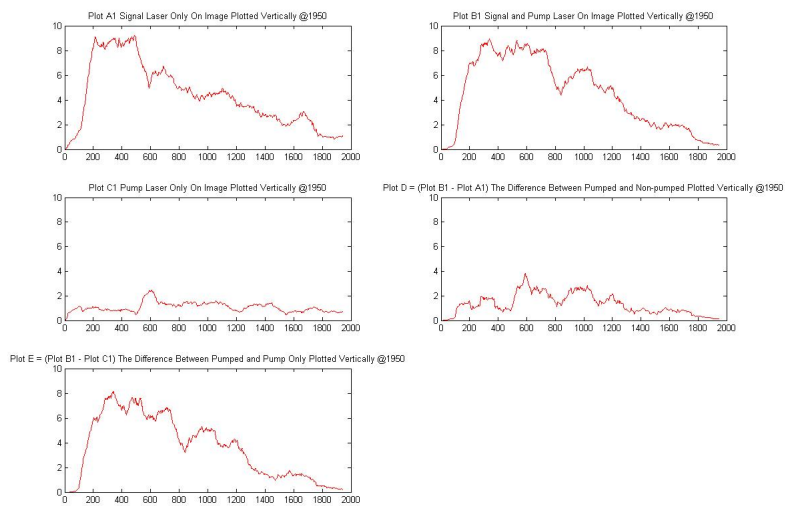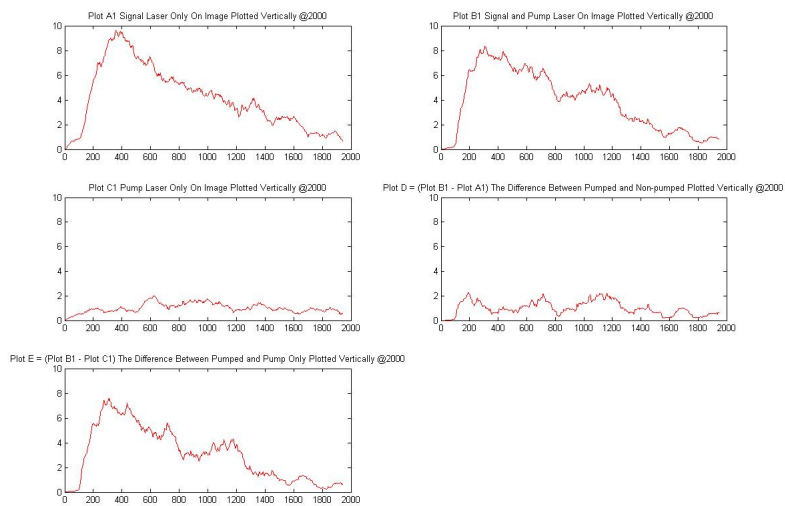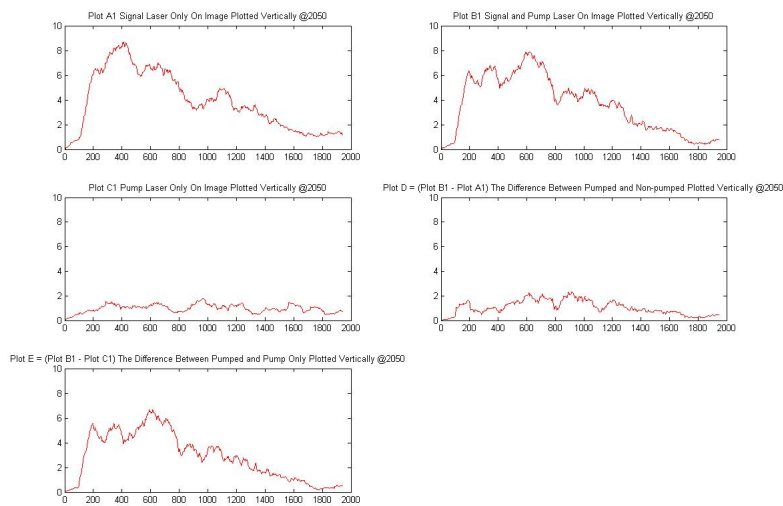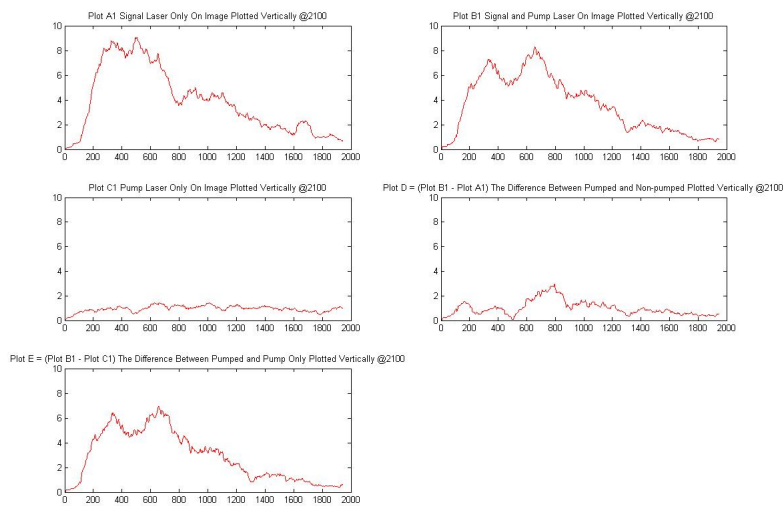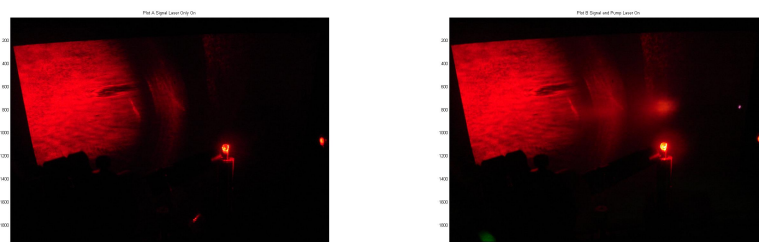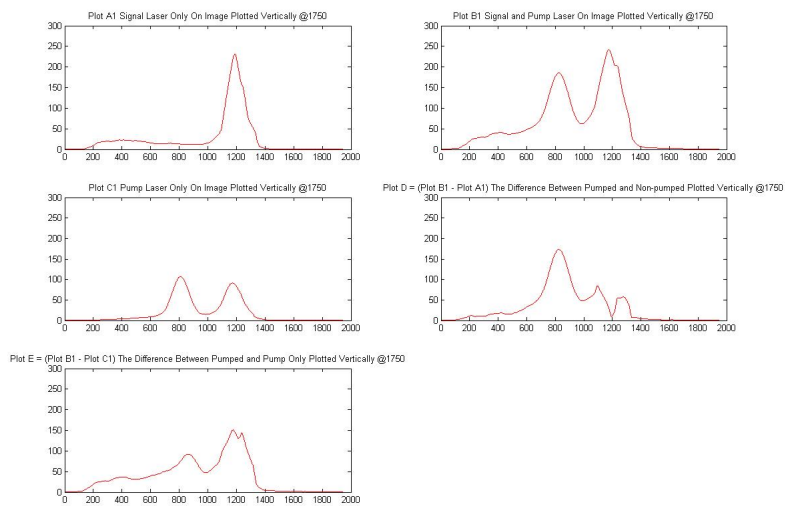Figure A.87: Pump Position C, Signal Polarization B at 1800

Plot A1 Signal Laser Only On Image Plotted Vertically @1850

Plot B1 Signal and Pump Laser On Image Plotted Vertically @1850

Plot C1 Pump Laser Only On Image Plotted Vertically @1850

Plot D = (Plot B1 - Plot A1) The Difference Between Pumped and Non-pumped Plotted Vertically @1850

Plot E = (Plot B1 - Plot C1) The Difference Between Pumped and Pump Only Plotted Vertically @1850

Figure A.88: Pump Position C, Signal Polarization B at 1850

Plot A1 Signal Laser Only On Image Plotted Vertically @1900

Plot B1 Signal and Pump Laser On Image Plotted Vertically @1900

Plot C1 Pump Laser Only On Image Plotted Vertically @1900

Plot D = (Plot B1 - Plot A1) The Difference Between Pumped and Non-pumped Plotted Vertically @1900

Plot E = (Plot B1 - Plot C1) The Difference Between Pumped and Pump Only Plotted Vertically @1900

Figure A.89: Pump Position C, Signal Polarization B at 1900

Plot A1 Signal Laser Only On Image Plotted Vertically @1950

Plot B1 Signal and Pump Laser On Image Plotted Vertically @1950

Plot C1 Pump Laser Only On Image Plotted Vertically @1950

Plot D = (Plot B1 - Plot A1) The Difference Between Pumped and Non-pumped Plotted Vertically @1950

Plot E = (Plot B1 - Plot C1) The Difference Between Pumped and Pump Only Plotted Vertically @1950

Figure A.90: Pump Position C, Signal Polarization B at 1950

Plot A1 Signal Laser Only On Image Plotted Vertically @2000

Plot B1 Signal and Pump Laser On Image Plotted Vertically @2000

Plot C1 Pump Laser Only On Image Plotted Vertically @2000

Plot D = (Plot B1 - Plot A1) The Difference Between Pumped and Non-pumped Plotted Vertically @2000

Plot E = (Plot B1 - Plot C1) The Difference Between Pumped and Pump Only Plotted Vertically @2000

Figure A.91: Pump Position C, Signal Polarization B at 2000

Figure A.92: Pump Position C, Signal Polarization B at 2050

Figure A.93: Pump Position C, Signal Polarization B at 2100

(a) Filtered Image Before Pumping

(b) Filtered Image After Pumping

(c) Filtered Image Pump Only On

Figure A.94: Pump Position C, Signal Polarization C

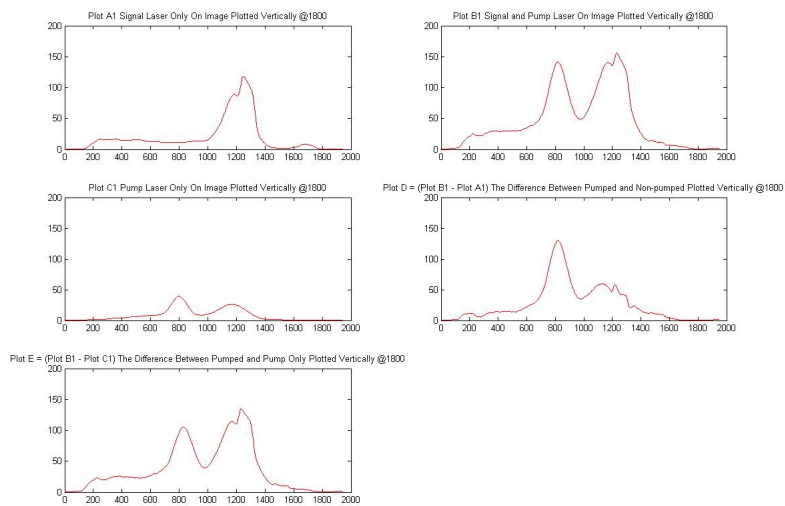Figure A.95: Pump Position C, Signal Polarization C at 1750

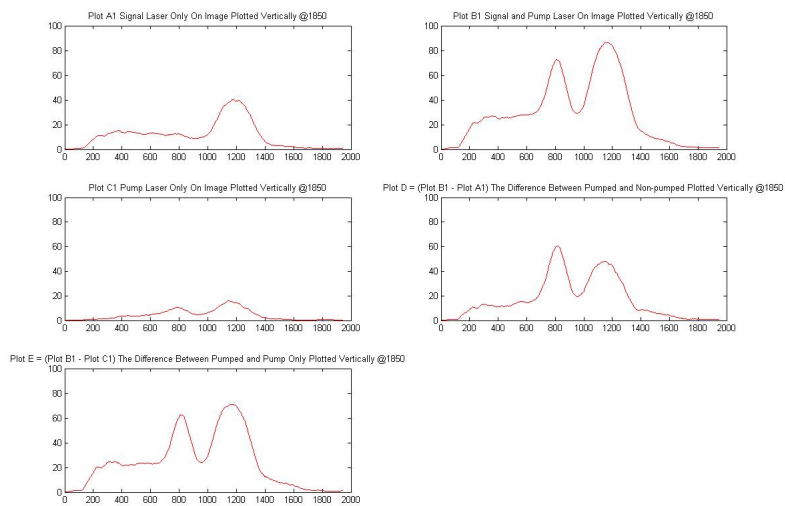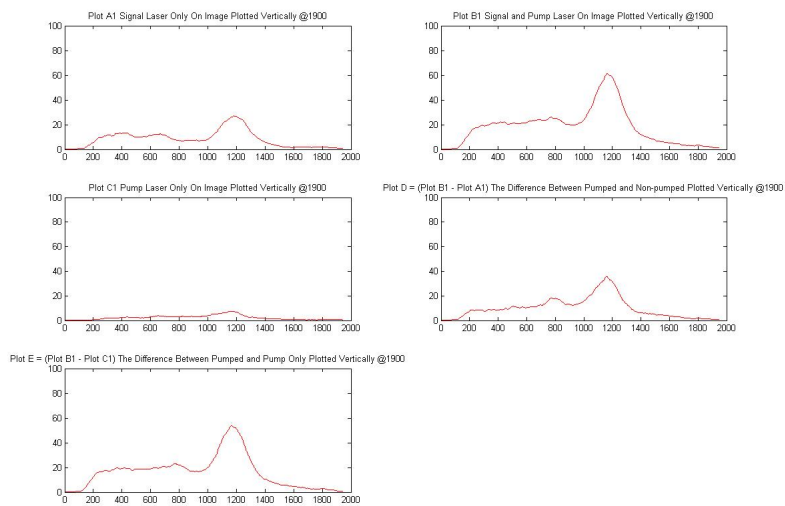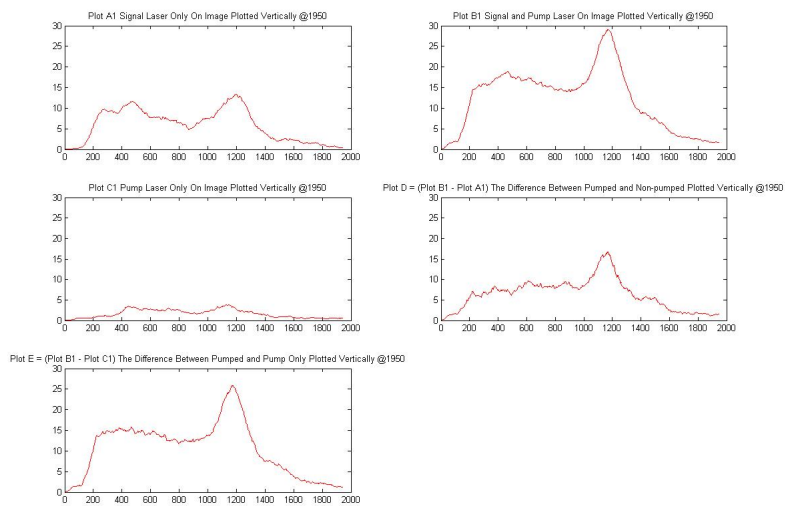Figure A.96: Pump Position C, Signal Polarization C at 1800

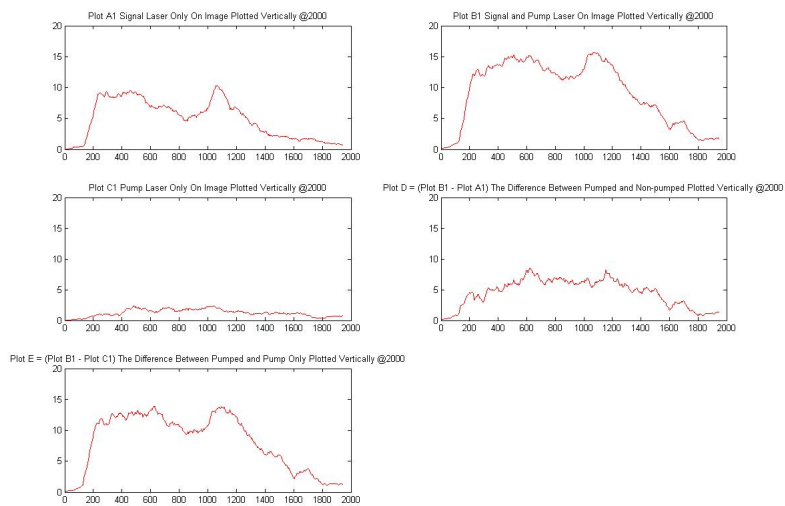Figure A.97: Pump Position C, Signal Polarization C at 1850

Figure A.98: Pump Position C, Signal Polarization C at 1900

Figure A.99: Pump Position C, Signal Polarization C at 1950

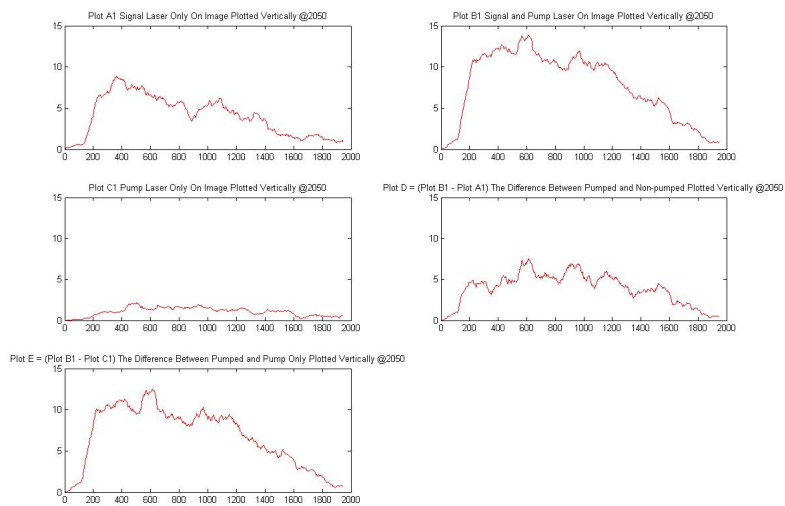Figure A.100: Pump Position C, Signal Polarization C at 2000

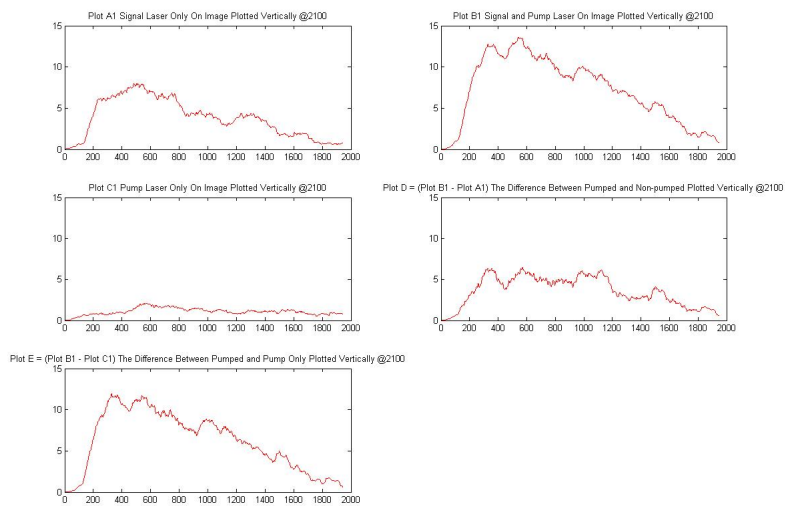Figure A.101: Pump Position C, Signal Polarization C at 2050

Figure A.102: Pump Position C, Signal Polarization C at 2100

(a) Filtered Image Before Pumping

(b) Filtered Image After Pumping

(c) Filtered Image Pump Only On
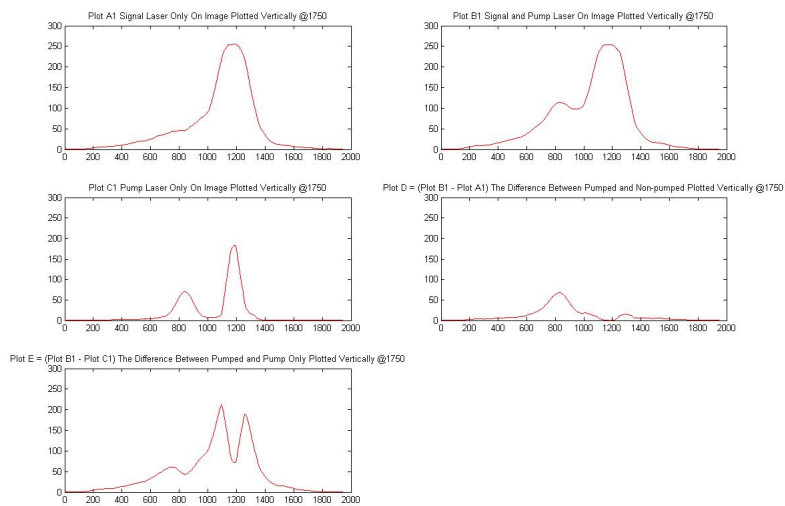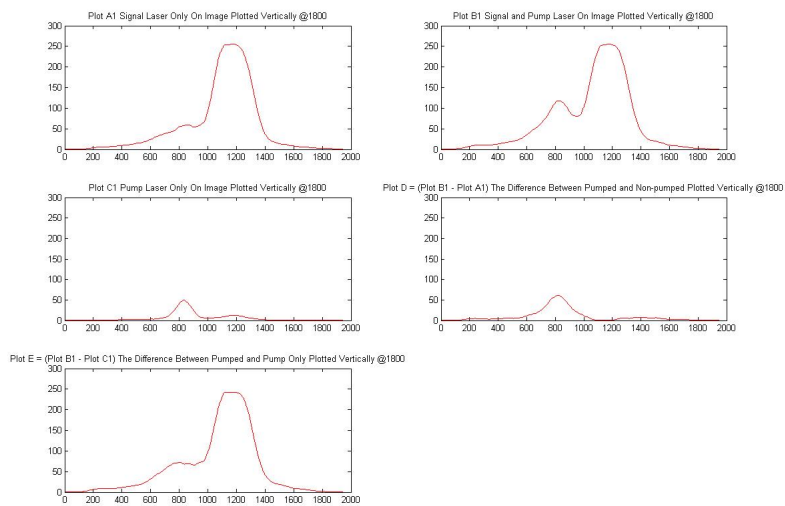
Figure A.103: Pump Position C, Signal Polarization D

Plot A1 Signal Laser Only On Image Plotted Vertically @1750

Plot B1 Signal and Pump Laser On Image Plotted Vertically @1750

Plot C1 Pump Laser Only On Image Plotted Vertically @1750

Plot D = (Plot B1 - Plot A1) The Difference Between Pumped and Non-pumped Plotted Vertically @1750

Plot E = (Plot B1 - Plot C1) The Difference Between Pumped and Pump Only Plotted Vertically @1750

Figure A.104: Pump Position C, Signal Polarization D at 1750

Plot A1 Signal Laser Only On Image Plotted Vertically @1800

Plot B1 Signal and Pump Laser On Image Plotted Vertically @1800

Plot C1 Pump Laser Only On Image Plotted Vertically @1800

Plot D = (Plot B1 - Plot A1) The Difference Between Pumped and Non-pumped Plotted Vertically @1800

Plot E = (Plot B1 - Plot C1) The Difference Between Pumped and Pump Only Plotted Vertically @1800

Figure A.105: Pump Position C, Signal Polarization D at 1800
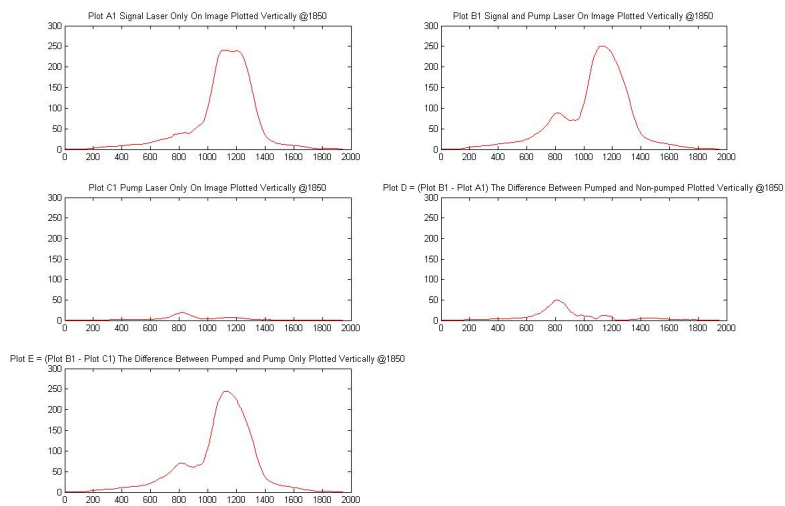
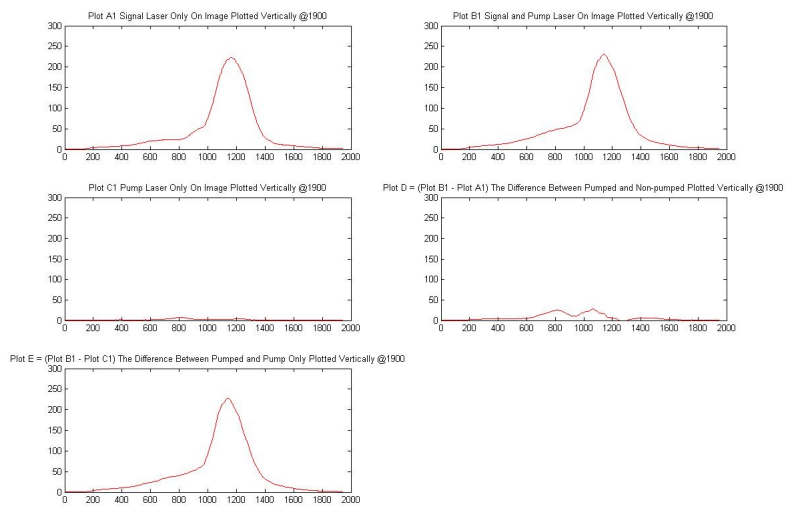Figure A.106: Pump Position C, Signal Polarization D at 1850

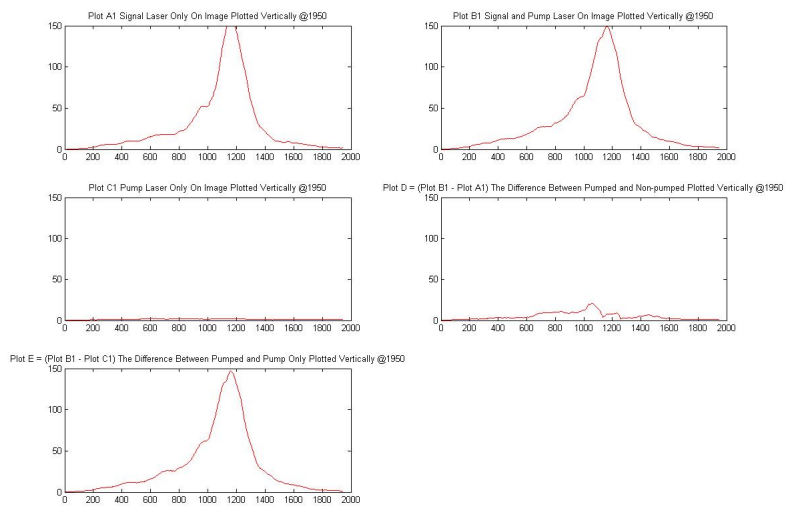Figure A.107: Pump Position C, Signal Polarization D at 1900

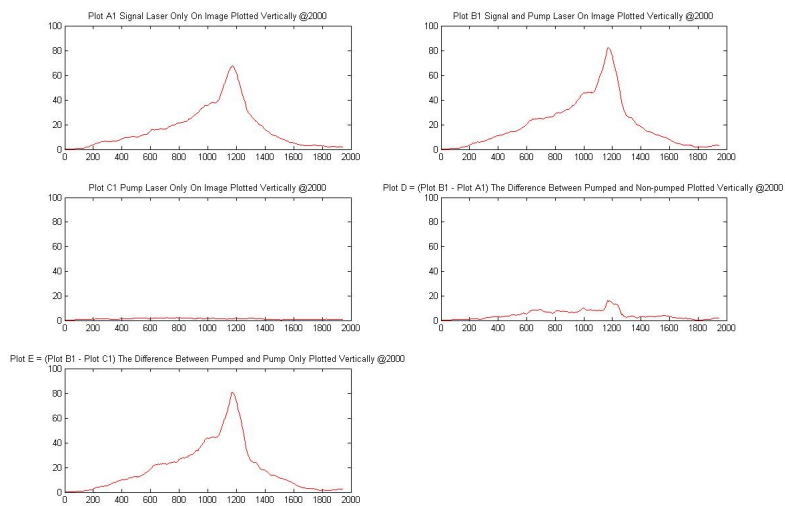Figure A.108: Pump Position C, Signal Polarization D at 1950

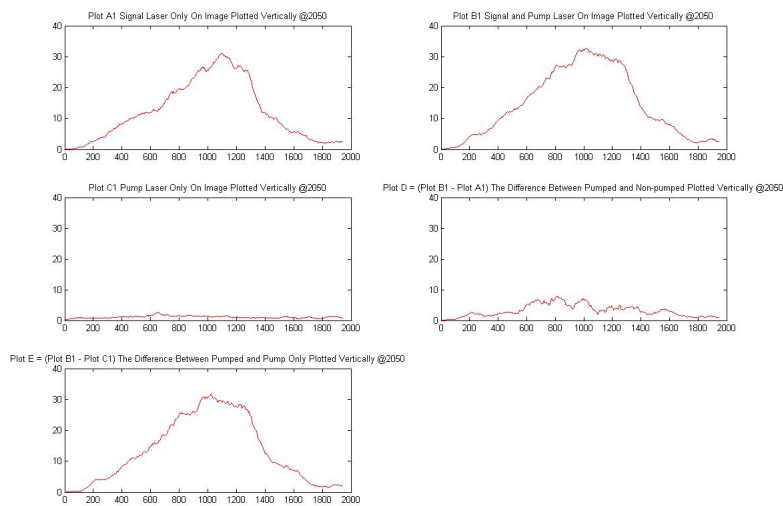Figure A.109: Pump Position C, Signal Polarization D at 2000

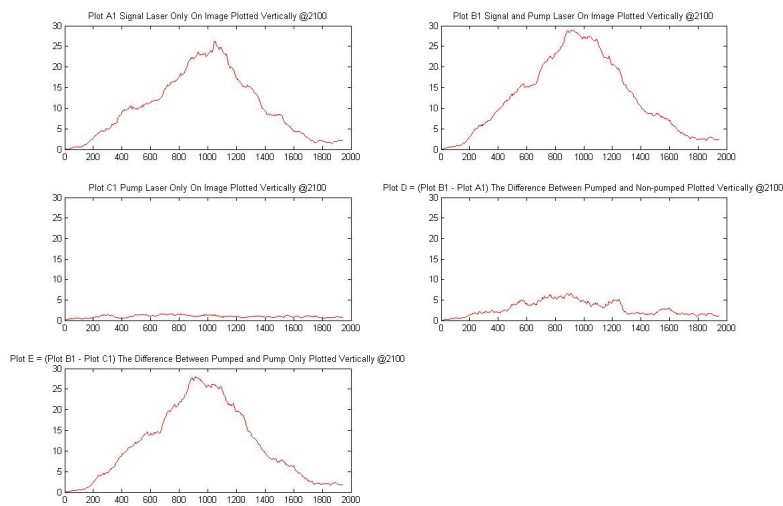Figure A.110: Pump Position C, Signal Polarization D at 2050

Figure A.111: Pump Position C, Signal Polarization D at 2100

APPENDIX B: SOURCE CODE